ELASTO-PLASTIC STRESS ANALYSIS IN TRANSVERSELY LOADED COMPOSITE LAMINATED PLATES

A Thesis Submitted to the

Graduate School of Natural and Applied Sciences of

Dokuz Eylül University

In Partial Fulfillment of the Requirements for

the Degree of Doctor of Philosophy in Mechanical Engineering, Mechanics Program

69026

by
Halil AYKUL

December,1998
İZMİR

Ph.D. THESIS EXAMINATION RESULT FORM

We certify that we have read this thesis and that in our opinion it is fully adequate, in scope and in quality, as a thesis for the degree of Doctor of Philosophy.

Prof. Dr. Onur SAYMAN

(Advisor)

Prof. Dr. Alâeddin Arpacı

(Committee Member)

Prof. Dr. Sami AKIŞ

(Committee Member)

Approved by the

Graduate School of Natural and Applied Sciences

Prof. Dr. Cahit Helvacı

Director

ACKNOWLEDGMENTS

I am deeply grateful to my thesis supervisor Prof. Dr. Onur SAYMAN, who has been my strongest supporter as I labored on this project, and there is no way that I could have done it without his encouragement, guidance, patience, and understanding.

I would like to thank my friends for their many helpful comments and suggestions.

Finally, I wish to express my heartfelt thank to my wife for her patience and tolerance.

Halil AYKUL

December, 1998
İzmir

ABSTRACT

Metal-matrix composites are new materials with superior properties. They provide high strength and stiffness, low density, resistance to corrosion, high creep and fatigue properties. These materials have gained a wide and popular range of use with several low cost manufacturing techniques developed in recent years.

Elasto-plastic stress analysis plays an important role in metal-matrix composite researches. In this study, a stainless steel fiber reinforced aluminum metal-matrix laminated plate is investigated. The plate is simply supported and transversely loaded. Elastic, elasto-plastic and residual stresses are calculated in the symmetric and/or antisymmetric cross-ply and angle-ply laminated plate for small deformations by using finite elements method. The expansion of plastic zone is illustrated by using AcadR14. The plate is examined either without or with a circular hole. Iteration numbers are chosen as 100, 150 and 200 for the plate without a hole. Iteration numbers are also chosen as 200, 400 and 600 for the plate with a circular hole. Isoparametric quadrilateral element with nine nodes is selected for the elasto-plastic analysis. Metal-matrix composite laminated plate is manufactured by using moulds under 30 MPa pressure and heating up to 600 ^{0}C. The first-order shear deformation theory is used. A computer program in Fortran77 is developed to solve the problem. This program can be used to make similar analyses. The engineering constants are obtained by using strain gages in the tensile testing machine after production of the stainless steel-aluminum composite material.

ÖZET

Metal-matriks kompozitler süper özelliklere yeni malzemelerdir. Bu kompozitler yüksek mukavemet ve direngenlik, düşük yoğunluk, korozyon dayanımı, yüksek sürünme ve yorulma özellikleri sağlar. Son yıllarda geliştirilen düşük maliyetli üretim teknikleri ile birlikte bu malzemeler geniş ve popüler bir kullanım alanına ulaşmıştır.

Elasto-plastik gerilme analizi metal-matriks kompozit çalışmalarında önemli bir rol oynar. Bu çalışmada paslanmaz çelik takviyeli aluminyum metal-matrix tabakalı bir plak incelendi. Plak sabit mesnetli ve düşey yüklüdür. Sonlu Elemanlar Metoduyla küçük deformasyonlar için simetrik ve antisimetrik $0^0/90^0$ ve açılı tabakalanmış plakta elastik, elastik-plastik ve artık gerilmeler hesaplanmıştır. Plastik bölgenin yayılması AcadR14 kullanılarak resmedildi. Delik bulunmayan plak için iterasyon sayıları 100, 150 ve 200 seçildi. Aynı şekilde delikli plak için iterasyon sayıları 200, 400 ve 600 seçildi. Elastik-plastik analiz için dokuz düğümlü izoparametrik dörtgen eleman geliştirildi. Metal-matriks kompozit tabakalı plak kalıp kullanılarak 30 MPa basınç altında 600 ^{0}C'ye kadar ısıtılarak üretildi. Birinci mertebe kayma-şekil değiştirme teorisi kullanıldı. Problemin çözümü için Fortran77'de otomatik bilgisayar programı geliştirildi. Bu program benzer analizlerin çözümü için de kullanılabilir. Mühendislik sabitleri, paslanmaz çelik-aluminyum kompozit malzemenin üretiminden sonra çekme deneyi ile strengeçler kullanılarak elde edilmiştir.

CONTENTS

Page

Acknowledgments..... I

Abstract..... II

Özet..... III

Contents..... IV

List of Tables..... VII

List of Figures..... X

Chapter One

INTRODUCTION

1.Introduction..... 1

Chapter Two

MACROMECHANICAL BEHAVIOR OF A LAMINATE

2.1 Introduction..... 5

2.2 Stress-Strain Relations For Plane Stress In An Orthotropic Material..... 5

2.3 Stress-Strain Relations For a laminae of Arbitrary Orientation..... 7

2.4 Stress-Strain Behavior in Laminated Composites..... 8

2.5. Strain and Stress Variation in a Laminate..... 9

2.6. Resultant Laminate Forces and Moments..... 12

2.7. Special Cases Of Laminate Stiffness..... 13
2.7.1. Single Layered Configurations..... 13
2.7.1.1. Single isotropic layer..... 13
2.7.1.2. Single specially orthotropic layer..... 14
2.7.1.3. Single generally orthotropic layer..... 15
2.7.1.4. Single anisotropic layer..... 16
2.7.2. Symmetric Laminates..... 16
2.7.2.1. Symmetric laminate with multiple isotropic layer..... 17
2.7.2.2. Symmetric laminate with multiple specially orthotropic layers..... 19
2.7.2.3. Symmetric laminate with multiple generally orthotropic layers..... 20
2.7.2.4. Symmetric laminates with multiple anisotropic layer..... 20
2.7.3. Antisymmetric Laminates..... 21
2.7.3.1. Antisymmetric cross-ply laminates..... 21
2.7.3.2. Antisymmetric angle-ply laminates..... 23

Chapter Three

ELASTO-PLASTIC STRESS ANALYSIS OF TRANSVERSELY LOADED LAMINATED PLATE

3.1. Mathematical Formulation..... 24
3.2. Finite Element Analysis..... ... 27
3.2.1. Finite Element Approach Elasto-Plastic Stress Analysis..... 27
3.2.2. Numerical Integration..... 32
3.3. Mesh, Geometry and Boundary Conditions..... 35
3.3.1. Geometry of The Plate 35
3.3.2. Mesh Generation and Boundary Conditions 35

Chapter Four
PRODUCTION OF LAMINATE

4.1. Specimen Preparation and Testing Procedure..... 37
4.2. Experimental Results 41
4.3. Production of Laminated Plates..... 42

Chapter Five
NUMERICAL RESULTS AND DISCUSSIONS

5.1. Transversely Loaded Plate Without a Hole..... 44
5.1.1. Symmetric or Antisymmetric Laminated Plates of Four Layers..... 44
5.1.2. Antisymmetric Laminated Plates of Four Layers..... 58
5.1.3. Antisymmetric Laminated Plates of Two Layers..... 67
5.2. Transversely Loaded Plate With a Circular Hole..... 76
5.2.1. Symmetric or Antisymmetric Laminated Plates of Four Layers..... 76
5.2.2. Antisymmetric Laminated Plates of Four Layers..... 92

Conclusions..... 104

References..... 106

LIST OF TABLES

Page

Table 3.1. Sampling points and weights in Gauss-Legendre numerical integration..... 34

Table 4.1. Mechanical properties and yield points of a layer..... 43

Table 5.1. The uniform transverse force at the yield points of the four laminated plates. (S: Symmetric laminate, A: Antisymmetric laminate)..... 45

Table 5.2. Elastic, elasto-plastic and residual stresses for symmetric cross-ply laminated plate $[(0/90)]_2$ at node 85 for 100-150-200 iterations..... 46

Table 5.3. Elastic, elasto-plastic and residual stresses for symmetric angle-ply laminated plate $[(30/-30)]_2$ at node 85 for 100-150-200 iterations..... 47

Table 5.4. Elastic, elasto-plastic and residual stresses for symmetric angle-ply laminated plate $[(45/-45)]_2$ at node 85 for 100-150-200 iterations..... 48

Table 5.5. Elastic, elasto-plastic and residual stresses in symmetric angle-ply laminated plates $[(60/-60)]_2$ at node 85 for 100-150-200 iterations..... 49

Table 5.6. Elastic, elasto-plastic and residual stresses in antisymmetric cross-ply laminated plates $[(0/90)]_2$ at node 85 for 100-150-200 iterations 51

Table 5.7. Elastic, elasto-plastic and residual stresses in antisymmetric angle-ply laminated plates $[(30/-30)]_2$ at node 85 for 100-150-200 iterations 53

Table 5.8. Elastic, elasto-plastic and residual stresses in antisymmetric angle-ply laminated plates $[(45/-45)]_2$ at node 85 for 100-150-200 iterations 55

Table 5.9. Elastic, elasto-plastic and residual stresses in antisymmetric angle-ply laminated plates $[(60/-60)]_2$ at node 85 for 100-150-200 iterations. 57

Table 5.10.. The uniform transverse force at the yield points of the antisymmetric four laminated plates. 58

Table 5.11. Elastic, elasto-plastic and residual stresses in antisymmetric cross-ply laminated plates $[(0)_2/(90)_2]$ at node 85 for 100-150-200 iterations 60
Table 5.12. Elastic, elasto-plastic and residual stresses in antisymmetric angle-ply laminated plates $[(30)_2/(-30)_2]$ at node 85 for 100-150-200 iterations 62
Table 5.13. Elastic, elasto-plastic and residual stresses in antisymmetric angle-ply laminated plates $[(45)_2/(-45)_2]$ at node 85 for 100-150-200 iterations 64
Table 5.14. Elastic, elasto-plastic and residual stresses in antisymmetric angle-ply laminated plates $[(60)_2/(-60)_2]$ at node 85 for 100-150-200 iterations 66
Table 5.15. The uniform transverse force at the yield points of the antisymmetric two laminated plates. 67
Table 5.16. Elastic, elasto-plastic and residual stresses in antisymmetric cross-ply (0/90) laminated plate at node 85 for 100-150-200 iterations 69
Table 5.17. Elastic, elasto-plastic and residual stresses in antisymmetric angle-ply laminated plates (30/-30) at node 85 for 100-150-200 iterations 71
Table 5.18. Elastic, elasto-plastic and residual stresses in antisymmetric angle-ply laminated plates (45/-45) at node 85 for 100-150-200 iterations 73
Table 5.19. Elastic, elasto-plastic and residual stresses in antisymmetric angle-ply laminated plates (60/-60) at node 85 for 100-150-200 iterations 75
Table 5.20. The uniform transverse force at the yield points of the four laminated plates. (S: Symmetric laminate, A: Antisymmetric laminate.) 76
Table 5.21. Elastic, elasto-plastic and residual stresses for symmetric cross-ply laminated plate with a circular hole $[(0/90)_2]$ at point A for 200-400-600 iterations..... 77
Table 5.22.. Elastic, elasto-plastic and residual stresses for symmetric angle-ply laminated plate with a circular hole $[(30/-30)_2]$ at point A 200-400-600 iterations..... 79
Table 5.23. Elastic, elasto-plastic and residual stresses for symmetric cross-ply laminated plate with a circular hole $[(45/-45)_2]$ at point A for 200-400-600 iterations. 80
Table 5.24.. Elastic, elasto-plastic and residual stresses for symmetric angle-ply laminated plate with a circular hole $[(60/-60)_2]$ at point A for 200-400-600 iterations. 82

Table 5.25.. Elastic, elasto-plastic and residual stresses for antisymmetric cross-ply laminated plate with a circular hole $[(0/90)_2]$ at point A for 200-400-600 iterations..... 84

Table 5.26.. Elastic, elasto-plastic and residual stresses for antisymmetric angle-ply laminated plate with a circular hole $[(30/-30)_2]$ at point A for 200-400-600 iterations. 87

Table 5.27. Elastic, elasto-plastic and residual stresses for antisymmetric angle-ply laminated plate with a circular hole $[(45/-45)_2]$ at point A for 200-400-600 iterations. 89

Table 5.28.. Elastic, elasto-plastic and residual stresses for antisymmetric angle-ply laminated plate with a circular hole $[(60/-60)]_2$ at point A for 200-400-600 iterations. 92

Table 5.29. The uniform transverse force at the yield points of the antisymmetric four laminated plates. 93

Table 5.30.. Elastic, elasto-plastic and residual stresses for antisymmetric cross-ply laminated plate with a circular hole $[(0)_2/(90)_2]$ at point A for 200-400-600 iterations. 95

Table 5.31. Elastic, elasto-plastic and residual stresses for antisymmetric angle-ply laminated plate with a circular hole $[(30)_2/(-30)_2]$ at point A for 200-400-600 iterations. 97

Table 5.32.. Elastic, elasto-plastic and residual stresses for antisymmetric angle-ply laminated plate with a circular hole $[(45)_2/(-45)_2]$ at point A for 200-400-600 iterations. 100

Table 5.33.. Elastic, elasto-plastic and residual stresses for antisymmetric angle-ply laminated plate with a circular hole $[(60)_2/(-60)_2]$ at point A for 200-400-600 iterations. 102

LIST OF FIGURES

Page

Fig. 2.1 Unidirectionally reinforced laminae..... 5

Fig. 2.2 a) Helically wound fiber-reinforced circular cylindrical shell
b) Positive rotation of principal material axes from arbitrary x, y-axes..... 8

Fig. 2.3. Geometry of deformation in the x-z plane..... 10

Fig. 2.4. Hypothetical variation of strain and stress through the laminate thickness..... 11

Fig. 2.5. Geometry of N-layered laminate..... 12

Fig. 2.6. Unbounded view of a four layered **a)** symmetric laminate with isotropic layers **b)** regular symmetric cross-ply laminate **c)** regular symmetric angle-ply laminate..... 19

Fig. 2.7. Unbounded view of a four layered regular antisymmetric **a)** cross-ply **b)** angle-ply laminate..... 22

Fig.3.1 Deformation assumptions in analysis of plate including shear deformations..... 25

Fig.3.2. Nine node Lagrangian finite element..... 28

Fig.3.3. Presentation of Gauss integration points..... 34

Fig.3.4. Geometry and coordinates..... 35

Fig.3.5. Mesh and boundary conditions for plate without a hole..... 36

Fig.3.6. Mesh and boundary conditions for plate with circular a hole..... 36

Fig.4.1. Uniaxial loading in the 1-direction..... 38

Fig.4.2. Uniaxial loading in the 2-direction..... 39

Fig.4.3. Uniaxial loading at 45^0 to the 1-direction..... 40

Fig.4.4. Uniaxial loading to the 1-direction..... 41

Fig.4.5. Production of composite layer..... 42

Fig. 5.1. Expansion of plastic zone in the symmetric $[(0/90)_2]$ laminated plate... 46
Fig. 5.2. Expansion of plastic zone in the symmetric $[(30/-30)_2]$ laminated plate 47
Fig. 5.3. Expansion of plastic zone in the symmetric $[(45/-45)_2]$ laminated plate 48
Fig. 5.4. Expansion of plastic zone in the symmetric $[(60/-60)_2]$ laminated plate 49
Fig. 5.5. Expansion of plastic zone in the antisymmetric $[(0/90)_2]$ laminated plate **(a)** At the upper surface **(b)** At the lower surface..... 50
Fig. 5.6. Expansion of plastic zone in the antisymmetric $[(30/-30)_2]$ laminated plate **(a)** At the upper surface **(b)** At the lower surface..... 52
Fig. 5.7. Expansion of plastic zone in the antisymmetric $[(45/-45)_2]$ laminated plate **(a)** At the upper surface **(b)** At the lower surface..... 54
Fig. 5.8. Expansion of plastic zone in the antisymmetric $[(60/-60)_2]$ laminated plate **(a)** At the upper surface **(b)** At the lower surface 56
Fig. 5.9. Expansion of the plastic zone in the antisymmetric $[(0)_2/(90)_2]$ laminated plate **(a)** At the upper surface **(b)** At the lower surface..... 59
Fig. 5.10. Expansion of the plastic zone in the antisymmetric $[(30)_2/(-30)_2]$ laminated plate **(a)** At the upper surface **(b)** At the lower surface..... 61
Fig. 5.11. Expansion of the plastic zone in the antisymmetric $[(45)_2/(-45)_2]$ laminated plate **(a)** At the upper surface **(b)** At the lower surface..... 63
Fig. 5.12.. Expansion of the plastic zone in the antisymmetric $[(60)_2/(-60)_2]$ laminated plate **(a)** At the upper surface **(b)** At the lower surface..... 65
Fig. 5.13.. Expansion of the plastic zone in the antisymmetric cross-ply (0/90) laminated plate **(a)** At the upper surface **(b)** At the lower surface..... 68
Fig. 5.14. Expansion of the plastic zone in the antisymmetric angle-ply (30/-30) laminated plate **(a)** At the upper surface **(b)** At the lower surface..... 70
Fig. 5.15. Expansion of the plastic zone in the antisymmetric angle-ply (45/-45) laminated plate **(a)** At the upper surface **(b)** At the lower surface..... 72
Fig. 5.16.. Expansion of the plastic zone in the antisymmetric angle-ply (60/-60) laminated plate **(a)** At the upper surface **(b)** At the lower surface..... 74
Fig. 5.17. Expansion of plastic zone in the symmetric $[(0/90)_2]$ laminated plate. 77
Fig. 5.18. The expansion of residual stress σ_x along AB in the symmetric $[(0/90)_2]$ laminated plate 78
Fig. 5.19. Expansion of plastic zone in the symmetric $[(30/-30)_2]$ laminated

plate..... 78

Fig. 5.20. The expansion of residual stress σ_x along AB in the symmetric $[(30/-30)_2]$ laminated plate..... 79

Fig. 5.21. Expansion of plastic zone in the symmetric $[(45/-45)_2]$ laminated plate..... 80

Fig. 5.22. The expansion of residual stress σ_x along AB in the symmetric $[(45/-45)_2]$ laminated plate..... 81

Fig. 5.23. Expansion of plastic zone in the symmetric $[(60/-60)_2]$ laminated plate..... 81

Fig. 5.24. The expansion of residual stress σ_x along AB in the symmetric $[(60/-60)_2]$ laminated plate..... 82

Fig. 5.25. Expansion of the plastic zone in the antisymmetric $[(0/90)_2]$ laminated plate **(a)** At the upper surface **(b)** At the lower surface..... 83

Fig. 5.26. The expansion of residual stress σ_x along AB in the antisymmetric $[(0/90)_2]$ laminated plate..... 85

Fig. 5.27. Expansion of the plastic zone in the antisymmetric $[(30/-30)_2]$ laminated plate **(a)** At the upper surface **(b)** At the lower surface..... 86

Fig. 5.28. The expansion of residual stress σ_x along AB in the antisymmetric $[(30/-30)_2]$ laminated plate..... 86

Fig. 5.29. Expansion of the plastic zone in the antisymmetric $[(45/-45)_2]$ laminated plate **(a)** At the upper surface **(b)** At the lower surface..... 88

Fig. 5.30. The expansion of residual stress σ_x along AB in the antisymmetric $[(45/-45)_2]$ laminated plate..... 90

Fig. 5.31. Expansion of the plastic zone in the antisymmetric $[(60/-60)_2]$ laminated plate **(a)** At the upper surface **(b)** At the lower surface..... 91

Fig. 5.32. The expansion of residual stress σ_x along AB in the antisymmetric $[(60/-60)_2]$ laminated plate..... 91

Fig. 5.33. Expansion of the plastic zone in the antisymmetric $[(0)_2/(90)_2]$ laminated plate **(a)** At the upper surface **(b)** At the lower surface..... 94

Fig. 5.34. The expansion of residual stress σ_x along AB in the antisymmetric $[(0)_2/(90)_2]$ laminated plate..... 94

Fig. 5.35. Expansion of the plastic zone in the antisymmetric $[(30)_2/(-30)_2]$

laminated plate **(a)** At the upper surface **(b)** At the lower surface..... 96

Fig. 5.36. The expansion of residual stress σ_x along AB in the antisymmetric $[(30)_2/(-30)_2]$ laminated plate..... 98

Fig. 5.37. Expansion of the plastic zone in the antisymmetric $[(45)_2/(-45)_2]$ laminated plate **(a)** At the upper surface **(b)** At the lower surface..... 99

Fig. 5.38. The expansion of residual stress σ_x along AB in the antisymmetric $[(45)_2/(-45)_2]$ laminated plate..... 99

Fig. 5.39. Expansion of the plastic zone in the antisymmetric $[(60)_2/(-60)_2]$ laminated plate **(a)** At the upper surface **(b)** At the lower surface..... 101

Fig. 5.40. The expansion of residual stress σ_x along AB in the antisymmetric $[(60)_2/(-60)_2]$ laminated plate..... 103

CHAPTER ONE
INTRODUCTION

The technology of metal matrix composite materials is developing very rapidly. Metal matrix composites consist of a ductile, usually low strength matrix reinforced with elastic or ductile and strong fibers. Ideally, the strength and rigidity of the fiber and the ductility of the matrix are combined to produce a new material with superior properties. Choosing the best combinations of fiber and matrix materials is a difficult task which involves conflicting demands and many compromises.

Plastic deformations and residual stresses are important in composite laminated plates. Residual stresses are used to raise the yield points of the plate. Bahei-El-Din & Dvorak (1982) have investigated the elastic-plastic behavior of symmetric metal-matrix composite laminates for the case of in-plane mechanical loading. In that study, aluminum matrix is reinforced by boron fibers. Metal-matrix composites consist of a ductile, usually low strength matrix reinforced with elastic brittle, or ductile strong fibers which provide a new material with superior properties such as high strength and stiffness, low density and resistance to corrosion high creep and fatigue properties (Yeh & Krempl 1993, Doghri *et al.* 1994, Canumalla & Dynan 1995). Continuous SiC fiber reinforced titanium or titanium alloy matrix composites are potential canditates for high temperature applications such as gas turbine engines and aircraft structural members since they have the potential for achieving a combination of low density, high strength to weight ratio, excellent corrosion resistance, high creep and fatigue properties. Common technique for the fabrication of continuous fiber metal-matrix composites involving minimal risk (matrix

contamination, fiber cracking, etc.) is the foil/fiber/foil technique. The foils first undergo a surface treatment step to remove surface oxides and other contaminants and are then stacked alternatively with fiber mats. Consolidation of the composite can be achieved by either HIP ing (where encapsulation is required) or hot pressing under high vacuum conditions. In that work, a simply geometry consisting of one layer of fibers sandwiched between two foils was examined (Nicolaou *et al.* 1994). Karakuzu & Özcan (1997) have given an exact solution to the elasto-plastic stress analysis of an aluminum metal-matrix composite beam reinforced by steel fibers. Continuous stainless steel reinforced aluminum matrix composites manufactured by die casting process provides higher mechanical properties.

Chou *et al.* (1985) reviewed the work on fibre-reinforced metal-matrix composites involving fabrication methods, mechanical properties, secondary working techniques and interfaces. G. Kang & S. Kang (1994) investigated the short fiber reinforced aluminum composite material, fabricated by stirring method and extruded at high temperatures at various extrusion ratios. The tensile strength of the hot extrusion billet was experimentally determined for different extrusion ratios, and compared with the theoretically calculated strength. Metal matrix composites provide a relatively new way of strengthening metals (Cöcen *et al.* 1997).

The die casting technique has recently been applied to investigate the fabrication possibilities of metal matrix composites. Among these fabrication methods, the squeeze casting technique appears to be the most effective in that it offers the following two advantages: (1) good suitability for mass production (2) a relatively simple process for manufacturing to near net shape in composites. G. Kang and S. Ku (1995) investigated the infiltration limits in the fabrication of Al_2O_3 short fiber reinforced composites for various processing conditions. Pitchumani *et al.* (1994) used an eddy current technique for the measurement of constituent volume fractions in a three-phase metal-matrix

composite. The volume fractions were calculated using eddy current measurements made on a wide range of silicon carbide particulate (SiCp) reinforced aluminum matrix composite extrusions. Ananth *et al.* (1995) investigated the application of push out test to characterize the mechanical behavior of interfaces in metallic and intermetallic matrix composites by using finite element method and also studied the effect of different material and testing variables on the experimental data.

The elasto-plastic stress analysis was carried out in an aluminum metal-matrix composite flat plate with "U" notch and an aluminum metal matrix rotating disc. Residual stresses are determined in metal matrix rotating discs with holes and flat plates containing notches by using finite element method and Tsai-Hill criterion is used as the failure criterion (Karakuzu & Sayman 1993, Karakuzu *et al.*1997).

Tensile residual stresses in the composite materials are particularly important because they may represent a significant fraction of the tensile strength of the polymer or metal matrix and can lead to premature or increased failure (Jeronimidis & Parkyn 1988, Unger & Hansen (1993). Pomies & Carlsson (1994) carried out micro mechanical finite element analysis of rigidity and strength of transverse tension loaded continuous fiber composites and compared their results with experimental data for dry and wet glass-epoxy, carbon-epoxy composites. In their study, transverse tensile strength predictions employed the combined mechanical and residual stress states at the fiber-matrix interface and in the matrix, in conjunction with debonding and matrix failure criteria. Zocher *et al.* (1995) presented numerically generated failure envelopes for several three-dimensional failure criteria and compared them with experimental data. Karakaya & Sehitoglu (1996) studied the improvement of the understanding of deformation and failure mechanisms of unidirectional carbon fiber reinforced plastics.

Linear or nonlinear finite element method can be used to analyze the laminated composites (Yang & He 1994, Hu & Schnobrich 1991, Choi & Kwak 1990). Owen (1983) studied elasto-plastic finite element analysis of anisotropic plates and shell. Theo (1981) investigated stress around rectangular holes in orthotropic plates.

In this study, aluminum metal matrix composite laminated plates reinforced by steel fibers are manufactured and analyzed by using the finite element technique. Isoparametric quadrilateral element with nine node is developed for the elasto-plastic analysis of the laminated plate. A stainless steel reinforced aluminum metal-matrix laminated, simply supported plate is loaded transversely. High material properties are obtained. Elasto-plastic stress analysis is carried out by using finite element method, and the residual stresses, together with the expansion of plastic zone are determined for small deformations.

This study is examined in some chapters. Macromechanical behavior of laminate is presented in Chapter 2. In Chapter 3, first mathametical formulation for elasto-plastic analysis, second finite element analysis and third boundary conditions, geometry and loading are presented. Experimental characterization, production of metal-matrix laminated composite are defined in Chapter 4. Numerical results are evaluated for plate without a hole and with a circular hole in Chapter 5.

CHAPTER TWO
MACROMECHANICAL BEHAVIOR OF A LAMINATE

2.1 Introduction

A laminate is two or more laminae bonded together to act as an integral structural element (Fig.2.1). The laminae principal material directions are oriented to produce a structural element capable of resisting load in several directions. The stiffness of such a composite material configuration is obtained from the properties of the constituent laminae. The procedures enable the analysis of laminates that have individual laminae with principal material directions oriented at arbitrary angles to the chosen or natural axes of the laminate. As a consequence of the arbitrary orientations, the laminate may not have definable principal directions.

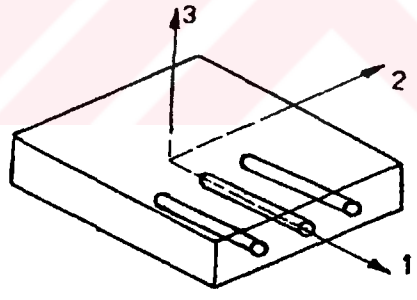

Fig.2.1 Unidirectionally reinforced laminae

2.2 Stress-Strain Relations For Plane Stress In An Orthotropic Material

For a lamina in the 1-2 plane as shown in Fig.2.1, a plane stress state is defined by setting

$$\sigma_3 = 0 \qquad \tau_{23} = 0 \; \tau_{31} = 0 \tag{2.1}$$

For orthotropic materials, such a procedure results in implied strains of

$$\varepsilon_3 = S_{13}\sigma_1 + S_{23}\sigma_2 \qquad \gamma_{23} = \gamma_{31} = 0 \tag{2.2}$$

The stress-strain relations are,

$$\begin{Bmatrix} \varepsilon_1 \\ \varepsilon_2 \\ \varepsilon_3 \end{Bmatrix} = \begin{bmatrix} S_{11} & S_{12} & 0 \\ S_{12} & S_{22} & 0 \\ 0 & 0 & S_{66} \end{bmatrix} \begin{Bmatrix} \sigma_1 \\ \sigma_2 \\ \tau_{12} \end{Bmatrix} \tag{2.3}$$

supplemented by Eq.(2.2) where

$$S_{11} = \frac{1}{E_1}, \qquad S_{22} = \frac{1}{E_2}, \qquad S_{66} = \frac{1}{G_{12}}, \qquad S_{12} = -\frac{\upsilon_{12}}{E_1} = -\frac{\upsilon_{21}}{E_2} \tag{2.4}$$

The strain-stress relations in Eq.(2.3) can be inverted to obtain the stress-strain relations:

$$\begin{Bmatrix} \sigma_1 \\ \sigma_2 \\ \tau_{12} \end{Bmatrix} = \begin{bmatrix} Q_{11} & Q_{12} & 0 \\ Q_{12} & Q_{22} & 0 \\ 0 & 0 & Q_{66} \end{bmatrix} \begin{Bmatrix} \varepsilon_1 \\ \varepsilon_2 \\ \gamma_{12} \end{Bmatrix} \tag{2.5}$$

where the Q_{ij}, the called reduced stiffnesses are

$$Q_{11} = \frac{E_1}{1-\upsilon_{12}\upsilon_{21}}, \; Q_{22} = \frac{E_2}{1-\upsilon_{12}\upsilon_{21}}, \; Q_{12} = \frac{\upsilon_{12}E_2}{1-\upsilon_{12}\upsilon_{21}} = \frac{\upsilon_{21}E_1}{1-\upsilon_{12}\upsilon_{21}}, \; Q_{66} = G_{12} \tag{2.6}$$

The processing stress-strain and strain-stress relations are basis for the stiffness and stress analysis an individual laminae subjected to forces in its own plane. The relations are therefore indispensable in the analysis of laminates.

2.3 Stress-Strain Relations For a Laminae of Arbitrary Orientation

The stress and strains were defined in the principal material directions for an orthotropic material. However the principal directions of orthotropy often do not coincide with coordinate directions that are geometrically natural to the solution of the problem. For example, consider the helically wound fiberglass-reinforced circular cylindrical shell in Fig.2.2(a). There, the coordinates natural to the solution of the shell problem are shell coordinates x, y, z whereas the principal material coordinates are x′, y′, z′. The wrap angle is defined by $Cos(y',y)=Cos\alpha$; also $z'=z$. Other examples include laminated plates with different orientations. Thus, a relation is needed between the stresses and strains in the principal material directions and those in the body coordinates. Then a method of transforming stress strain relations from one coordinate system to another is also needed. At this point, from elementary mechanics of materials, the transformation equations for expressing stresses in an *x-y* coordinate system in terms of stresses in a *1-2* coordinate system are,

$$\begin{Bmatrix}\sigma_x\\ \sigma_y\\ \tau_{xy}\end{Bmatrix}=\begin{bmatrix}m^2 & n^2 & -2mn\\ n^2 & m^2 & 2mn\\ mn & -mn & m^2-n^2\end{bmatrix}\begin{Bmatrix}\sigma_1\\ \sigma_2\\ \tau_{12}\end{Bmatrix}\text{and}\begin{Bmatrix}\varepsilon_x\\ \varepsilon_y\\ \gamma_{xy}\end{Bmatrix}=\begin{bmatrix}m^2 & n^2 & -2mn\\ n^2 & m^2 & 2mn\\ 2mn & -2mn & m^2-n^2\end{bmatrix}\begin{Bmatrix}\varepsilon_1\\ \varepsilon_2\\ \gamma_{12}\end{Bmatrix} \qquad (2.7)$$

where $m=Cos\theta$ and $n=Sin\theta$ and θ is the angle from the *x*-axis to the *1*-axis (Fig.2.2(b)). This square matrix *[T]* is transformation matrix. The stress-strain relations in *x-y* coordinates are,

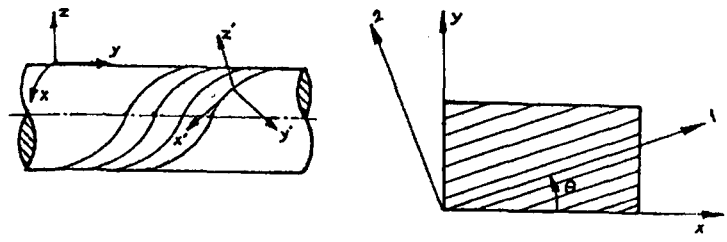

(a) (b)

Fig.2.2 a) Helically wound fiber-reinforced circular cylindrical shell **b)** Positive rotation of principal material axes from arbitrary x, y-axes

$$\begin{Bmatrix}\sigma_x\\ \sigma_y\\ \tau_{xy}\end{Bmatrix}=[\overline{Q}]\begin{Bmatrix}\varepsilon_x\\ \varepsilon_y\\ \gamma_{xy}\end{Bmatrix}=\begin{bmatrix}\overline{Q_{11}} & \overline{Q_{12}} & \overline{Q_{16}}\\ \overline{Q_{12}} & \overline{Q_{22}} & \overline{Q_{26}}\\ \overline{Q_{16}} & \overline{Q_{26}} & \overline{Q_{66}}\end{bmatrix}\begin{Bmatrix}\varepsilon_x\\ \varepsilon_y\\ \gamma_{xy}\end{Bmatrix} \tag{2.8}$$

in which,

$$\overline{Q_{11}}=Q_{11}m^4+2(Q_{12}+2Q_{66})m^2n^2+Q_{22}n^4$$

$$\overline{Q_{22}}=Q_{11}n^4+2(Q_{12}+2Q_{66})m^2n^2+Q_{22}m^4$$

$$\overline{Q_{12}}=(Q_{11}+Q_{22}-4Q_{66})m^2n^2+Q_{12}(n^4+m^4)$$

$$\overline{Q_{16}}=(Q_{11}-Q_{12}-2Q_{66})m^3n+(Q_{12}-Q_{22}+Q_{66})n^3m$$

$$\overline{Q_{26}}=(Q_{11}-Q_{12}-2Q_{66})n^3m+(Q_{12}-Q_{22}+Q_{66})m^3n$$

$$\overline{Q_{66}}=(Q_{11}+Q_{22}-2Q_{66})m^2n^2+Q_{66}(n^4+m^4)$$

Where the bar over the $\overline{Q_{ij}}$ matrix denotes that it is dealing with the transformed reduced stiffnesses instead of the reduced stiffnesses, Q_{ij}.

2.4 Stress-Strain Behavior in Laminated Composites

The stress-strain relations in principal material coordinates for a lamina of an orthotropic material under plane stress are

$$\begin{Bmatrix} \sigma_x \\ \sigma_y \\ \tau_{xy} \end{Bmatrix} = \begin{bmatrix} \overline{Q_{11}} & \overline{Q_{12}} & \overline{Q_{16}} \\ \overline{Q_{12}} & \overline{Q_{22}} & \overline{Q_{26}} \\ \overline{Q_{16}} & \overline{Q_{26}} & \overline{Q_{66}} \end{bmatrix} \begin{Bmatrix} \varepsilon_x \\ \varepsilon_y \\ \gamma_{xy} \end{Bmatrix} \tag{2.9}$$

Eqs.(2.9) can be thought of as stress-strain relations for the k^{th} layer of a multilayered laminate. Thus, Eq.(2.9) can be written as

$$\{\sigma\}_k = [\overline{Q}]_k \{\varepsilon\}_k \tag{2.10}$$

It will be proceeded in this section to define the strain and stress variations through the thickness of a laminate.

2.5. Strain and Stress Variation in a Laminate

Knowledge of the variation of stress and strain through the laminate thickness is essential to the definition of the extensional and bending stiffnesses of a laminate. The laminate is presumed to consist of perfectly bonded laminae. Moreover, the bonds are presumed to be infinitesimally thin as well as non-shear deformable. That is, the displacements are continuous across lamina boundaries so that no laminae can slip relative to another. Thus the laminate acts as a single layer with very special properties, but nevertheless acts as a single layer of material. The implications of the Kirchoff-Love hypothesis on the laminate displacements u, v and w in the x, y and z directions are derived by use of the laminate cross section in the x-z plane shown in Fig 2.3. The displacement in the x direction of point B from the undeformed to the deformed middle surface is u_0. Since line ABCD remains straight under deformation of laminate,

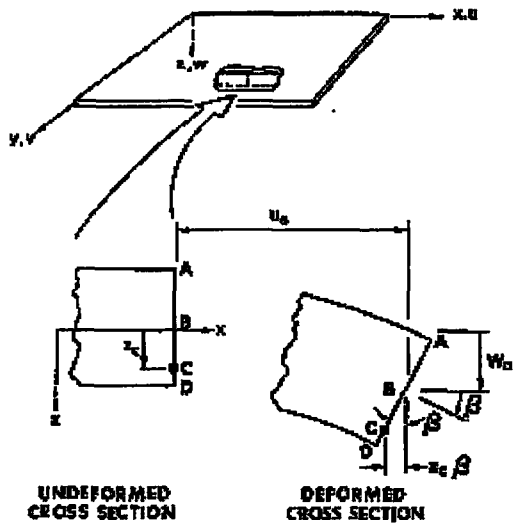

Fig. 2.3. Geometry of deformation in the x-z plane.

$u_c = u_0 - z_c\beta$

$$\beta = \frac{\partial w_o}{\partial x} \tag{2.11}$$

Then the displacement u, v at any point z through the laminate thickness is

$$u = u_o - z\frac{\partial w_o}{\partial x}$$
$$v = v_o - z\frac{\partial w_o}{\partial y} \tag{2.12}$$

Thus for the derived displacements u and v in Eq.(2.12), the strains are

$$\begin{Bmatrix} \varepsilon_x \\ \varepsilon_x \\ \gamma_{xy} \end{Bmatrix} = \begin{Bmatrix} \dfrac{\partial u_0}{\partial x} \\ \dfrac{\partial v_0}{\partial y} \\ \dfrac{\partial u_0}{\partial y} + \dfrac{\partial v_0}{\partial x} \end{Bmatrix} + z\begin{Bmatrix} \dfrac{\partial \beta_x}{\partial x} \\ -\dfrac{\partial \beta_y}{\partial y} \\ \dfrac{\partial \beta_x}{\partial y} - \dfrac{\partial \beta_y}{\partial x} \end{Bmatrix}$$

$$\begin{Bmatrix} \varepsilon_x \\ \varepsilon_x \\ \gamma_{xy} \end{Bmatrix} = \begin{Bmatrix} \varepsilon_x^0 \\ \varepsilon_y^0 \\ \gamma_{xy}^0 \end{Bmatrix} + z \begin{Bmatrix} K_x \\ K_y \\ K_{xy} \end{Bmatrix} \tag{2.13}$$

where the middle surface strains and middle surface curvature are respectively,

$$\begin{Bmatrix} \varepsilon_x^0 \\ \varepsilon_y^0 \\ \gamma_{xy}^0 \end{Bmatrix} = \begin{Bmatrix} \dfrac{\partial u_0}{\partial x} \\ \dfrac{\partial v_0}{\partial y} \\ \dfrac{\partial u_0}{\partial y} + \dfrac{\partial v_0}{\partial x} \end{Bmatrix}$$

(2.14)

$$\begin{Bmatrix} K_x \\ K_y \\ K_{xy} \end{Bmatrix} = -\begin{Bmatrix} \dfrac{\partial^2 w_0}{\partial x^2} \\ \dfrac{\partial^2 w_0}{\partial y^2} \\ \dfrac{2\partial^2 w_0}{\partial x \partial y} \end{Bmatrix}$$

Since the $\bar{Q}_{ij}$ can be different for each layer of the laminate , the stress variation through the laminate thickness is not necessarily linear, even though the strain variation is linear. Instead typical strain and stress variations are shown in Fig 2.4.

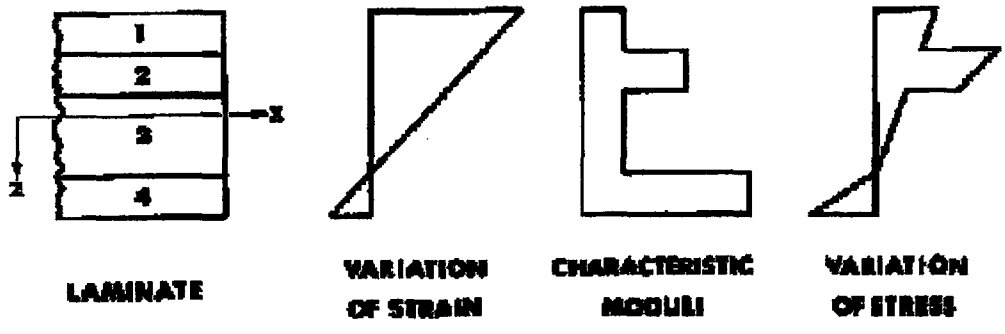

Fig. 2.4. Hypothetical variation of strain and stress through the laminate thickness.

The stresses in the k^{th} layer can be expressed in terms of the laminate middle surface strains and curvature as

$$\begin{Bmatrix}\sigma_x\\ \sigma_y\\ \tau_{xy}\end{Bmatrix}_k = \begin{bmatrix}\overline{Q_{11}} & \overline{Q_{12}} & \overline{Q_{16}}\\ \overline{Q_{12}} & \overline{Q_{22}} & \overline{Q_{26}}\\ \overline{Q_{16}} & \overline{Q_{26}} & \overline{Q_{66}}\end{bmatrix}_k \left\{\begin{Bmatrix}\varepsilon_x^0\\ \varepsilon_y^0\\ \gamma_{xy}^0\end{Bmatrix} + z\begin{Bmatrix}K_x\\ K_y\\ K_{xy}\end{Bmatrix}\right\} \tag{2.15}$$

2.6. Resultant Laminate Forces and Moments

Force and moment resultants for an N-layered laminate is defined as

$$\begin{Bmatrix}N_x\\ N_y\\ N_{xy}\end{Bmatrix} = \int_{-t/2}^{t/2}\begin{Bmatrix}\sigma_x\\ \sigma_y\\ \sigma_{xy}\end{Bmatrix}dz = \sum_{k=1}^{N}\int_{z_{k-1}}^{z_k}\begin{Bmatrix}\sigma_x\\ \sigma_y\\ \sigma_{xy}\end{Bmatrix}_k dz$$
$$\begin{Bmatrix}M_x\\ M_y\\ M_{xy}\end{Bmatrix} = \int_{-t/2}^{t/2}\begin{Bmatrix}\sigma_x\\ \sigma_y\\ \sigma_{xy}\end{Bmatrix}zdz = \sum_{k=1}^{N}\int_{z_{k-1}}^{z_k}\begin{Bmatrix}\sigma_x\\ \sigma_y\\ \sigma_{xy}\end{Bmatrix}_k zdz \tag{2.16}$$

where z_k and z_{k-1} are defined in Fig 2.5. Note that z_o=-t/2.

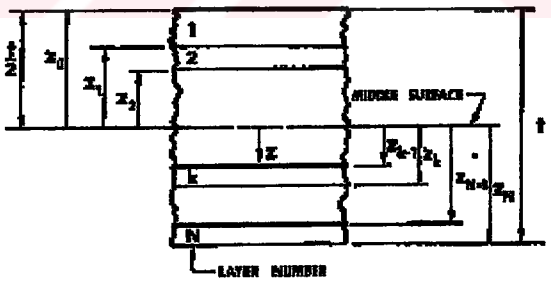

Fig. 2.5. Geometry of N-layered laminate

When the stress-strain relations Eq.2.15 are substituted

$$\begin{Bmatrix}N_x\\ N_y\\ N_{xy}\end{Bmatrix}_k = \sum_{k=1}^{N}\begin{bmatrix}\overline{Q_{11}} & \overline{Q_{12}} & \overline{Q_{16}}\\ \overline{Q_{12}} & \overline{Q_{22}} & \overline{Q_{26}}\\ \overline{Q_{16}} & \overline{Q_{26}} & \overline{Q_{66}}\end{bmatrix}_k \left\{\int_{z_{k-1}}^{z_k}\begin{Bmatrix}\varepsilon_x^0\\ \varepsilon_y^0\\ \gamma_{xy}^0\end{Bmatrix}dz + \int_{z_{k-1}}^{z_k}\begin{Bmatrix}K_x\\ K_y\\ K_{xy}\end{Bmatrix}zdz\right\}$$

$$\begin{Bmatrix} M_x \\ M_y \\ M_{xy} \end{Bmatrix}_k = \sum_{k=1}^{N} \begin{bmatrix} \overline{Q_{11}} & \overline{Q_{12}} & \overline{Q_{16}} \\ \overline{Q_{12}} & \overline{Q_{22}} & \overline{Q_{26}} \\ \overline{Q_{16}} & \overline{Q_{26}} & \overline{Q_{66}} \end{bmatrix}_k \left\{ \int_{z_{k-1}}^{z_k} \begin{Bmatrix} \varepsilon_x^0 \\ \varepsilon_y^0 \\ \gamma_{xy}^0 \end{Bmatrix} z dz + \int_{z_{k-1}}^{z_k} \begin{Bmatrix} K_x \\ K_y \\ K_{xy} \end{Bmatrix} z^2 dz \right\} \tag{2.17}$$

Eq. (2.17) can be written as

$$\begin{Bmatrix} N_x \\ N_y \\ N_{xy} \end{Bmatrix} = \begin{bmatrix} A_{11} & A_{12} & A_{16} \\ A_{12} & A_{22} & A_{26} \\ A_{16} & A_{26} & A_{66} \end{bmatrix} \begin{Bmatrix} \varepsilon_x^0 \\ \varepsilon_y^0 \\ \gamma_{xy}^0 \end{Bmatrix} + \begin{bmatrix} B_{11} & B_{12} & B_{16} \\ B_{12} & B_{22} & B_{26} \\ B_{16} & B_{26} & B_{66} \end{bmatrix} \begin{Bmatrix} K_x \\ K_y \\ K_{xy} \end{Bmatrix}$$

$$\begin{Bmatrix} M_x \\ M_y \\ M_{xy} \end{Bmatrix} = \begin{bmatrix} B_{11} & B_{12} & B_{16} \\ B_{12} & B_{22} & B_{26} \\ B_{16} & B_{26} & B_{66} \end{bmatrix} \begin{Bmatrix} \varepsilon_x^0 \\ \varepsilon_y^0 \\ \gamma_{xy}^0 \end{Bmatrix} + \begin{bmatrix} D_{11} & D_{12} & D_{16} \\ D_{12} & D_{22} & D_{26} \\ D_{16} & D_{26} & D_{66} \end{bmatrix} \begin{Bmatrix} K_x \\ K_y \\ K_{xy} \end{Bmatrix} \tag{2.18}$$

where

$$\begin{aligned} A_{ij} &= \sum_{k=1}^{N} \left(\bar{Q}_{ij} \right)_k (z_k - z_{k-1}) \\ B_{ij} &= \frac{1}{2} \sum_{k=1}^{N} \left(\bar{Q}_{ij} \right)_k (z_k^2 - z_{k-1}^2) \\ D_{ij} &= \frac{1}{3} \sum_{k=1}^{N} \left(\bar{Q}_{ij} \right)_k (z_k^3 - z_{k-1}^3) \end{aligned} \tag{2.19}$$

2.7. Special Cases Of Laminate Stiffness

2.7.1. Single Layered Configurations

The special single-layered configurations are isotropic, specially orthotropic, generally orthotropic and anisotropic.

2.7.1.1. Single isotropic layer

For a single isotropic layer with material properties E, ν and thickness t,

$$
\begin{aligned}
A_{11} &= \frac{Et}{1-\nu^2} = A & D_{11} &= \frac{Et^3}{12(1-\nu^2)} = D \\
A_{12} &= \nu A & D_{12} &= \nu D \\
A_{22} &= A & D_{22} &= D \\
A_{16} &= 0 \qquad B_{ij}=0 & D_{16} &= 0 \\
A_{26} &= 0 & D_{26} &= 0 \\
A_{66} &= \frac{Et}{2(1+\nu)} = \frac{1-\nu}{2}A & D_{66} &= \frac{Et^3}{24(1+\nu)} = \frac{1-\nu}{2}D
\end{aligned}
\qquad (2.20)
$$

whereupon the resultant forces are dependent only on their surface strains of the laminate middle surface and the resultant moments are dependent only on the curvatures of the middle surface:

$$
\begin{Bmatrix} N_x \\ N_y \\ N_{xy} \end{Bmatrix} = \begin{bmatrix} A & \nu A & 0 \\ \nu A & A & 0 \\ 0 & 0 & \frac{1-\nu}{2}A \end{bmatrix} \begin{Bmatrix} \varepsilon_x^{\,0} \\ \varepsilon_y^{\,0} \\ \gamma_{xy}^{\,0} \end{Bmatrix}
$$

$$
\begin{Bmatrix} M_x \\ M_y \\ M_{xy} \end{Bmatrix} = \begin{bmatrix} D & \nu D & 0 \\ \nu D & D & 0 \\ 0 & 0 & \frac{1-\nu}{2}D \end{bmatrix} \begin{Bmatrix} K_x \\ K_y \\ K_{xy} \end{Bmatrix} \qquad (2.21)
$$

Thus, there is no coupling between bending and extension of a single isotropic layer. Also note that

$$D = \frac{At^2}{12}$$

2.7.1.2. Single specially orthotropic layer

For a single specially orthotropic layer of thickness t, and lamina stifness Q_{ij}, the laminate stifnesses are,

$$
\begin{aligned}
A_{11} &= Q_{11}t \\
A_{12} &= Q_{12}t \\
A_{22} &= Q_{22}t \\
A_{16} &= 0 \\
A_{26} &= 0 \\
A_{66} &= Q_{66}t
\end{aligned}
\qquad B_{ij}=0 \qquad
\begin{aligned}
D_{11} &= \frac{Q_{11}t^3}{12} \\
D_{12} &= \frac{Q_{12}t^3}{12} \\
D_{22} &= \frac{Q_{22}t^3}{12} \\
D_{16} &= 0 \\
D_{26} &= 0 \\
D_{66} &= \frac{Q_{66}t^3}{12}
\end{aligned}
\qquad (2.22)
$$

$$
\begin{Bmatrix} N_x \\ N_y \\ N_{xy} \end{Bmatrix} = \begin{bmatrix} A_{11} & A_{12} & 0 \\ A_{12} & A_{22} & 0 \\ 0 & 0 & A_{66} \end{bmatrix} \begin{Bmatrix} \varepsilon_x^{\,0} \\ \varepsilon_y^{\,0} \\ \gamma_{xy}^{\,0} \end{Bmatrix}
$$

$$
\begin{Bmatrix} M_x \\ M_y \\ M_{xy} \end{Bmatrix} = \begin{bmatrix} D_{11} & D_{12} & 0 \\ D_{12} & D_{22} & 0 \\ 0 & 0 & D_{66} \end{bmatrix} \begin{Bmatrix} K_x \\ K_y \\ K_{xy} \end{Bmatrix} \qquad (2.23)
$$

2.7.1.3. Single generally orthotropic layer

For a single generally orthotropic layer of thickness t, and lamina stifness $\bar{Q}_{ij}$, the laminate stifnesses are,

$$
A_{ij} = \bar{Q}_{ij}t \qquad B_{ij} = 0 \qquad D_{ij} = \frac{\bar{Q}_{ij}t^3}{12} \qquad (2.24)
$$

Again, there is no coupling between and extension so the force and moment resultants are,

$$\begin{Bmatrix} N_x \\ N_y \\ N_{xy} \end{Bmatrix} = \begin{bmatrix} A_{11} & A_{12} & A_{16} \\ A_{12} & A_{22} & A_{26} \\ A_{16} & A_{26} & A_{66} \end{bmatrix} \begin{Bmatrix} \varepsilon_x^0 \\ \varepsilon_y^0 \\ \gamma_{xy}^0 \end{Bmatrix}$$

$$\begin{Bmatrix} M_x \\ M_y \\ M_{xy} \end{Bmatrix} = \begin{bmatrix} D_{11} & D_{12} & D_{16} \\ D_{12} & D_{22} & D_{26} \\ D_{16} & D_{26} & D_{66} \end{bmatrix} \begin{Bmatrix} K_x \\ K_y \\ K_{xy} \end{Bmatrix} \qquad (2.25)$$

Note, in contrast to both an isotropic layer and a specially ortotropic layer, that the extensional forces depend on shearing strain as well as on extensional strain. Also, the resultant shearing force N_{xy} depends on the extensional strains ε_x and ε_y as well as on the shear strain γ_{xy}^0.Smilarly the moment resultants all depend on both curvatures K_x and K_y and on the twist K_{xy}.

2.7.1.4. Single anisotropic layer

The only difference in appearance between a single generally orthotropic layer and an anisotropic layer is that the latter has lamina stiffnesses Q_{ij}, whereas the generally orthotropic layer has stiffnesses $\bar{Q}_{ij}$. The laminate stiffnesses are

$$A_{ij}=Q_{ij}t \qquad B_{ij}=0 \qquad D_{ij}=\frac{Q_{ij}t^3}{12} \qquad (2.26)$$

The force and moment resultants are given by Eq.(2.25).

2.7.2. Symmetric Laminates

For laminates that are symmetric in both geometry and material properties about the middle surface. The general stiffness,

$$A_{ij} = \sum_{k=1}^{N} \left(\bar{Q}_{ij}\right)_k (z_k - z_{k-1})$$
$$B_{ij} = \frac{1}{2} \sum_{k=1}^{N} \left(\bar{Q}_{ij}\right)_k (z_k^2 - z_{k-1}^2) \qquad (2.27)$$
$$D_{ij} = \frac{1}{3} \sum_{k=1}^{N} \left(\bar{Q}_{ij}\right)_k (z_k^3 - z_{k-1}^3)$$

In particular, because of symmetry of the $(\bar{Q}_{ij})_k$ and the thickness t_k, all the coupling stiffnesses, that is the B_{ij} can be shown to be zero. The elimination of the coupling between bending and extension has two important practical ramifications. First, such laminates are usually much easier to analyze than laminates with coupling. Second, symmetric laminates do not have a tendency to twist from the inevitable thermally induced contractions that occur during cooling following the curing process. Consequently, symmetric laminates are commonly used unless special circumstances require an unsymmetric laminate.

The force and moment resultants for a symmetric laminate are,

$$\begin{Bmatrix} N_x \\ N_y \\ N_{xy} \end{Bmatrix} = \begin{bmatrix} A_{11} & A_{12} & A_{16} \\ A_{12} & A_{22} & A_{26} \\ A_{16} & A_{26} & A_{66} \end{bmatrix} \begin{Bmatrix} \varepsilon_x^0 \\ \varepsilon_y^0 \\ \gamma_{xy}^0 \end{Bmatrix}$$

$$\begin{Bmatrix} M_x \\ M_y \\ M_{xy} \end{Bmatrix} = \begin{bmatrix} D_{11} & D_{12} & D_{16} \\ D_{12} & D_{22} & D_{26} \\ D_{16} & D_{26} & D_{66} \end{bmatrix} \begin{Bmatrix} K_x \\ K_y \\ K_{xy} \end{Bmatrix} \qquad (2.28)$$

2.7.2.1. Symmetric laminate with multiple isotropic layer

If multiple isotropic layers of various thicknesses are arranged symmetrically about a middle surface from both a geometric and a material property standpoint, the resulting laminate does not exhibit coupling between bending and extension.

The extensional and bending stiffnesses for a general case are calculated from Eq.(2.27) wherein for the k^{th} layer

$$(Q_{11})_k=(Q_{22})_k=\frac{E_k}{1-\nu_k^2} \qquad (Q_{16})_k=(Q_{26})_k=0$$

$$(Q_{12})_k=\frac{\nu_k E_k}{1-\nu_k^2} \qquad (Q_{12})_k=\frac{E_k}{2(1+\nu_k)} \tag{2.29}$$

The force and moment resultants take the form

$$\begin{Bmatrix} N_x \\ N_y \\ N_{xy} \end{Bmatrix} = \begin{bmatrix} A_{11} & A_{12} & 0 \\ A_{12} & A_{22} & 0 \\ 0 & 0 & A_{66} \end{bmatrix} \begin{Bmatrix} \varepsilon_x^{\,0} \\ \varepsilon_y^{\,0} \\ \gamma_{xy}^{\,0} \end{Bmatrix}$$

$$\begin{Bmatrix} M_x \\ M_y \\ M_{xy} \end{Bmatrix} = \begin{bmatrix} D_{11} & D_{12} & 0 \\ D_{12} & D_{22} & 0 \\ 0 & 0 & D_{66} \end{bmatrix} \begin{Bmatrix} K_x \\ K_y \\ K_{xy} \end{Bmatrix} \tag{2.30}$$

wherein, for isotropic layers $A_{11}=A_{22}$ and $D_{11}=D_{22}$ because of the condition of the Eq.(2.29). A simple example of a symmetric laminate with four isotropic layers is shown in Fig. 2.6.a.

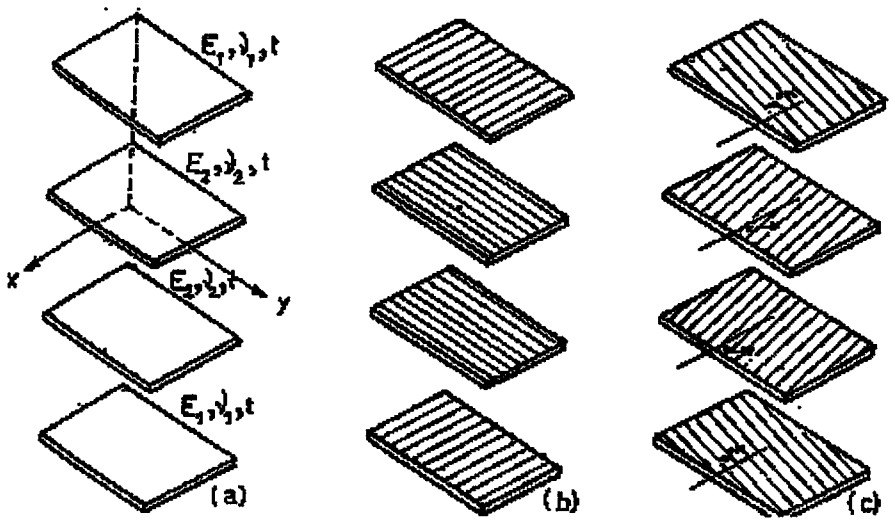

Fig 2.6. Unbounded view of a four layered **a)** symmetric laminate with isotropic layers **b)** regular symmetric cross-ply laminate **c)** regular symmetric angle-ply laminate

2.7.2.2. Symmetric laminate with multiple specially orthotropic layers

Because of the analytical complications involving the stiffnesses A_{16}, A_{26}, D_{16} and D_{26}, a laminate is desired that does not have these stiffnesses. Laminates can be made with orthotropic layers that have principal material directions aligned with the laminate axes. If the thickness, locations and material properties of the laminae are symmetric about the middle surface of the laminate, there is no coupling between bending and extension. The extensional and bending stiffnesses case are calculated from Eq.(2.27) wherein for the k^{th} layer

$$
\begin{aligned}
(\bar{Q}_{11})_k &= \frac{E_1^k}{1-\nu_{12}^k\nu_{21}^k} & (\bar{Q}_{16})_k &= (\bar{Q}_{26})_k = 0 \\
(\bar{Q}_{12})_k &= \frac{\nu_{21}^k E_1^k}{1-\nu_{12}^k\nu_{21}^k} & (\bar{Q}_{22})_k &= \frac{E_k}{(1-\nu_{12}^k\nu_{21}^k)} \\
(\bar{Q}_{66})_k &= G_{12}^k
\end{aligned}
\qquad (2.31)
$$

Because $(\bar{Q}_{16})_k$ and $(\bar{Q}_{26})_k$ are zero, the stiffnesses A_{16}, A_{26}, D_{16} and D_{26} vanish. Also the stiffnesses B_{ij} are zero because of symmetry. The force and moment resultants take the form of Eq.11. A very common special case of symmetric

laminates with multiple specially orthotropic layers occurs when the laminae are all of the same thickness and material properties, but have their major principal material directions alternating at 0^0 and 90^0 to the laminate axes, for example , $0^0/90^0/90^0/0^0$. A simple example of regular symmetric cross-ply laminate with four layers is shown in Fig. 2.6.b. Such laminates are called regular symmetric cross-ply laminates.

2.7.2.3. Symmetric laminate with multiple generally orthotropic layers

A laminate of multiple generally orthotropic layers that are symmetrically disposed about the middle surface exhibits no coupling between bending and extension; the B_{ij} are zero. Therefore the force and moment resultants are represented by Eq.(2.28). There all the A_{ij} and D_{ij} are required because of coupling between normal forces and shearing strain, shearing force and normal strains, normal moments and twist, twisting moment and normal curvatures. Such coupling is evidenced by the A_{16}, A_{26}, D_{16} and D_{26} stiffnesses. A special subclass of this class of symmetric laminates is the regular symmetric angle-ply laminate. Such laminates have orthotropic laminae of equal thicknesses. The adjacent laminae have opposite signs of the angle of orientation of the principal material properties with respect to the laminate axes, for example $30^0/-30^0/-30^0/30^0$. A simple example of regular symmetric angle-ply laminate with four layers is shown in Fig. 2.6.c.

2.7.2.4. Symmetric laminates with multiple anisotropic layer

The general case of a laminate with multiple anisotropic layers symmetrically disposed about the middle surface does not have any stiffness simplifications other than the elimination of the B_{ij} by virtue of symmetry. The A_{16}, A_{26}, D_{16} and D_{26} stiffnesses all exist and do not necessarily go to zero as the number of layers is increased.

2.7.3. Antisymmetric Laminates

Symmetry of the laminate about the middle surface is often desirable to avoid coupling between bending and extension. However, many physical applications of laminated composites, require nonsymmetric laminates to achieve design requirements. For example , coupling is necessary feature to make jet turbine fan blades with pretwist. The orientation for an antisymmetric laminate with four layers alternate from layer to layer , e.g., $30^0/-30^0/30^0/-30^0$. Therefore, symmetry about the middle surface is destroyed and the behavioral characteristics of the laminate can be substantially changed from the symmetric case. The general class of antisymmetric laminates must have an even number of layers if adjacent laminae have alternating signs of the principal material property directions with respect to the laminate axes. In addition, each pair of laminae must have the same thickness.

The coupling stiffnesses B_{ij} vary for different classes of antisymmetric laminates of generally orthotropic laminae and in fact no general representation exists other than in the following force and moment resultants

$$\begin{Bmatrix} N_x \\ N_y \\ N_{xy} \end{Bmatrix} = \begin{bmatrix} A_{11} & A_{12} & 0 \\ A_{12} & A_{22} & 0 \\ 0 & 0 & A_{66} \end{bmatrix} \begin{Bmatrix} \varepsilon_x^0 \\ \varepsilon_y^0 \\ \gamma_{xy}^0 \end{Bmatrix} + \begin{bmatrix} B_{11} & B_{12} & B_{16} \\ B_{12} & B_{22} & B_{26} \\ B_{16} & B_{26} & B_{66} \end{bmatrix} \begin{Bmatrix} K_x \\ K_y \\ K_{xy} \end{Bmatrix}$$

$$\begin{Bmatrix} M_x \\ M_y \\ M_{xy} \end{Bmatrix} = \begin{bmatrix} B_{11} & B_{12} & B_{16} \\ B_{12} & B_{22} & B_{26} \\ B_{16} & B_{26} & B_{66} \end{bmatrix} \begin{Bmatrix} \varepsilon_x^0 \\ \varepsilon_y^0 \\ \gamma_{xy}^0 \end{Bmatrix} + \begin{bmatrix} D_{11} & D_{12} & 0 \\ D_{12} & D_{22} & 0 \\ 0 & 0 & D_{66} \end{bmatrix} \begin{Bmatrix} K_x \\ K_y \\ K_{xy} \end{Bmatrix} \quad (2.32)$$

2.7.3.1. Antisymmetric cross-ply laminates

An antisymmetric cross-ply laminate consists of an even number of orthotropic laminae laid on each other with principal material directions alternating at 0^0 and 90^0 to the laminate axes. Such laminates do not have A_{16}, A_{26}, D_{16} and D_{26}, but do have coupling between bending and extension.

The force and moment resultants are

$$\begin{Bmatrix} N_x \\ N_y \\ N_{xy} \end{Bmatrix} = \begin{bmatrix} A_{11} & A_{12} & 0 \\ A_{12} & A_{22} & 0 \\ 0 & 0 & A_{66} \end{bmatrix} \begin{Bmatrix} \varepsilon_x^0 \\ \varepsilon_y^0 \\ \gamma_{xy}^0 \end{Bmatrix} + \begin{bmatrix} B_{11} & 0 & 0 \\ 0 & -B_{11} & 0 \\ 0 & 0 & 0 \end{bmatrix} \begin{Bmatrix} K_x \\ K_y \\ K_{xy} \end{Bmatrix}$$

$$\begin{Bmatrix} M_x \\ M_y \\ M_{xy} \end{Bmatrix} = \begin{bmatrix} B_{11} & 0 & 0 \\ 0 & -B_{11} & 0 \\ 0 & 0 & 0 \end{bmatrix} \begin{Bmatrix} \varepsilon_x^0 \\ \varepsilon_y^0 \\ \gamma_{xy}^0 \end{Bmatrix} + \begin{bmatrix} D_{11} & D_{12} & 0 \\ D_{12} & D_{22} & 0 \\ 0 & 0 & D_{66} \end{bmatrix} \begin{Bmatrix} K_x \\ K_y \\ K_{xy} \end{Bmatrix} \quad (2.33)$$

A regular antisymmetric cross-ply laminate is defined to have laminae all of equal thickness and is common because of simplicity of fabrication. As the number of layers increases the coupling stiffness B_{11} can be shown to approach zero. A simple example of regular antisymmetric cross-ply laminate with four layers is shown in Fig. 2.7.a.

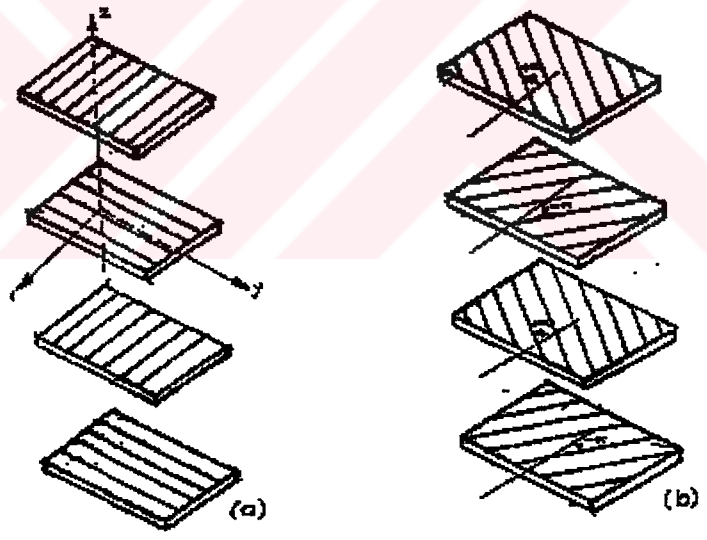

Fig. 2.7. Unbounded view of a four layered regular antisymmetric
a) cross-ply **b)** angle-ply laminate

2.7.3.2. Antisymmetric angle-ply laminates

An antisymmetric angle-ply laminate has laminae oriented at $+\alpha$ degrees to the laminate coordinate axes on one side of the middle surface and corresponding equal thickness laminae oriented at $-\alpha$ degrees on the other side. A regular antisymmetric angle-ply laminate has laminae all of the same thickness. A simple example of regular antisymmetric cross-ply laminate with four layers is shown in Fig. 2.7.b.

The force and moment resultants for an antisymmetric angle-ply laminate are

$$\begin{Bmatrix} N_x \\ N_y \\ N_{xy} \end{Bmatrix} = \begin{bmatrix} A_{11} & A_{12} & 0 \\ A_{12} & A_{22} & 0 \\ 0 & 0 & A_{66} \end{bmatrix} \begin{Bmatrix} \varepsilon_x^0 \\ \varepsilon_y^0 \\ \gamma_{xy}^0 \end{Bmatrix} + \begin{bmatrix} 0 & 0 & B_{16} \\ 0 & 0 & B_{26} \\ B_{16} & B_{26} & 0 \end{bmatrix} \begin{Bmatrix} K_x \\ K_y \\ K_{xy} \end{Bmatrix}$$

$$\begin{Bmatrix} M_x \\ M_y \\ M_{xy} \end{Bmatrix} = \begin{bmatrix} 0 & 0 & B_{16} \\ 0 & 0 & B_{26} \\ B_{16} & B_{26} & 0 \end{bmatrix} \begin{Bmatrix} \varepsilon_x^0 \\ \varepsilon_y^0 \\ \gamma_{xy}^0 \end{Bmatrix} + \begin{bmatrix} D_{11} & D_{12} & 0 \\ D_{12} & D_{22} & 0 \\ 0 & 0 & D_{66} \end{bmatrix} \begin{Bmatrix} K_x \\ K_y \\ K_{xy} \end{Bmatrix} \quad (2.34)$$

the coupling stiffnesses B_{16} and B_{26} can be shown to go to zero as the number of layers in the laminate increases for a fixed laminate thickness.

CHAPTER THREE

ELASTO-PLASTIC STRESS ANALYSIS OF TRANSVERSELY LOADED LAMINATED PLATE

3.1. Mathematical Formulation

The plate elements formulation based on the theory of plates with transverse shear deformations included. This theory uses the assumption that "particles of the plate originally on a line during deformation, but this line is not necessarily normal to the deformed middle surface". With this assumption, the displacement components of a point of coordinates *x, y, z* are in the small displacement bending theory:

$$\begin{aligned} u(x,y,z) &= u_0(x,y) + z\beta_x(x,y); \\ v(x,y,z) &= v_0(x,y) - z\beta_y(x,y) \\ w(x,y,z) &= w(x,y) \end{aligned} \tag{3.1}$$

where u_0, v_0, and w are the displacements at any point of the middle surface, and β_x, β_y are the rotations of the normal to the undeformed middle surface in the *x-z* and *y-z* planes, respectively, see Fig.3.1. It is instructive to note that in the kirchhoff plate theory excluding shear deformations, $\beta_x = -w_{,x}$ and $\beta_y = w_{,y}$.

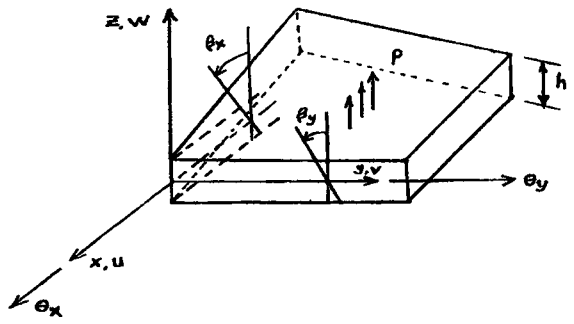

Fig.3.1 Deformation assumptions in analysis of plate including shear deformations

The bending strains vary linearly through the plate thickness, whereas shear strains are assumed to constant through the thickness as,

$$\begin{Bmatrix} \varepsilon_x \\ \varepsilon_x \\ \gamma_{xy} \end{Bmatrix} = \begin{Bmatrix} \varepsilon_x^0 \\ \varepsilon_y^0 \\ \gamma_{xy}^0 \end{Bmatrix} + z \begin{Bmatrix} K_x \\ K_y \\ K_{xy} \end{Bmatrix} \tag{3.2}$$

where the middle surface strains and middle surface curvature are respectively,

$$\begin{Bmatrix} \varepsilon_x^0 \\ \varepsilon_y^0 \\ \gamma_{xy}^0 \end{Bmatrix} = \begin{Bmatrix} \dfrac{\partial u_0}{\partial x} \\ \dfrac{\partial v_0}{\partial y} \\ \dfrac{\partial u_0}{\partial y} + \dfrac{\partial v_0}{\partial x} \end{Bmatrix}$$

$$\begin{Bmatrix} K_x \\ K_y \\ K_{xy} \end{Bmatrix} = \begin{Bmatrix} \dfrac{\partial \beta_x}{\partial x} \\ -\dfrac{\partial \beta_y}{\partial y} \\ \dfrac{\partial \beta_x}{\partial y} - \dfrac{\partial \beta_y}{\partial x} \end{Bmatrix} = -\begin{Bmatrix} \dfrac{\partial^2 w_0}{\partial x^2} \\ \dfrac{\partial^2 w_0}{\partial y^2} \\ \dfrac{2\partial^2 w_0}{\partial x \partial y} \end{Bmatrix} \tag{3.3}$$

whereas the transverse shear strains are assumed to be constant through the thickness

$$\begin{Bmatrix}\gamma_{yz}\\ \gamma_{xz}\end{Bmatrix}=\begin{Bmatrix}\dfrac{\partial w}{\partial y}-\beta_y\\ \dfrac{\partial w}{\partial x}+\beta_x\end{Bmatrix} \tag{3.4}$$

and stresses

$$\begin{Bmatrix}\sigma_x\\ \sigma_y\\ \tau_{xy}\end{Bmatrix}=\begin{bmatrix}\overline{Q_{11}} & \overline{Q_{22}} & \overline{Q_{16}}\\ \overline{Q_{12}} & \overline{Q_{22}} & \overline{Q_{26}}\\ \overline{Q_{16}} & \overline{Q_{26}} & \overline{Q_{66}}\end{bmatrix}\left\{\begin{Bmatrix}\varepsilon_x^0\\ \varepsilon_y^0\\ \gamma_{xy}^0\end{Bmatrix}+z\begin{Bmatrix}K_x\\ K_y\\ K_{xy}\end{Bmatrix}\right\} \tag{3.5}$$

$$\begin{Bmatrix}\tau_{yz}\\ \tau_{xz}\end{Bmatrix}=\begin{bmatrix}Q_{44} & Q_{45}\\ Q_{45} & Q_{55}\end{bmatrix}\begin{Bmatrix}\gamma_{yz}\\ \gamma_{xz}\end{Bmatrix}$$

The total potential energy of a laminated plate under static loading is given as

$$\Pi = U_b + U_s + V \tag{3.6}$$

where U_b is the strain energy of bending, U_s is the strain energy of shear and V represents potential energy of external forces. They are as,

$$U_b = \frac{1}{2}\int_{-\frac{h}{2}}^{\frac{h}{2}}\left[\int_A\left(\sigma_x\varepsilon_x+\sigma_y\varepsilon_y+\tau_{xy}\gamma_{xy}\right)dA\right]dz$$

$$U_s = \frac{1}{2}\int_{-\frac{h}{2}}^{\frac{h}{2}}\left[\int_A\left(\tau_{xz}\gamma_{xz}+\tau_{yz}\gamma_{yz}\right)dA\right]dz \tag{3.7}$$

$$V = -\int_A wp\,dA - \int_{\partial R}\left(\overline{N}_n^b u_n^0 + \overline{N}_s^b u_s^0\right)ds$$

where $dA=dx.dy$, p is the transverse loading Per unit area, and $\overline{N_n^b}$ and $\overline{N_s^b}$ are the inplane loads applied to the boundary ∂R .

In plane forces N_x, N_y and N_{xy} and moments M_x, M_y, and M_{xy} defined Per unit length are given as,

$$\begin{bmatrix} N_x & M_x \\ N_y & M_y \\ N_{xy} & M_{xy} \end{bmatrix} = \int_{-\frac{h}{2}}^{\frac{h}{2}} \begin{bmatrix} \sigma_x \\ \sigma_y \\ \tau_{xy} \end{bmatrix} (1,z)dz \tag{3.8}$$

$$\begin{Bmatrix} Q_x \\ Q_y \end{Bmatrix} = \int_{-\frac{h}{2}}^{\frac{h}{2}} \begin{bmatrix} \tau_{xz} \\ \tau_{yz} \end{bmatrix} dz$$

Equilibrium requires that Π is stationary or Π is a minimum, that is the second variation of Π is positive at the stationary point. It may be regarded as the principal of virtual displacements. By using the finite element method, the total potential energy is expressed as a function of displacement components as,

$$\Pi = \Pi\left(u_0, v_0, w, \beta_x, \beta_y\right) \tag{3.9}$$

3.2. Finite Element Analysis

3.2.1. Finite Element Approach For Elasto-Plastic Stress Analysis

The symmetric or antisymmetric laminated plate is composed of four or two layers. A typical finite element for a symmetric and an antisymmetric lamination is divided into 8 imaginary layers for obtaining the finite element results more accurately.

The nine node finite element is used in this study (Fig. 3.2). The quadratic interpolation functions for the nine-node Lagrangian finite element are given as:

$$N_1(r,s) = \frac{1}{4}(1-r)(1-s)rs$$

$$N_2(r,s) = -\frac{1}{2}(1-r^2)(1-s)s$$

$$N_3(r,s) = -\frac{1}{4}(1+r)(1-s)rs$$

$$N_4(r,s) = \frac{1}{2}(1+r)(1-s^2)r$$

$$N_5(r,s) = \frac{1}{4}(1+r)(1+s)rs$$

$$N_6(r,s) = \frac{1}{2}(1-r^2)(1+s)s$$

$$N_7(r,s) = -\frac{1}{4}(1-r)(1+s)rs \qquad (3.10)$$

$$N_8(r,s) = -\frac{1}{2}(1-r)(1-s^2)r$$

$$N_9(r,s) = (1-r^2)(1-s^2)$$

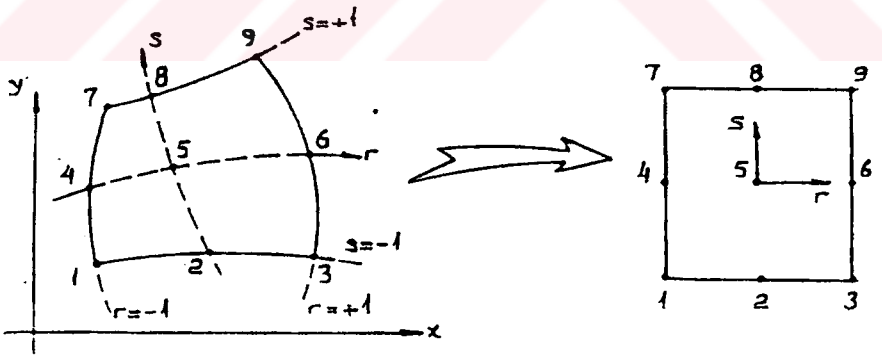

Fig. 3.2. Nine node Lagrangian finite element

The displacement field can be expressed in the following matrix form as,

$$[d]=\begin{bmatrix} u_0 \\ v_0 \\ w \\ \beta_x \\ \beta_y \end{bmatrix}=\sum_{i=1}^{n}\begin{bmatrix} N_i & 0 & 0 & 0 & 0 \\ 0 & N_i & 0 & 0 & 0 \\ 0 & 0 & N_i & 0 & 0 \\ 0 & 0 & 0 & N_i & 0 \\ 0 & 0 & 0 & 0 & N_i \end{bmatrix}\begin{bmatrix} u_0 \\ v_0 \\ w \\ \beta_x \\ \beta_y \end{bmatrix}_i \tag{3.11}$$

in which n is the total number of nodes and N_i is the shape function at node i.

The relationship between strains and displacements can be written in the matrix form as,

$$\begin{Bmatrix} \varepsilon_x^0 \\ \varepsilon_y^0 \\ \gamma_{xy}^0 \\ K_x \\ K_y \\ K_{xy} \end{Bmatrix}_i=\begin{bmatrix} N_{i,x} & 0 & 0 & 0 & 0 \\ 0 & N_{i,y} & 0 & 0 & 0 \\ N_{i,y} & N_{i,x} & 0 & 0 & 0 \\ 0 & 0 & 0 & N_{i,x} & 0 \\ 0 & 0 & 0 & 0 & -N_{i,y} \\ 0 & 0 & 0 & N_{i,y} & -N_{i,x} \end{bmatrix}_i\begin{Bmatrix} u_0 \\ v_0 \\ w \\ \beta_x \\ \beta_y \end{Bmatrix}_i \tag{3.12}$$

or symbolically as,

$$\{\varepsilon_{bi}\}=[B_{bi}]\{u_i\} \tag{3.13}$$

in which i is the node number, and commas represent the partial derivation.

The relationship between the transverse shear strains and displacement components can be written as,

$$\begin{Bmatrix} \gamma_{yz} \\ \gamma_{xz} \end{Bmatrix}_i=\begin{bmatrix} 0 & 0 & N_{i,y} & 0 & -N_i \\ 0 & 0 & N_{i,x} & N_i & 0 \end{bmatrix}_i\begin{Bmatrix} u_0 \\ v_0 \\ w \\ \beta_x \\ \beta_y \end{Bmatrix}_i \tag{3.14}$$

or symbolically as,

$$\{\varepsilon_{si}\}=[B_{si}]\{u_i\} \tag{3.15}$$

The stiffness matrix of the plate element is obtained by using the minimum potential energy method or the principle of virtual displacements. Bending and shear stiffness matrices are,

$$[K_b]=\int_A [B_b]^T [D_b][B_b]dA \tag{3.16}$$

$$[K_s]=\int_A [B_s]^T [D_s][B_s]dA$$

where,

$$[D_b]=\begin{bmatrix} A_{ij} & B_{ij} \\ B_{ij} & D_{ij} \end{bmatrix}$$

$$[D_s]=\begin{bmatrix} k_1^2 A_{44} & 0 \\ 0 & k_2^2 A_{55} \end{bmatrix} \tag{3.17}$$

$$(A_{ij}, B_{ij}, D_{ij})=\int_{-\frac{h}{2}}^{\frac{h}{2}} Q_{ij}(1, z, z^2)dz \qquad (i,j=1,2,6)$$

$$(A_{44}, A_{55})=\int_{-\frac{h}{2}}^{\frac{h}{2}} (Q_{44}, Q_{55})dz$$

$|B_b|_{6x45}, |B_s|_{2x45}$ and D_b and D_s are the bending and shear parts of the material matrix, respectively; A_{45} is neglected in comparison with A_{44}, A_{55} and shear correction factors for rectangular cross-sections are given as, $k_1^2 = k_2^2 = 5/6$. [Lin, 1989].

In the elasto-plastic solution the tangential modular matrix is used instead of the elasticity matrix [Crisfield, 1991]. The yield function f is as,

$$f = \sigma_e - \sigma_o = 0 \tag{3.18}$$

where σ_e is the effective stress and σ_o is the yield stress. The tangential modular matrix is found as ,

$$C_t = C\,(I - aa^T C / a^T C a) \tag{3.19}$$

where C, I and a are the elasticity matrix, unit matrix and flow vector, respectively.

The flow vector a is found by using the Prandtl- Reuss equations as,

$$a = \partial f / \partial \sigma \tag{3.20}$$

Once the nodal displacements are calculated, the strain components of each layer can be found by using Eqn.(3.13) and (3.15). And the stress components can be calculated and used to check the yield state of the material.

Since the calculated stresses do not generally coincide with the true stresses in a non-linear problem, the unbalanced nodal forces and the equivalent nodal forces must be calculated. The equivalent nodal point forces corresponding to the element stresses at each iteration can be calculated as:

$$\{R\}_{\text{equivalent}} = \int_{vol} [B]^T [\sigma] \; dA = \int_{vol} [B_b]^T [\sigma_b] \; dA + \int_{vol} [B_s]^T [\sigma_s] \; dA \tag{3.21}$$

When the equivalent nodal forces are known, the unbalanced nodal forces can be found by

$$\{R\}_{\text{unbalanced}} = \{R\}_{\text{applied}} - \{R\}_{\text{equivalent}} \tag{3.22}$$

These unbalanced nodal forces are applied for obtaining increments in the solution and must satisfy the convergence tolerance in a non-linear analysis. A widely used iteration procedure is the modified Newton iteration method as [Bathe, 1982]. This iterative scheme can be derived from the Newton- Raphson method equations. The method is quite effective in many analysis and contains the basic solution steps used in practically all incremental solution strategies. But various other procedures are effective in only some individual problems.

The equations used in the modified Newton iteration are, for the number of i=1,2,3,...,

$$ {}^{t}K\Delta U^{(i)} = \{R\}_{unbalanced} = {}^{t+\Delta t}\{R\}_{applied} - {}^{t+\Delta t}\{R\}_{equivalent}^{(i-1)} \qquad (3.23) $$

$$ {}^{t+\Delta t}U^{(i)} = {}^{t+\Delta t}U^{(i-1)} + \Delta U^{(i)} $$

with the initial condition

$$ {}^{t+\Delta t}U^{(0)} = {}^{t}U, \qquad {}^{t+\Delta t}F^{(0)} = {}^{t}F \qquad (3.24) $$

where t, Δt, U and K are time, time interval, overall displacement vector and stiffness matrix, respectively.

The difference between the plastic and elastic solution gives the residual stresses. The residual stresses may increase the possibility failure of the laminated plates.

3.2.2. Numerical Integration

An important aspect of isoparametric and related finite element analysis is required numerical integration. The required matrix integral in two dimensional finite element analysis is practice evaluated numerically using

$$\int F(r,s)drds = \sum_{i,j} \alpha_{ij} F(r_i, s_i) + R_n \tag{3.25}$$

where the summations extend over all i and j specified, the α_{ij} is weighting factor. $F(r_i, s_i)$is the matrices F(r, s) evaluated at the points specified in the arguments. R_n is error matrix, in practice is not evaluated. Thus Eq. (3.25) becomes

$$\int F(r,s)drds = \sum_{i,j} \alpha_{ij} F(r_i, s_i) \tag{3.26}$$

An important point is the integration accuracy that is needed the number of integration points required in the element formation. In finite element analysis, the integration of matrix means that each element of the matrix considered is integrated individually. Hence, for the derivation of the numerical integration formulas considered a typical element of a matrix F.

Two dimensional integrals need be evaluated in two dimensional finite element analysis. A two dimensional integral is below

$$\begin{aligned} \int_{-1}^{+1}\int_{-1}^{+1} F(r,s)drds &= \sum_i \alpha_i \int_{-1}^{+1} F(r_i, s)ds \\ \int_{-1}^{+1}\int_{-1}^{+1} F(r,s)drds &= \sum_i \alpha_i \alpha_j F(r_i, s_j) \end{aligned} \tag{3.27}$$

where $\alpha_i\alpha_j=\alpha_{ij}$ and α_i, α_j are the integration weights.

The above procedure is directly applicable to the evaluation of matrices of rectangular elements in which all integration limits are –1 to +1. Hence in the evaluation of a two dimensional finite element, the integration can be carried out for each entry of the bending, shear and geometric stiffness matrices and load vectors. Some common Gauss quadrate rules for two dimensional analysis are given in Table 3.1. and the locations of integration points are presented in Fig. 3.3.

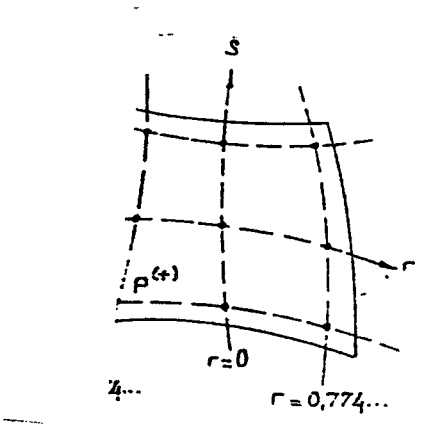

Fig. 3.3. Presentation of Gauss integration points

Table 3.1. Sampling points and weights in Gauss-Legendre numerical integration

Number of points, n	Location, r_i	Weights, w_i
1	0.0	2.0
2	±0.577350269189626	1.0
3	±0.774596669241483 0.0	0.55555555555556 0.88888888888889
4	±0.861136311594053 ±0.339981043584856	0.347854845137454 0.642145154862546
5	±0.906179845938664 ±0.538469310105683 0.0	0.236926885056189 0.478628670499362 0.568888888888889
6	±0.932469514203152 ±0.661209386466265 ±0.238619186083197	0.107324492379170 0.360761573048139 0.467913934572691

3.3. Mesh, Geometry and Boundary Conditions

3.3.1. Geometry of The Plate

In this study, a stainless steel fiber reinforced aluminum metal matrix laminated is loaded transversely. The laminated plate is assumed simple supported plate. The plate is assumed of geometric shape without hole and with circular hole. The dimension of the plate are 300*300 mm. The laminated plates are bonded symmetrically and antisymmetrically about the middle surface of plate. Detailed information symmetrically and antisymmetrically laminated plates is given in Chapter two. Cartesian coordinates (x, y, z) are used for the plate coordinates where x-y plane coincides wiht the middle surface of the plate and z denotes the transverse axes, as shown in Fig 3.4.

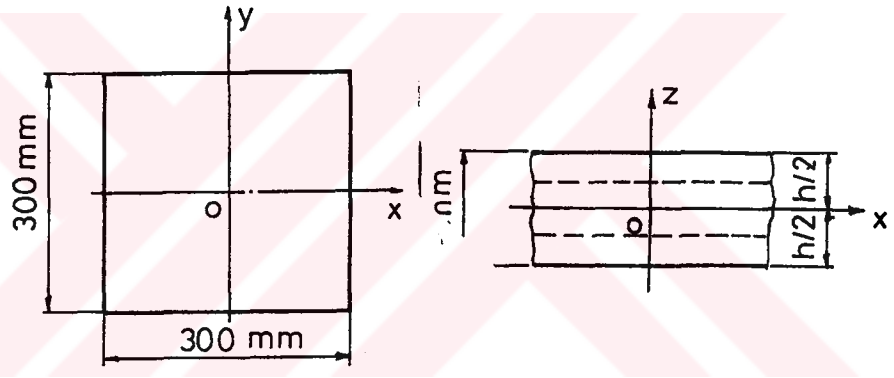

Fig 3.4. Geometry and coordinates

3.3.2. Mesh Generation and Boundary Conditions

Fist, the plates without a hole are divided 36 elements and 169 nodes, as shown in Fig 3.5. The boundary conditions are given in Fig 3.5.

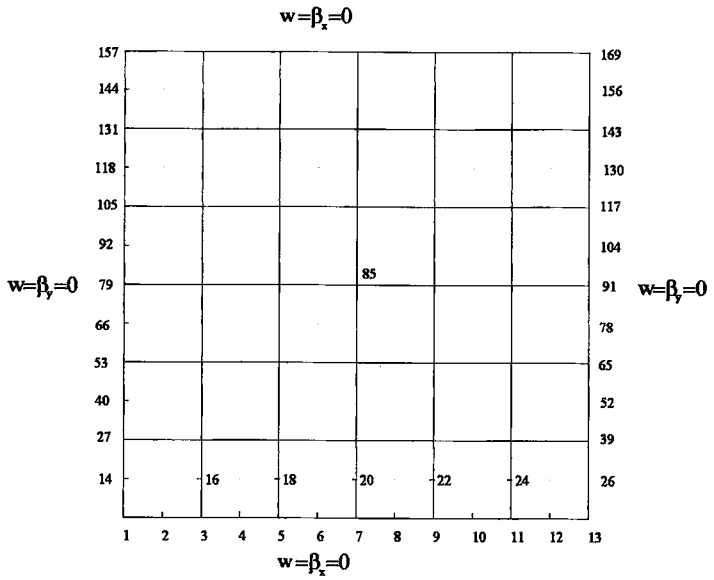

Fig 3.5. Mesh and boundary conditions for plate without a hole

Second, the plates with a circular hole are divided 32 elements and 144 nodes, as shown in Fig 3.6. The boundary conditions are given in Fig 3.6.

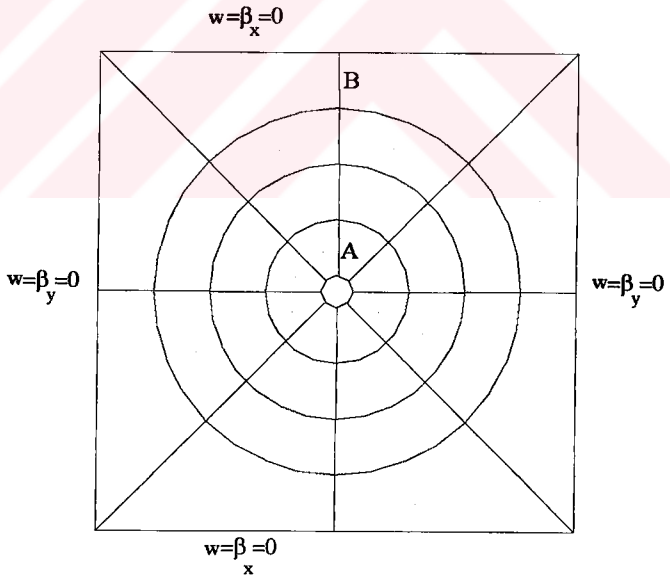

Fig 3.6. Mesh and boundary conditions for plate with a circular hole

CHAPTER FOUR
PRODUCTION OF LAMINATE

4.1.Specimen Preparation and Testing Procedure

For orthotropic material properties in tension, certain basic experiments can be performed to obtain the properties in the principal material directions. The experiments, if conducted properly, generally reveal both the strength and stiffness characteristics of the material. These stiffness characteristics are,

E_1=Young's modulus in the 1-direction.

E_2=Young's modulus in the 2-direction.

$\upsilon_{12} = -\frac{\varepsilon_2}{\varepsilon_1}$ for $\sigma_1=\sigma$ and all other stresses are zero

$\upsilon_{21} = -\frac{\varepsilon_1}{\varepsilon_2}$ for $\sigma_2=\sigma$ and all other stresses are zero

G_{12}= Shear modulus in the 1-2 plane

where only three of E_1, E_2, υ_{12}, υ_{21} are independent and the strength characteristics are,

X=Axial or longitudinal strength (1-direction)

Y =Transverse strength (2-direction)

S =Shear strength (1-2 plane)

In addition, the other required characteristics are,

k =Plasticity constant

n =Strain-hardening exponent (or slope of the curve)

The specimens were prepared to find required (above) characteristics. Four types of specimens are enough to find these values. From every mold we took out at least four specimens. The specimens were cut off and processed carefully to achieved the experiments.

First, consider a uniaxial tension test in the 1-direction on a flat piece of unidirectionally reinforced lamina as shown in Fig.4.1.

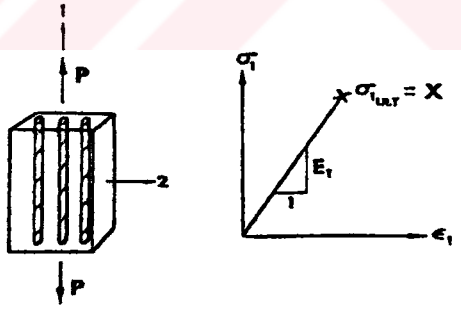

Fig.4.1. Uniaxial loading in the 1-direction.

The strains ε_1 and ε_2 were measured in the test where upon, by definition,

$\sigma_1 = P/A$

$$E_1=\sigma_1/\varepsilon_1$$

$$\upsilon_{12} = -\frac{\varepsilon_2}{\varepsilon_1} \tag{4.1}$$

$$X=P_{ult}/A$$

where A is the cross-sectional area of the specimen and perpendicular to the applied load.

Second, consider a uniaxial tension test in the 2-direction on a flat piece of unidirectionally reinforced lamina as in Fig.4.2.

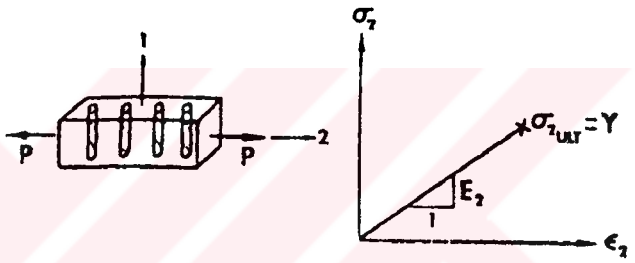

Fig.4.2. Uniaxial loading in the 2-direction

As in the first experiment, ε_1 and ε_2 were measured so,

$$\sigma_2=P/A$$

$$E_2=\sigma_2/\varepsilon_2$$

$$\upsilon_{21} = -\frac{\varepsilon_1}{\varepsilon_2} \tag{4.2}$$

$$Y=P_{ult}/A$$

where again A is the cross-sectional area of the specimen.

At this point, the stiffness properties should satisfy the reciprocal relations.

$$\frac{\upsilon_{12}}{E_1} = \frac{\upsilon_{21}}{E_2} \tag{4.3}$$

Third consider a uniaxial tension test at 45^0 to the 1-direction on a flat place of lamina as shown in Fig.4.3. By measurement of ε_x alone, obviously

$$E_x = \frac{P/A}{\varepsilon_x} \tag{4.4}$$

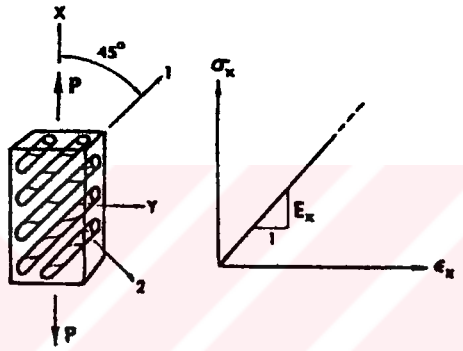

Fig.4.3. Uniaxial loading at 45^0 to the 1-direction .

Then by use of the transformation relations in following equation,

$$\frac{1}{E_x} = \frac{1}{4}\left(\frac{1}{E_1} - \frac{2\upsilon_{12}}{E_1} + \frac{1}{G_{12}} + \frac{1}{E_2}\right) \tag{4.5}$$

wherein G_{12} is the only unknown, thus,

$$G_{12} = \frac{1}{\left(\frac{4}{E_x} - \frac{1}{E_1} - \frac{1}{E_2} + \frac{2\upsilon_{12}}{E_1}\right)} \tag{4.6}$$

This experiment can not be related upon to determines, the ultimate shear stress since a pure shear deformation mode has not been excited with accompanying failure in shear. Accordingly, the following approach to obtaining S must be used.

The last, to find shear stress T specimens were prepared as shown in Fig.4.4.

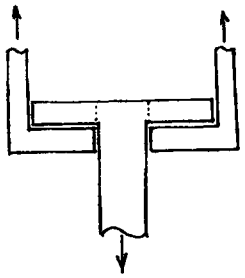

Fig.4.4. Uniaxial loading to the 1-direction.

To achieve the experiment cross-section of the specimen prepared closely to square otherwise during the loading operation the specimen may be twisted. By defining P_{ult}, we found S from the following equation.

$$S = \tau = \frac{P_{ult}}{2A} \tag{4.7}$$

The other characteristics (k, n) can be found from above designs.

4.2.Experimental Results

In the composite material, the ratio of the volume the steel fiber V_f and of the aluminum matrix V_m are 0.15 and 0.85 respectively. The densities fiber and matrix are ρ_f=7850 kg/m^3 and ρ_m=2560 kg/m^3 respectively. The density of the composite is obtained from

$$\rho_c = V_f\rho_f + V_m\rho_m \quad (4.8)$$

as ρ_c=3300 kg/m^3

4.3 Production Of Laminated Plates

The composite layer consists of stainless steel fiber and aluminum matrix. The production has been realized by using moulds which consist of upper and lower parts. Electrical resistance has been used heat the moulds and material which are insulated, as illustrated in Figure 4.5.

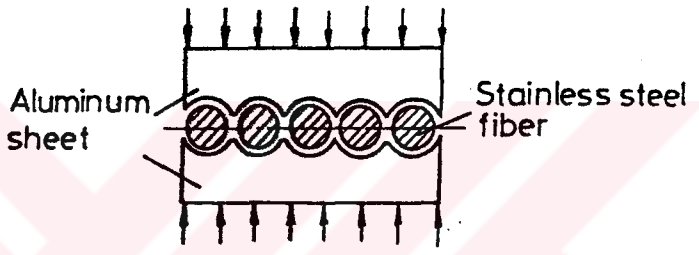

Fig. 4.5. Production of composite layer

The hydraulic press has been used to obtain a pressure of 30 MPa to the upper mould. Manufacturing set has been heated 600 ^{0}C. In these conditions, the yield strength of aluminum is exceed and good bonding between matrix and fiber has been realized. The mechanical properties, yield points and plastic parameters are given in Table 4.1. Mechanical properties of a layer were found by using strain gages. The laminated plate was manufactured by using four and two layers symmetrically or antisymmetrically.

The stress-strain relation in plastic region is given by Ludwik equation as,

$$\sigma = \sigma_0 + k\varepsilon_P^{\,n} \quad (4.9)$$

Table 4.1. Mechanical properties and yield points of a layer

Mechanical properties

E_1	86 GPa
E_2	74 GPa
G_{12}	32 GPa
ν_{12}	0.30

Yield strengths and parameters

Axial Strength	X	228.3 MPa
Transverse Strength	Y	24.2 MPa
Shear Strength	S	47.6 MPa
Hardening Parameter	k	1254 MPa
Strain Hardening Parameter	n	0.7

In the plastic solution Tsai-Hill criterion was used as a yield criterion. It is assumed that the yield point in the Z direction is equal to Y, the yield points of τ_{xz}, τ_{yz} are equal to S.

$$\left(\frac{\sigma_1}{X}\right)^2-\left(\frac{\sigma_1\sigma_2}{X}\right)^2+\left(\frac{\sigma_2}{Y}\right)^2+\left(\frac{\tau_{12}}{S}\right)^2+\left(\frac{\tau_{23}}{S}\right)^2+\left(\frac{\tau_{13}}{S}\right)^2=1 \tag{4.10}$$

$$\bar{\sigma}_e^{\,2}=\sigma_1^2-\sigma_1\sigma_2+\left(\frac{\sigma_2 X}{Y}\right)^2+\left(\frac{\tau_{12}X}{S}\right)^2+\left(\frac{\tau_{23}X}{S}\right)^2+\left(\frac{\tau_{13}X}{S}\right)^2=X^2$$

CHAPTER FIVE
NUMERICAL RESULTS AND DISCUSSIONS

5. NUMERICAL RESULTS AND DISCUSSIONS

In this study, aluminum metal matrix composite laminated plates reinforced by steel fibers are manufactured and analyzed by using the finite element technique. A stainless steel reinforced aluminum metal-matrix laminated, simply supported plate is loaded transversely. High material properties are obtained. The laminated plate is assumed to be under uniform forces on the upper surface. They are composed of four or two orthotropic or generally orthotropic layers bonded symmetrically or antisymmetrically. Elasto-plastic stress analysis is carried out by using finite element method, and the residual stresses, together with the expansion of plastic zone are determined for small deformations. The difference between the elasto-plastic and elastic solutions gives residual stresses. The load is increased from the yield point for transversely loaded composite laminated plate to 100, 150 and 200 iterations for plates without a hole, incrementally. The load also is increased 200, 400 and 600 iterations for plates with a circular hole, incrementally. The external force is increased 0.0001 Mpa at each step.

5.1. Transversely Loaded Plate Without a Hole

5.1.1. Symmetric or Antisymmetric Laminated Plates of Four Layers

Symmetric or antisymmetric laminated plates of four layers are bonded in the symmetric and antisymmetric form as cross-ply laminated plate $[(0^0/90^0)_2]$ and angle-ply

laminated plates $[(30^0/-30^0)_2]$, $[(45^0/-45^0)_2]$, $[(60^0/-60^0)_2]$. $[(0^0/90^0)_2]$ is the abbreviation of $0^0/90^0/90^0/0^0$ for symmetric and $0^0/90^0/0^0/90^0$ for antisymmetric laminated plates of four layers. The transverse uniform load at the yield points of the symmetric and antisymmetric laminated plates are given in Table 5.1. It shows that the transverse uniform load for the symmetrically laminated plates at the yield point points are higher than those for the antisymmetric ones.

Table 5.1. The uniform transverse force at the yield points of the four laminated plates. (S: Symmetric laminate, A: Antisymmetric laminate.)

	$[(0^0/90^0)_2]$	$[(30^0/-30^0)_2]$	$[(45^0/-45^0)_2]$	$[(60^0/-60^0)_2]$
S (MPa)	0.0726	0.0726	0.0727	0.0726
A (MPa)	0.0715	0.0724	0.0723	0.0724

The expansion of the plastic zone for symmetric cross-ply $[(0^0/90^0)_2]$ laminated plate is shown in Figure 5.1. The expansion of plastic zone is the same at the upper and lower surfaces in the symmetric laminated plates. Therefore it is given only at the upper surface. Stress components at the upper and lower surfaces in the symmetric laminated plates are the same in absolutely. Elasto-plastic, elastic and residual stresses at the mid-point of upper surface of the cross-ply laminated plate (node number is 85) for 100, 150, 200 iterations are given in Table 5.2.

The expansion of the plastic zone for symmetric angle-ply $[(30^0/-30^0)_2]$ laminated plate is shown in Figure 5.2. It expands along the diagonal at the plate. Elasto-plastic, elastic and residual stresses at the mid-point of upper surface of the angle-ply laminated plate for 100, 150, 200 iterations are given in Table 5.3.

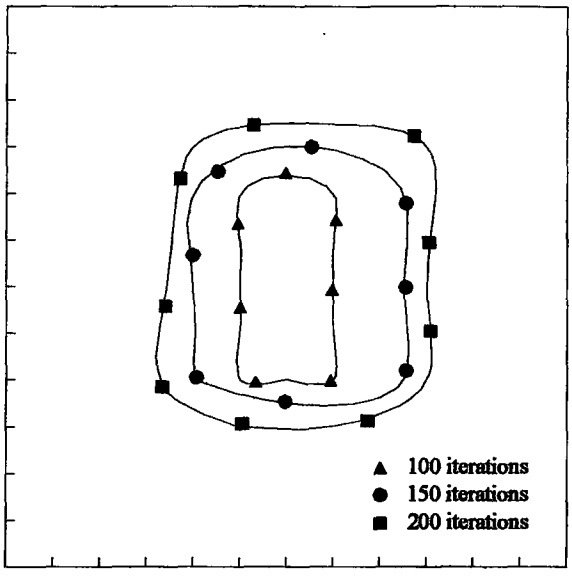

Fig. 5.1. Expansion of plastic zone in the symmetric $[(0^0/90^0)_2]$ laminated plate

Table 5.2. Elastic, elasto-plastic and residual stresses for symmetric cross-ply laminated plate $[(0^0/90^0)_2]$ at node 85 for 100-150-200 iterations.

Iterations	Stress	σ_x (MPa)	σ_y(MPa)	τ_{xy}(MPa)	τ_{yz}(MPa)	τ_{xz}(MPa)
100	Elasto-Plastic	-30.147	-23.958	0.034	0.052	0.071
	Elastic	-30.553	-27.308	0.030	0.055	0.064
	Residual	0.406	3.350	0.004	-0.003	0.007
150	Elasto-Plastic	-31.846	-23.943	0.037	0.053	0.073
	Elastic	-32.409	-28.967	0.032	0.058	0.068
	Residual	0.563	5.024	0.005	-0.005	0.005
200	Elasto-Plastic	-33.543	-23.927	0.039	0.057	0.074
	Elastic	-34.265	-30.626	0.034	0.062	0.072
	Residual	0.722	6.699	0.005	-0.005	0.002

The expansion of the plastic zone for symmetric angle-ply $[(45^0/-45^0)_2]$ laminated plate is shown in Figure 5.3. Elasto-plastic, elastic and residual stresses at the mid-point

of upper surface of the angle-ply laminated plate for 100, 150, 200 iterations are given in Table 5.4.

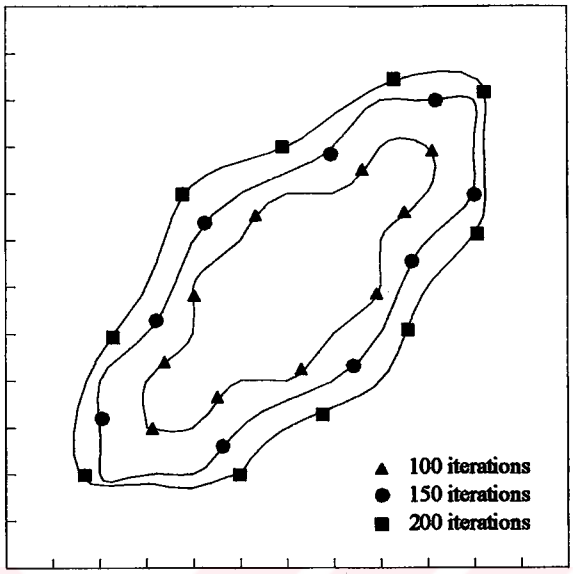

Fig. 5.2. Expansion of plastic zone in the symmetric $[(30^0/-30^0)_2]$ laminated plate

Table 5.3. Elastic, elasto-plastic and residual stresses for symmetric angle-ply laminated plate $[(30^0/-30^0)_2]$ at node 85 for 100-150-200 iterations.

Iterations	Stress	σ_x (MPa)	σ_y(MPa)	τ_{xy}(MPa)	τ_{yz}(MPa)	τ_{xz}(MPa)
100	Elasto-Plastic	-28.282	-24.969	-2.116	0.106	0.096
	Elastic	-29.423	-27.816	-1.068	0.082	0.093
	Residual	1.141	2.847	-1.047	0.024	0.003
150	Elasto-Plastic	-29.609	-25.242	-2.751	0.100	0.097
	Elastic	-31.204	-29.499	-1.133	0.087	0.099
	Residual	1.596	4.257	-1.618	0.013	-0.002
200	Elasto-Plastic	-30.952	-25.530	-3.405	0.107	0.101
	Elastic	-32.985	-31.183	-1.198	0.092	0.104
	Residual	2.033	5.653	-2.207	0.015	-0.003

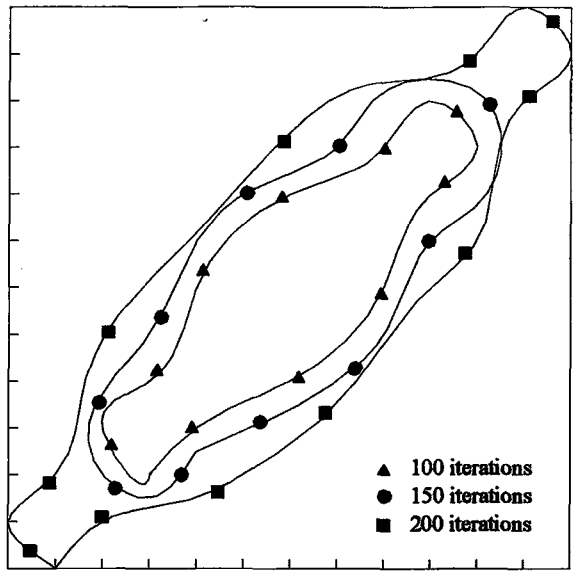

Fig. 5.3. Expansion of plastic zone in the symmetric $[(45^0/-45^0)_2]$ laminated plate

Table 5.4. Elastic, elasto-plastic and residual stresses for symmetric angle-ply laminated plate $[(45^0/-45^0)]_2$ at node 85 for 100-150-200 iterations.

Iterations	Stress	σ_x (MPa)	σ_y(MPa)	τ_{xy}(MPa)	τ_{yz}(MPa)	τ_{xz}(MPa)
100	Elasto-Plastic	-26.493	-26.490	-2.525	0.105	0.105
	Elastic	-28.557	-28.557	-1.238	0.087	0.087
	Residual	2.064	2.067	-1.287	0.018	0.018
150	Elasto-Plastic	-27.259	-27.254	-3.303	0.104	0.104
	Elastic	-30.284	-30.284	-1.313	0.092	0.092
	Residual	3.024	3.029	-1.990	0.012	0.012
200	Elasto-Plastic	-28.058	-28.051	-4.115	0.125	0.125
	Elastic	-32.010	-32.010	-1.388	0.097	0.097
	Residual	3.952	3.959	-2.727	0.028	0.027

The expansion of the plastic zone for symmetric angle-ply $[(60^0/-60^0)_2]$ laminated plate is shown in Figure 5.4. Elasto-plastic, elastic and residual stresses at the mid-point

of upper surface of the angle-ply laminated plate for 100, 150, 200 iterations are given in Table 5.5.

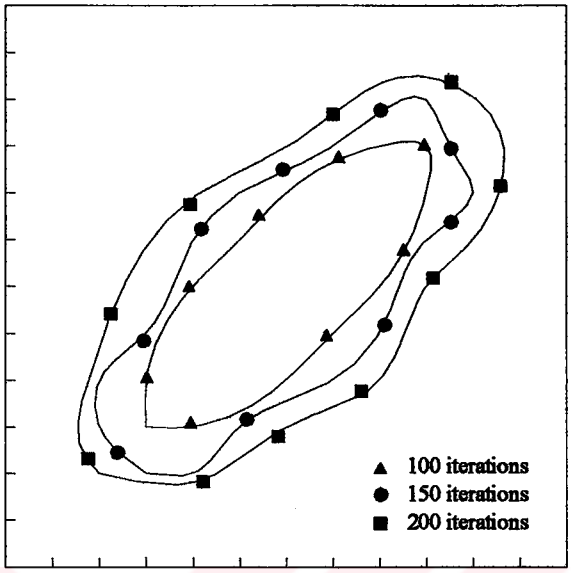

Fig. 5.4. Expansion of plastic zone in the symmetric $[(60^0/-60^0)_2]$ laminated plate

Table 5.5. Elastic, elasto-plastic and residual stresses in symmetric angle-ply laminated plates $[(60^0/-60^0)_2]$ at node 85 for 100-150-200 iterations .

Iterations	Stress	σ_x (MPa)	σ_y(MPa)	τ_{xy}(MPa)	τ_{yz}(MPa)	τ_{xz}(MPa)
100	Elasto-Plastic	-24.970	-28.279	-2.116	0.096	0.107
	Elastic	-27.816	-29.423	-1.068	0.093	0.082
	Residual	2.846	1.144	-1.048	0.003	0.024
150	Elasto-Plastic	-25.244	-29.604	-2.752	0.097	0.100
	Elastic	-29.499	-31.204	-1.133	0.099	0.087
	Residual	4.255	1.600	-1.619	-0.002	0.013
200	Elasto-Plastic	-25.533	-30.947	-3.407	0.101	0.108
	Elastic	-31.183	-32.985	-1.198	0.104	0.092
	Residual	5.650	2.038	-2.209	-0.003	0.015

The expansion of the plastic zone at the upper and lower surfaces for antisymmetric cross-ply $[(0^0/90^0)_2]$ laminated plate are shown in Figure 5.5 (a) and (b). In

antisymmetric plate, the plastic zone at the upper and lower surface is different. Elasto-plastic, elastic and residual stresses at the mid-point of upper and lower surfaces of the cross-ply laminated plate (node number is 85) for 100, 150, 200 iterations are shown in Table 5.6.

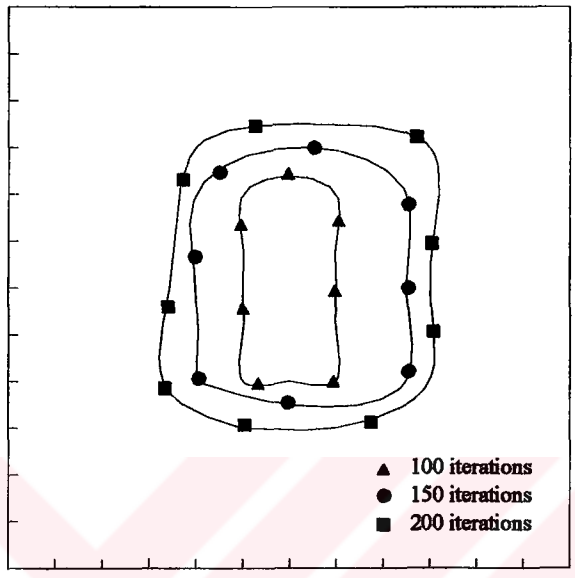

(a)

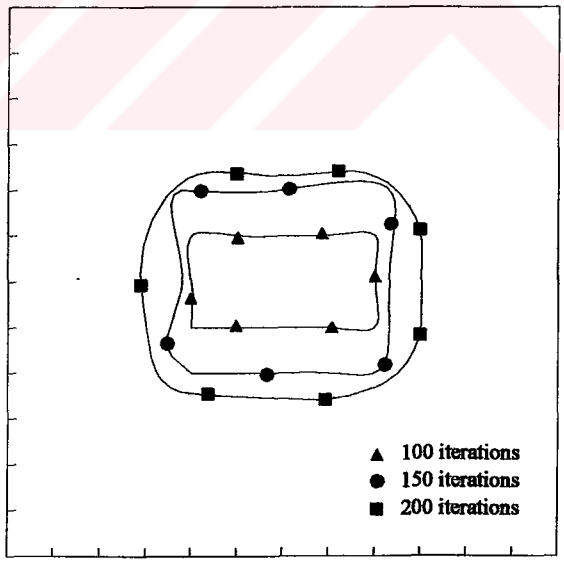

(b)

Fig. 5.5. Expansion of plastic zone in the antisymmetric $[(0^0/90^0)_2]$ laminated plate

(a) At the upper surface **(b)** At the lower surface

As seen from these Figures plastic zone expands in different directions at the upper and lower surfaces of the plate.

Table 5.6. Elastic, elasto-plastic and residual stresses in antisymmetric cross-ply laminated plates $[(0^0/90^0)]_2$ at node 85 for 100-150-200 iterations .

Iteration	Stress	Layer	σ_x(MPa)	σ_y(MPa)	τ_{xy}(MPa)	τ_{yz}(MPa)	τ_{xz}(MPa)
100	Elasto-Plastic	1	-28.894	-23.968	0.048	0.097	0.097
		8	23.968	28.882	-0.057	0.097	0.097
	Elastic	1	-29.648	-27.368	0.049	0.091	0.091
		8	27.360	29.638	-0.057	0.091	0.091
	Residual	1	0.754	3.401	-0.001	0.006	0.006
		8	-3.393	-0.755	0.000	0.006	0.006
150	Elasto-Plastic	1	-30.416	-23.955	0.050	0.099	0.098
		8	23.955	30.424	-0.068	0.099	0.098
	Elastic Stress	1	-31.467	-29.047	0.052	0.096	0.096
		8	29.039	31.456	-0.060	0.096	0.096
	Residual	1	1.051	5.092	-0.002	0.003	0.002
		8	-5.084	-1.032	-0.008	0.003	0.002
200	Elasto-Plastic	1	-31.922	-23.942	0.056	0.103	0.102
		8	23.942	31.925	-0.076	0.103	0.102
	Elastic	1	-33.286	-30.726	0.055	0.102	0.102
		8	30.717	33.274	-0.064	0.102	0.102
	Residual	1	1.364	6.784	0.001	0.001	0.000
		8	-6.775	-1.350	-0.012	0.001	0.000

The expansion of the plastic zone at the upper and lower surfaces for antisymmetric angle-ply $[(30^0/-30^0)_2]$ laminated plate are shown in Figure 5.6 (a) and (b). Elasto-plastic, elastic and residual stresses at the mid-point of upper and lower surface of the angle-ply laminated plate for 100, 150, 200 iterations are shown in Table 5.7.

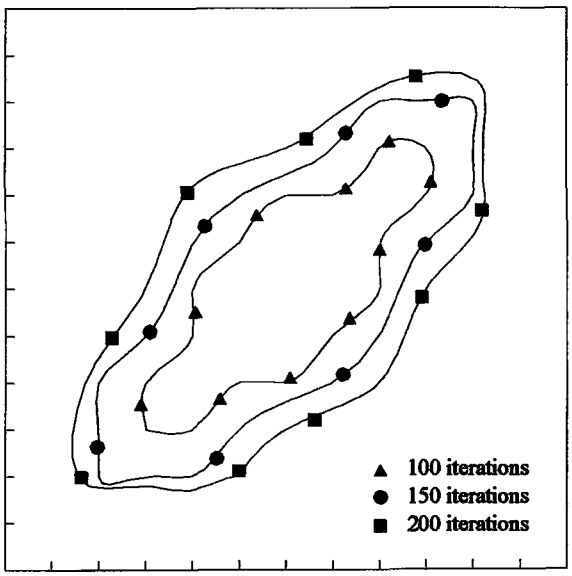

(a)

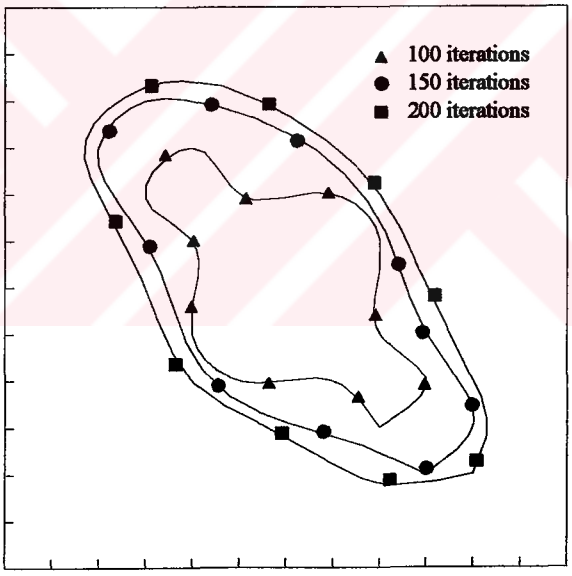

(b)

Fig. 5.6. Expansion of plastic zone in the antisymmetric $[(30^0/-30^0)_2]$ laminated plate

(a) At the upper surface **(b)** At the lower surface

As seen from these Figures the plastic zone is different and spreads in different directions at the upper and lower surfaces of the plate.

Table 5.7. Elastic, elasto-plastic and residual stresses in antisymmetric angle-ply laminated plates $[(30^0/-30^0)_2]$ at node 85 for 100-150-200 iterations .

Iteration	Stress	Layer	σ_x(MPa)	σ_y(MPa)	τ_{xy}(MPa)	τ_{yz}(MPa)	τ_{xz}(Mpa)
100	Elasto-Plastic	1	-28.116	-24.872	-1.982	0.105	0.101
		8	28.179	24.916	-2.095	0.090	0.128
	Elastic	1	-29.323	-27.723	-0.911	0.085	0.094
		8	29.331	27.727	-1.019	0.085	0.094
	Residual	1	1.206	2.851	-1.071	0.021	0.007
		8	-1.152	-2.811	-1.075	0.005	0.034
150	Elasto-Plastic	1	-29.424	-25.171	-2.633	0.100	0.103
		8	29.492	25.218	-2.751	0.087	0.133
	Elastic	1	-31.102	-29.405	-0.967	0.090	0.100
		8	31.111	29.410	-1.081	0.090	0.100
	Residual	1	1.678	4.234	-1.667	0.011	0.003
		8	-1.618	-4.191	-1.670	-0.002	0.033
200	Elasto-Plastic	1	-30.769	-25.447	-3.277	0.105	0.110
		8	30.835	25.506	-3.405	0.090	0.148
	Elastic	1	-32.881	-31.088	-1.022	0.095	0.106
		8	32.890	31.092	-1.143	0.095	0.106
	Residual	1	2.112	5.641	-2.255	0.010	0.004
		8	-2.055	-5.586	-2.262	-0.005	0.042

The expansion of the plastic zone at the upper and lower surfaces for antisymmetric angle-ply $[(45^0/-45^0)_2]$ laminated plate are shown in Figure 5.7 (a) and (b). Elasto-plastic, elastic and residual stresses at the mid-point of upper and lower surfaces of the angle-ply laminated plate for 100, 150, 200 iterations are shown in Table 5.8.

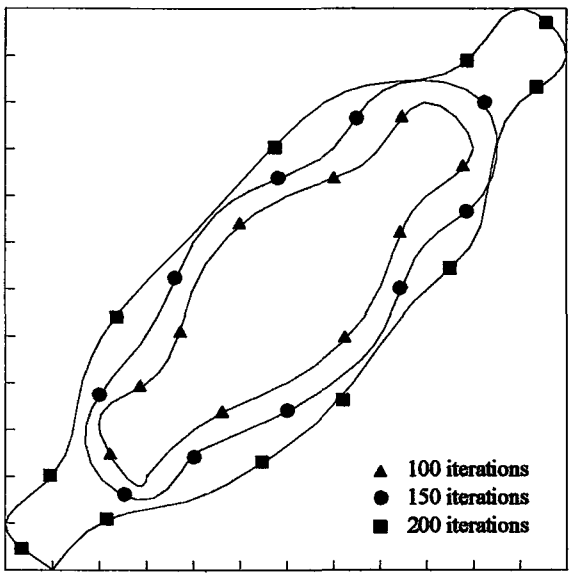

(a)

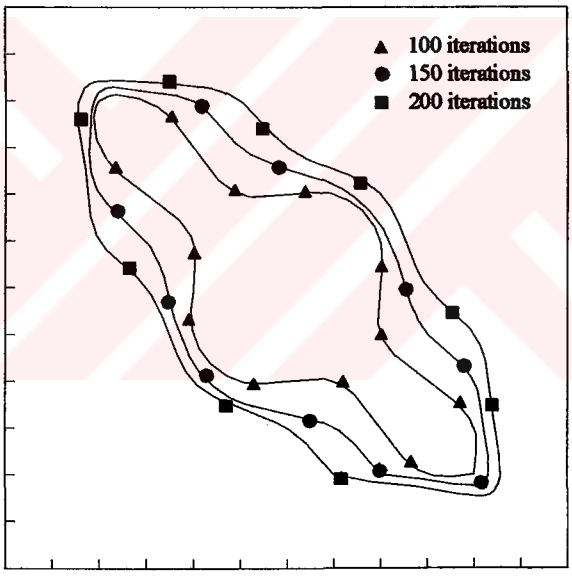

(b)

Fig. 5.7. Expansion of plastic zone in the antisymmetric $[(45^0/-45^0)_2]$ laminated plate

(a) At the upper surface **(b)** At the lower surface

As seen from these Figures the plastic zone is different and expands in different directions at the upper and lower surfaces of the plate.

Table 5.8. Elastic, elasto-plastic and residual stresses in antisymmetric angle-ply laminated plates $[(45^0/-45^0)_2]$ at node 85 for 100-150-200 iterations .

Iteration	Stress	Layer	σ_x(MPa)	σ_y(MPa)	τ_{xy}(MPa)	τ_{yz}(MPa)	τ_{xz}(MPa)
100	Elasto-Plastic	1	-26.344	-26.341	-2.374	0.108	0.108
		8	26.392	26.386	-2.489	0.110	0.110
	Elastic	1	-28.384	-28.385	-1.054	0.089	0.089
		8	28.392	28.391	-1.162	0.089	0.089
	Residual	1	2.040	2.043	-1.320	0.019	0.019
		8	-2.000	-2.005	-1.327	0.021	0.021
150	Elasto-Plastic	1	-27.133	-27.128	-3.174	0.108	0.107
		8	27.185	-27.176	-3.294	0.110	0.110
	Elastic	1	-30.108	-30.109	-1.118	0.094	0.094
		8	30.117	30.116	-1.233	0.094	0.094
	Residual	1	2.976	2.981	-2.056	0.013	0.013
		8	-2.932	-2.939	-2.061	0.015	0.015
200	Elasto-Plastic	1	-27.921	-27.914	-3.975	0.127	0.127
		8	27.981	27.972	-4.104	0.130	0.130
	Elastic	1	-31.833	-31.833	-1.182	0.100	0.100
		8	31.841	31.840	-1.304	0.100	0.100
	Residual	1	3.911	3.919	-2.793	0.028	0.027
		8	-3.861	-3.869	-2.800	0.031	0.030

The expansion of the plastic zone at the upper and lower surfaces for antisymmetric angle-ply $[(60^0/-60^0)_2]$ laminated plate are shown in Figure 5.8 (a) and (b). Elasto-plastic, elastic and residual stresses at the mid-point of upper and lower surfaces of the angle-ply laminated plate for 100, 150, 200 iterations are shown in Table 5.9.

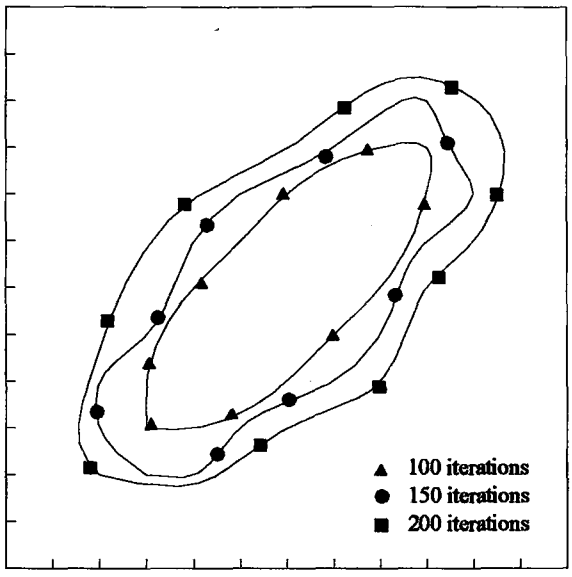

(a)

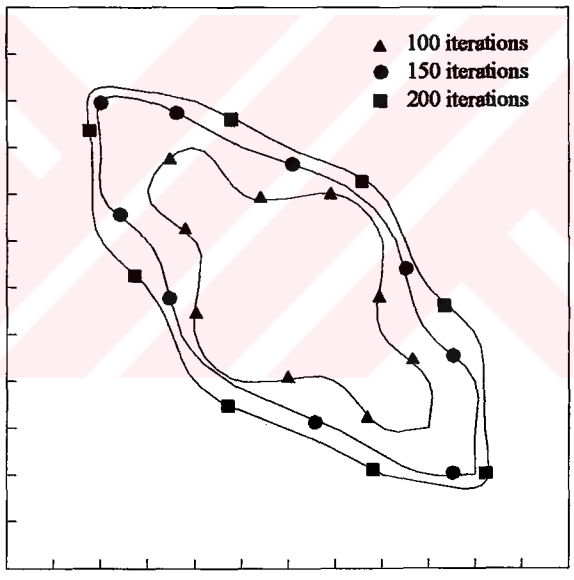

(b)

Fig. 5.8. Expansion of plastic zone in the antisymmetric $[(60^0/-60^0)_2]$ laminated plate

(a) At the upper surface **(b)** At the lower surface

As seen from the Figures the plastic zone is different and expands in different directions at the upper and lower surfaces of the plate.

Table 5.9. Elastic, elasto-plastic and residual stresses in antisymmetric angle-ply laminated plates $[(60^0/-60^0)_2]$ at node 85 for 100-150-200 iterations .

Iteration	Stress	Layer	σ_x(MPa)	σ_y(MPa)	τ_{xy}(MPa)	τ_{yz}(MPa)	τ_{xz}(MPa)
100	Elasto-Plastic	1	-24.871	-28.114	-1.981	0.101	0.106
		8	24.918	28.173	-2.094	0.128	0.090
	Elastic	1	-27.722	-29.323	-0.910	0.094	0.085
		8	27.728	29.330	-1.018	0.094	0.085
	Residual	1	2.851	1.209	-1.071	0.007	0.021
		8	-2.810	-1.157	-1.076	0.034	0.006
150	Elasto-Plastic	1	-25.169	-29.419	-2.631	0.103	0.101
		8	25.220	29.483	-2.749	0.133	0.088
	Elastic	1	-29.404	-31.102	-0.965	0.100	0.090
		8	29.410	31.110	-1.080	0.100	0.090
	Residual	1	4.235	1.683	-1.666	0.003	0.011
		8	-4.191	-1.626	-1.669	0.033	-0.002
200	Elasto-Plastic	1	-25.444	-30.762	-3.273	0.110	0.106
		8	25.506	30.826	-3.402	0.149	0.090
	Elastic	1	-31.087	-32.882	-1.021	0.106	0.095
		8	31.093	32.889	-1.142	0.106	0.095
	Residual	1	6.357	2.064	-2.252	0.004	0.011
		8	-5.587	-2.063	-2.260	0.043	-0.005

As seen from the Figures the plastic zone is the same at the upper and lower surfaces of the plate in symmetric cases. It is different and expands in different directions at the upper and lower surfaces of the plate in antisymmetric cases. As seen from the Tables when we increase the iteration numbers the residual stress becomes greater.

5.1.2 Antisymmetric Laminated Plates of Four Layers

In this case, the layers are bonded antisymmetrically, as $[(0^0)_2/(90^0)_2]$, $[(30^0)_2/(-30^0)_2]$, $[(45^0)_2/(-45^0)_2]$ and $[(60^0)_2/(-60^0)_2]$. $[(0^0)_2/(90^0)_2]$ is the abbreviation of $0^0/0^0/90^0/90^0$ for antisymmetric laminated plates of four layers. The transverse uniform load at the yield point of the plates are given in Table 5.10. The yield point of laminated plate is smallest for cross-ply $[(0^0)_2/(90^0)_2]$ and greatest for angle-ply $[(30^0)_2/(-30^0)_2]$ and $[(60^0)_2/(-60^0)_2]$ laminated plates. As seen from these Tables the yield points are less than $[(0^0/90^0)_2]$, $[(30^0/-30^0)_2]$, $[(45^0/-45^0)_2]$, $[(60^0/-60^0)_2]$, symmetric and antisymmetric cases.

Table 5.10. The uniform transverse force at the yield points of the antisymmetric four laminated plates.

	$[(0^0)_2/(90^0)_2]$	$[(30^0)_2/(-30^0)_2]$	$[(45^0)_2/(-45^0)_2]$	$[(60^0)_2/(-60^0)_2]$
Transverse load (MPa)	0.0704	0.0714	0.0711	0.0714

The expansion of the plastic zone at the upper and lower surfaces for antisymmetric cross-ply $[(0^0)_2/(90^0)_2]$ laminated plate are shown in Figure 5.9 (a) and (b). In antisymmetric plate, the plastic zone at the upper and lower surface is different. Elasto-plastic, elastic and residual stresses at the mid-point of upper and lower surfaces of the cross-ply laminated plate (node number is 85) for 100, 150, 200 iterations are shown in Table 5.11.

The expansion of the plastic zone at the upper and lower surfaces for antisymmetric angle-ply $[(30^0)_2/(-30^0)_2]$ laminated plate are shown in Figure 5.10. (a) and (b). Elasto-plastic, elastic and residual stresses at the mid-point of upper and lower surfaces of the angle-ply laminated plate for 100, 150, 200 iterations are shown in Table 5.12.

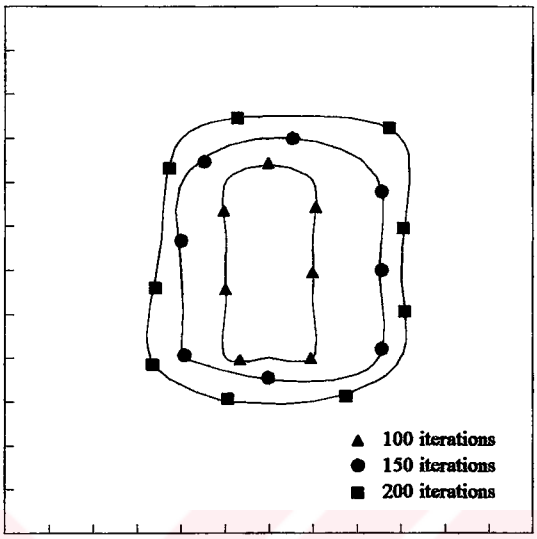

(a)

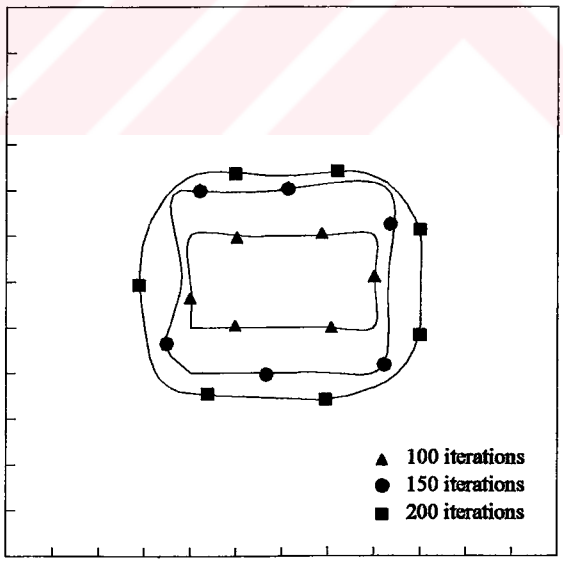

(b)

Fig. 5.9. Expansion of the plastic zone in the antisymmetric $[(0^0)_2/(90^0)_2]$ laminated plate

(a) At the upper surface **(b)** At the lower surface

As seen from these Figures the plastic zone spreads in different directions at the upper and lower surfaces of the plate.

Table 5.11. Elastic, elasto-plastic and residual stresses in antisymmetric cross-ply laminated plates $[(0^0)_2/(90^0)_2]$ at node 85 for 100-150-200 iterations .

Iterations	Stress	Layer	σ_x(MPa)	σ_y(MPa)	τ_{xy}(MPa)	τ_{yz}(MPa)	τ_{xz}(MPa)
100	Elasto-Plastic	1	-28.116	-23.973	0.043	0.096	0.095
		8	23.969	28.089	-0.061	0.096	0.096
	Elastic	1	-28.867	-27.410	0.044	0.089	0.089
		8	27.395	28.845	-0.060	0.089	0.089
	Residual	1	0.750	3.436	0.00	0.006	0.006
		8	-3.426	-0.756	-0.001	0.007	0.007
150	Elasto-Plastic	1	-29.600	-23.962	0.048	0.097	0.097
		8	23.957	29.566	-0.068	0.097	0.097
	Elastic	1	-30.622	-29.114	0.047	0.095	0.095
		8	29.099	30.638	-0.064	0.095	0.095
	Residual	1	1.062	5.152	0.001	0.002	0.002
		8	-5.141	-1.073	-0.004	0.003	0.002
200	Elasto-Plastic	1	-31.071	-23.950	0.055	0.104	0.104
		8	23.945	31.028	-0.077	0.105	0.105
	Elastic	1	-32.457	-30.819	0.049	0.100	0.100
		8	30.803	32.432	-0.068	0.100	0.100
	Residual	1	1.387	6.869	0.006	0.004	0.003
		8	-6.857	-1.404	-0.010	0.004	0.004

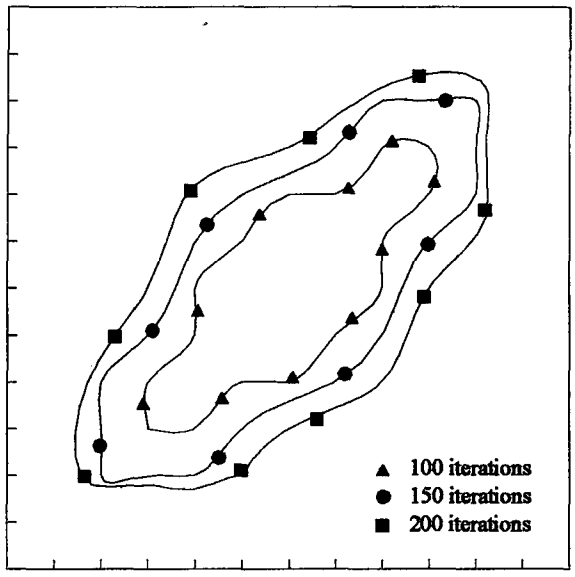

(a)

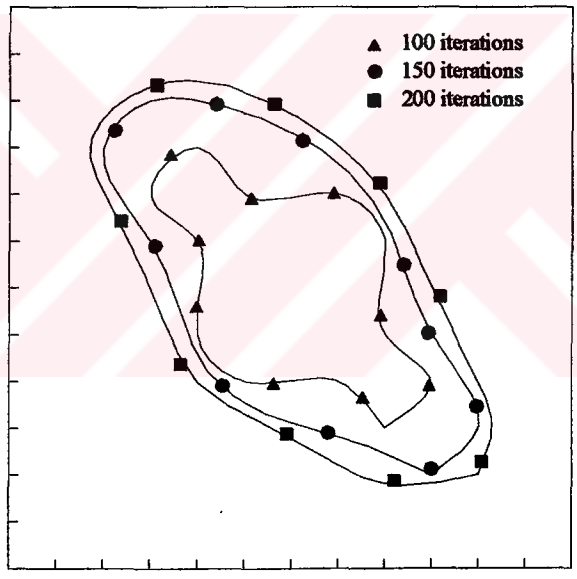

(b)

Fig. 5.10. Expansion of the plastic zone in the antisymmetric $[(30^0)_2/(-30^0)_2]$ laminated plate **(a)** At the upper surface **(b)** At the lower surface

Table 5.12. Elastic, elasto-plastic and residual stresses in antisymmetric angle-ply laminated plates $[(30^0)_2/(-30^0)_2]$ at node 85 for 100-150-200 iterations .

Iterations	Stress	Layer	σ_x(MPa)	σ_y(MPa)	τ_{xy}(MPa)	τ_{yz}(MPa)	τ_{xz}(MPa)
100	Elasto-Plastic	1	-27.811	-24.557	-1.616	0.105	0.101
		8	27.846	24.573	-1.726	0.090	0.128
	Elastic	1	-28.997	-27.426	-0.533	0.084	0.093
		8	29.003	27.427	-0.640	0.084	0.093
	Residual	1	1.186	2.869	-1.083	0.021	0.007
		8	-1.157	-2.854	-1.086	0.006	0.034
150	Elasto-Plastic	1	-29.127	-24.837	-2.253	0.100	0.103
		8	29.168	24.856	-2.367	0.087	0.132
	Elastic	1	-30.778	-29.111	-0.566	0.089	0.099
		8	30.784	29.111	-0.680	0.089	0.099
	Residual	1	1.651	4.274	-1.686	0.011	0.003
		8	-1.616	-4.255	-1.688	-0.002	0.033
200	Elasto-Plastic	1	-30.508	-25.075	-2.873	0.110	0.114
		8	30.548	25.110	-3.002	0.092	0.157
	Elastic	1	-32.559	-30.795	-0.599	0.094	0.105
		8	32.566	30.796	-0.719	0.094	0.105
	Residual	1	2.051	5.720	-2.274	0.016	0.009
		8	-2.018	-5.686	-2.283	-0.002	0.052

The expansion of the plastic zone at the upper and lower surfaces for antisymmetric angle-ply $[(45^0)_2/(-45^0)_2]$ laminated plate are shown in Figure 5.11. (a) and (b). Elasto-plastic, elastic and residual stresses at the mid-point of upper and lower surfaces of the angle-ply laminated plate for 100, 150, 200 iterations are shown in Table 5.13.

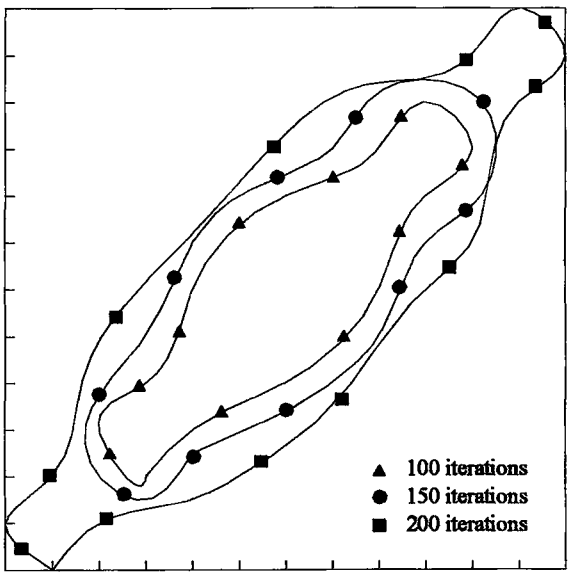

(a)

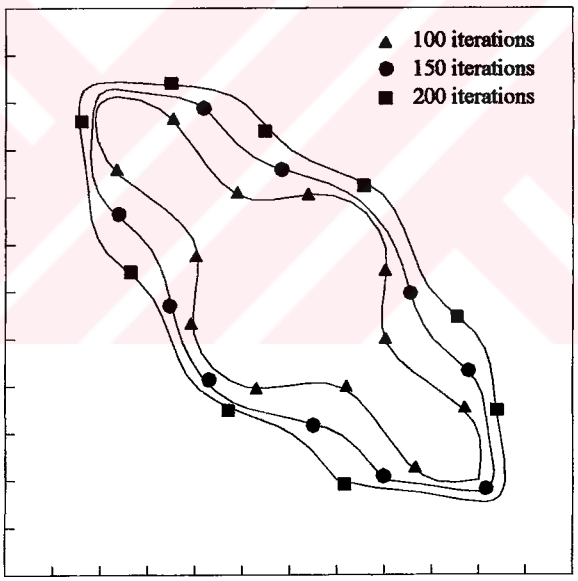

(b)

Fig 5.11. Expansion of the plastic zone in the antisymmetric $[(45^0)_2/(-45^0)_2]$ laminated plate **(a)** At the upper surface **(b)** At the lower surface

Table 5.13. Elastic, elasto-plastic and residual stresses in antisymmetric angle-ply laminated plates $[(45^0)_2/(-45^0)_2]$ at node 85 for 100-150-200 iterations .

Iterations	Stress	Layer	σ_x(MPa)	σ_y(MPa)	τ_{xy}(MPa)	τ_{yz}(MPa)	τ_{xz}(MPa)
100	Elasto-Plastic	1	-25.944	-25.942	-1.968	0.108	0.108
		8	25.994	25.986	-2.082	0.110	0.110
	Elastic	1	-28.013	-28.015	-0.617	0.088	0.088
		8	28.019	28.017	-0.725	0.088	0.088
	Residual	1	2.069	2.073	-1.351	0.020	0.020
		8	-2.025	-2.031	-1.357	0.022	0.022
150	Elasto-Plastic	1	-26.721	-26.717	-2.756	0.107	0.107
		8	26.775	26.765	-2.873	0.109	0.109
	Elastic	1	-29.741	-29.742	-0.656	0.093	0.093
		8	29.746	29.744	-0.769	0.093	0.093
	Residual	1	3.019	3.025	-2.101	0.014	0.014
		8	-2.971	-2.979	-2.104	0.016	0.016
200	Elasto-Plastic	1	-27.510	-27.499	-3.554	0.135	0.135
		8	27.572	27.556	-3.681	0.138	0.138
	Elastic	1	-31.468	-31.469	-0.694	0.098	0.098
		8	31.474	31.472	-0.814	0.098	0.098
	Residual	1	3.958	3.970	-2.861	0.036	0.036
		8	-3.902	-3.916	-2.867	0.039	0.039

The expansion of the plastic zone at the upper and lower surfaces for antisymmetric angle-ply $[(60^0)_2/(-60^0)_2]$ laminated plate are shown in Figure 5.12. (a) and (b). Elasto-plastic, elastic and residual stresses at the mid-point of upper and lower surfaces of the angle-ply laminated plate for 100, 150, 200 iterations are shown in Table 5.14.

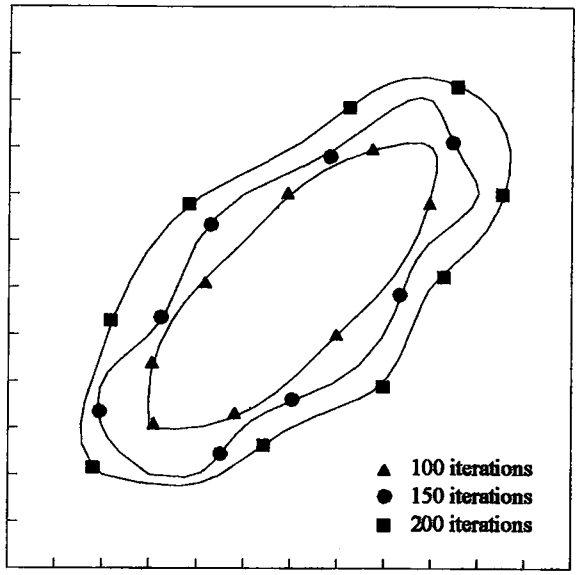

(a)

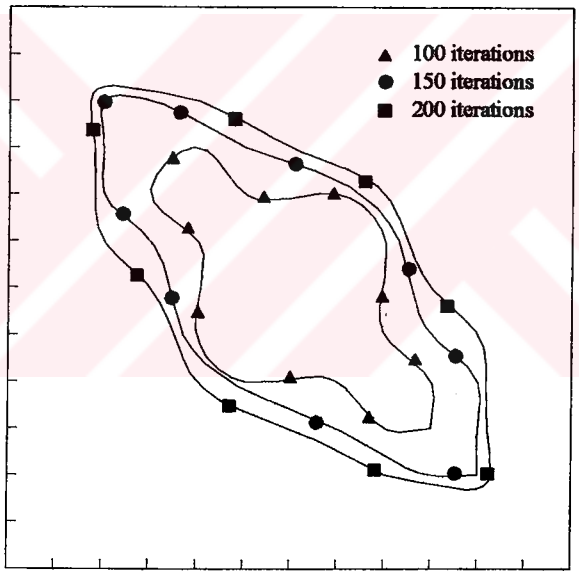

(b)

Fig. 5.12. Expansion of the plastic zone in the antisymmetric $[(60^0)_2/(-60^0)_2]$ laminated plate **(a)** At the upper surface **(b)** At the lower surface

Table 5.14. Elastic, elasto-plastic and residual stresses in antisymmetric angle-ply laminated plates $[(60^0)_2/(-60^0)_2]$ at node 85 for 100-150-200 iterations.

Iterations	Stress	Layer	σ_x(MPa)	σ_y(MPa)	τ_{xy}(MPa)	τ_{yz}(MPa)	τ_{xz}(MPa)
100	Elasto-Plastic	1	-24.555	-27.809	-1.614	0.101	0.105
		8	24.576	27.839	-1.725	0.128	0.090
	Elastic	1	-27.424	-28.998	-0.531	0.093	0.084
		8	27.428	29.001	-0.638	0.093	0.084
	Residual	1	2.869	1.189	-1.082	0.007	0.021
		8	-2.852	-1.162	-1.087	0.034	0.006
150	Elasto-Plastic	1	-24.833	-29.122	-2.248	0.103	0.100
		8	24.859	29.157	-2.365	0.132	0.087
	Elastic	1	-29.109	-30.779	-0.564	0.099	0.089
		8	29.113	30.782	-0.677	0.099	0.089
	Residual	1	4.276	1.657	-1.685	0.003	0.011
		8	-4.254	-1.625	-1.687	0.033	-0.002
200	Elasto-Plastic	1	-25.071	-30.501	-2.869	0.114	0.110
		8	25.111	30.535	-2.998	0.157	0.092
	Elastic	1	-30.793	-32.560	-0.596	0.105	0.094
		8	30.798	32.563	-0.717	0.105	0.094
	Residual	1	5.722	2.059	-2.272	0.009	0.016
		8	-5.686	-2.028	-2.281	0.052	-0.002

As seen from these Figures the plastic zone is different and expands in different directions at the upper and lower surfaces of the plate in all cases. When we increase the iteration numbers the residual stress becomes greater.

5.1.3. Antisymmetric laminated Plates of Two Layers

In this case, the layers are bonded antisymmetrically, as (0^0/90^0), (30^0/-30^0), (45^0/-45^0) and (60^0/-60^0). Plate thickness is 4 mm. The transverse uniform load at the yield point of the plates is given in Table 5.15. Only in this case the load is increased 0.00002 Mpa at each iteration, incrementally. Iteration numbers are chosen as 100, 150 and 200. The yield point of (0^0/90^0) and (45^0/-45^0) is the same and smallest. The yield point of (30^0/-30^0) and (60^0/-60^0) is the same and greatest.

Table 5.15. The uniform transverse force at the yield points of the antisymmetric two laminated plates.

	(0^0/ 90^0)	(30^0/-30^0)	(45^0/-45^0)	(60^0/-60^0)
Transverse load (MPa)	0.0177	0.0179	0.0177	0.0179

The expansion of the plastic zone at the upper and lower surfaces for antisymmetric cross-ply (0^0/90^0) laminated plate are shown in Figure 5.13. (a) and (b). In antisymmetric plate, the plastic zone at the upper and lower surface is different. Elasto-plastic, elastic and residual stresses at the mid-point of upper and lower surfaces of the cross-ply laminated plate (node number is 85) for 100, 150, 200 iterations is represented in Table 5.16.

The expansion of the plastic zone at the upper and lower surfaces for antisymmetric angle-ply (30^0/-30^0) laminated plate are illustrated in Figure 5.14. (a) and (b). Elasto-plastic, elastic and residual stresses at the mid-point of upper and lower surfaces of the angle-ply laminated plate for 100, 150, 200 iterations are given in Table 5.17.

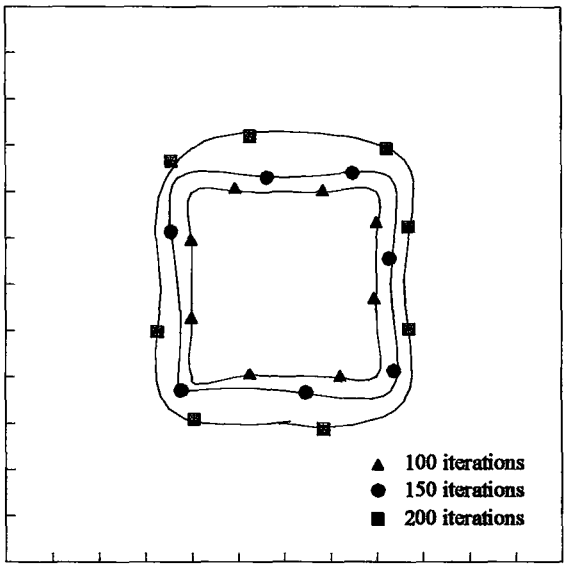

(a)

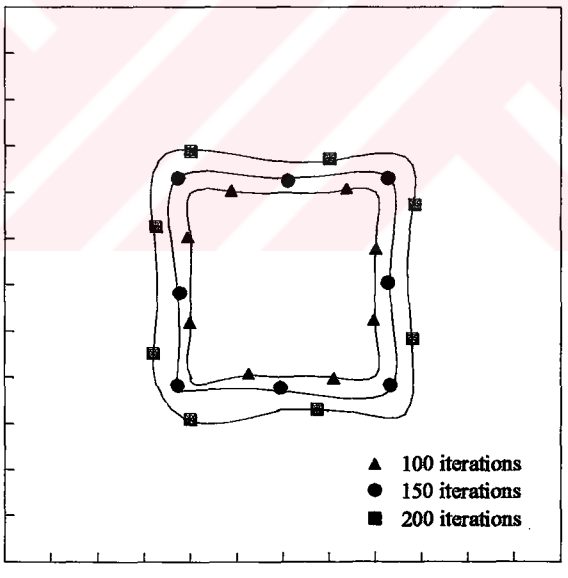

(b)

Fig. 5.13.. Expansion of the plastic zone in the antisymmetric cross-ply ($0^0/90^0$) laminated plate **(a)** At the upper surface **(b)** At the lower surface

Table 5.16. Elastic, elasto-plastic and residual stresses in antisymmetric cross-ply ($0^0/90^0$) laminated plate at node 85 for 100-150-200 iterations .

Iterations	Stress	Layer	σ_x(MPa)	σ_y(MPa)	τ_{xy}(MPa)	τ_{yz}(MPa)	τ_{xz}(MPa)
100	Elasto-Plastic	1	-27.523	-23.978	0.041	0.054	0.054
		8	23.978	27.497	-0.057	0.054	0.054
	Elastic	1	-28.227	-26.802	0.042	0.051	0.051
		8	26.787	28.205	-0.058	0.051	0.051
	Residual	1	0.705	2.824	-0.001	0.002	0.003
		8	-2.809	-0.708	0.001	0.002	0.003
150	Elasto-Plastic	1	-28.715	-23.969	0.044	0.054	0.054
		8	23.969	28.684	-0.063	0.054	0.055
	Elastic	1	-29.660	-28.162	0.044	0.054	0.054
		8	28.147	29.637	-0.061	0.054	0.054
	Residual	1	0.945	4.193	0.000	0.000	0.001
		8	-4.178	-0.953	-0.002	0.001	0.001
200	Elasto-Plastic	1	-29.906	-23.960	0.047	0.055	0.055
		8	23.960	29.869	-0.068	0.055	0.055
	Elastic	1	-31.093	-29.523	0.046	0.056	0.056
		8	29.507	31.069	-0.064	0.056	0.056
	Residual	1	1.187	5.563	0.001	-0.001	-0.001
		8	-5.547	-1.200	-0.004	-0.001	-0.001

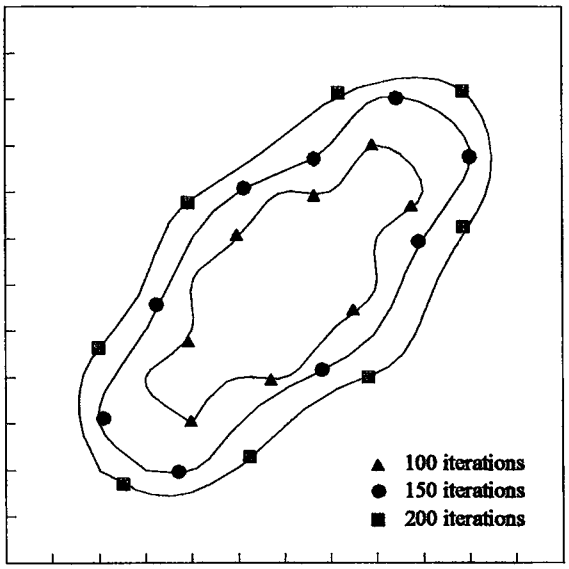

(a)

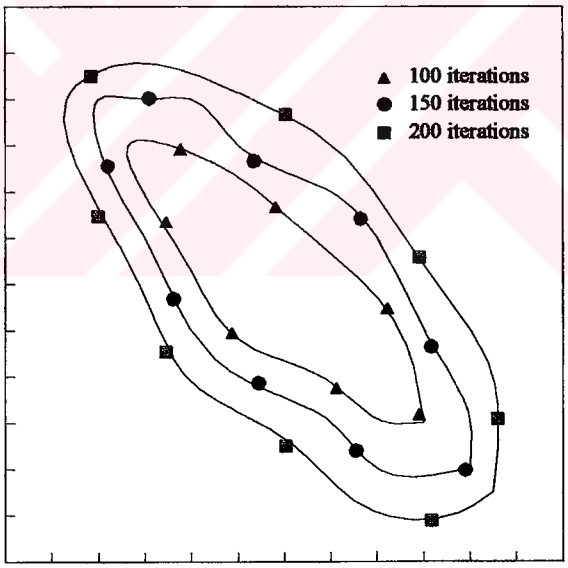

(b)

Fig. 5.14. Expansion of the plastic zone in the antisymmetric angle-ply (30^0/-30^0) laminated plate **(a)** At the upper surface **(b)** At the lower surface

Table 5.17. Elastic, elasto-plastic and residual stresses in antisymmetric angle-ply laminated plates (30^0/-30^0) at node 85 for 100-150-200 iterations .

Iterations	Stress	Layer	σ_x(MPa)	σ_y(MPa)	τ_{xy}(MPa)	τ_{yz}(MPa)	τ_{xz}(MPa)
100	Elasto-Plastic	1	-27.259	-24.435	-1.346	0.060	0.059
		8	27.307	24.470	-1.458	0.053	0.076
	Elastic	1	-28.291	-26.761	-0.521	0.047	0.054
		8	28.297	26.762	-0.624	0.047	0.054
	Residual	1	1.032	2.326	-0.824	0.012	0.006
		8	-0.990	-2.292	-0.834	0.006	0.022
150	Elasto-Plastic	1	-28.280	-24.658	-1.844	0.057	0.061
		8	28.339	24.697	-1.964	0.051	0.080
	Elastic	1	-29.713	-28.106	-0.548	0.050	0.056
		8	29.718	28.107	-0.655	0.050	0.056
	Residual	1	1.432	3.448	-1.296	0.007	0.004
		8	-1.379	-3.410	-1.308	0.002	0.023
200	Elasto-Plastic	1	-29.338	-24.885	-2.358	0.054	0.061
		8	29.401	24.928	-2.483	0.050	0.080
	Elastic	1	-31.134	-29.451	-0.574	0.052	0.059
		8	31.140	29.452	-0.687	0.052	0.059
	Residual	1	1.796	4.566	-1.784	0.002	0.002
		8	-1.740	-4.523	-1.796	-0.002	0.021

The expansion of the plastic zone at the upper and lower surfaces for antisymmetric angle-ply (45^0/-45^0) laminated plate are represented in Figure 5.15. (a) and (b). Elasto-plastic, elastic and residual stresses at the mid-point of upper and lower surfaces of the angle-ply laminated plate for 100, 150, 200 iterations are given in Table 5.18.

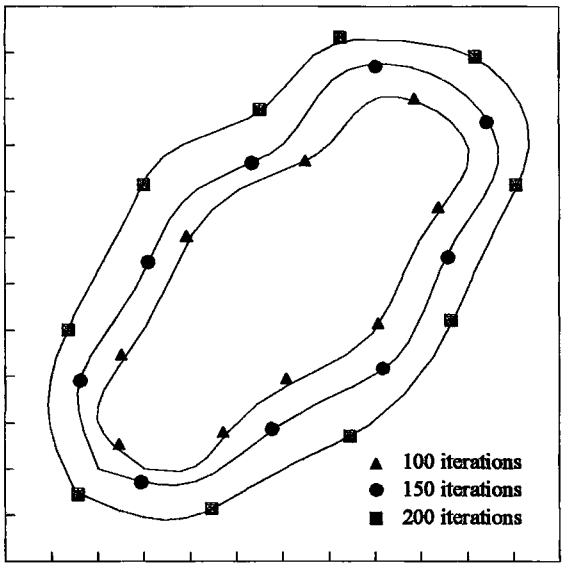

(a)

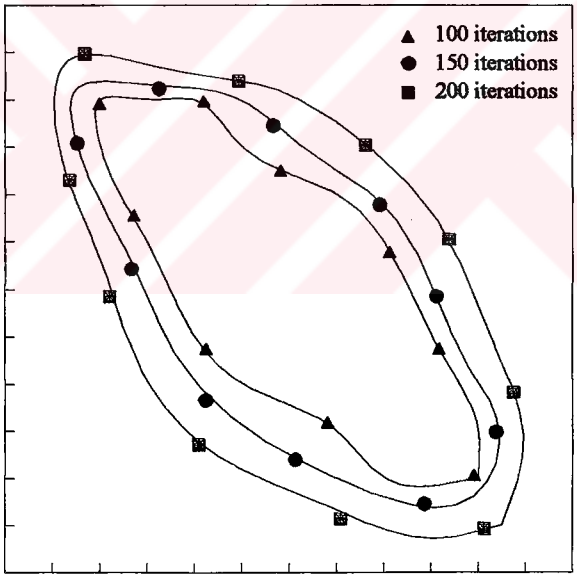

(b)

Fig 5.15. Expansion of the plastic zone in the antisymmetric angle-ply (45^0/-45^0) laminated plate **(a)** At the upper surface **(b)** At the lower surface

Table 5.18. Elastic, elasto-plastic and residual stresses in antisymmetric angle-ply laminated plates ($45^0/-45^0$) at node 85 for 100-150-200 iterations .

Iterations	Stress	Layer	σ_x(MPa)	σ_y(MPa)	τ_{xy}(MPa)	τ_{yz}(MPa)	τ_{xz}(MPa)
100	Elasto-Plastic	1	-25.471	-25.469	-1.620	0.066	0.065
		8	25.488	25.490	-1.728	0.067	0.066
	Elastic	1	-27.159	-27.161	-0.600	0.050	0.050
		8	27.165	27.163	-0.702	0.050	0.050
	Residual	1	1.689	1.692	-1.020	0.016	0.016
		8	-1.676	-1.673	-1.026	0.017	0.017
150	Elasto-Plastic	1	-26.081	-26.078	-2.238	0.066	0.066
		8	26.110	26.110	-2.358	0.067	0.067
	Elastic	1	-28.538	-28.540	-0.630	0.052	0.052
		8	28.544	28.542	-0.737	0.052	0.052
	Residual	1	2.457	2.462	-1.608	0.014	0.014
		8	-2.434	-2.432	-1.620	0.015	0.015
200	Elasto-Plastic	1	-26.705	-26.700	-2.871	0.065	0.065
		8	26.739	26.737	2.996	0.066	0.065
	Elastic	1	-29.917	-29.918	-0.661	0.055	0.055
		8	29.922	29.920	-0.773	0.055	0.055
	Residual	1	3.212	3.218	-2.211	0.011	0.010
		8	-3.184	-3.184	-2.223	0.011	0.011

The expansion of the plastic zone at the upper and lower surfaces for antisymmetric angle-ply ($60^0/-60^0$) laminated plate are shown in Figure 5.16. (a) and (b). Elasto-plastic, elastic and residual stresses at the mid-point of upper and lower surfaces of the angle-ply laminated plate for 100, 150, 200 iterations is given in Table 5.19.

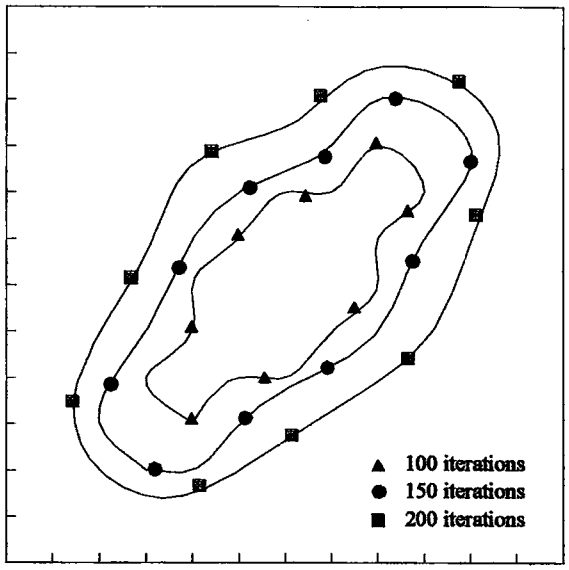

(a)

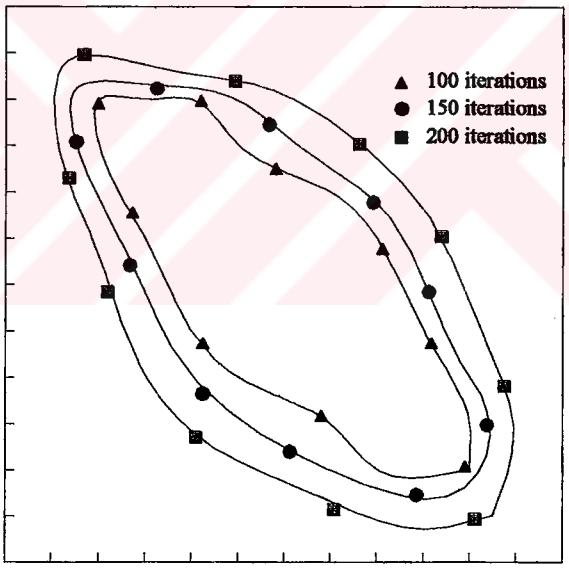

(b)

Fig. 5.16. Expansion of the plastic zone in the antisymmetric angle-ply (60^0/-60^0) laminated plate **(a)** At the upper surface **(b)** At the lower surface

Table 5.19. Elastic, elasto-plastic and residual stresses in antisymmetric angle-ply laminated plates (60^0/-60^0) at node 85 for 100-150-200 iterations .

Iterations	Stress	Layer	σ_x(MPa)	σ_y(MPa)	τ_{xy}(MPa)	τ_{yz}(MPa)	τ_{xz}(MPa)
100	Elasto-Plastic	1	-24.433	-27.258	-1.343	0.059	0.060
		8	24.472	27.301	-1.456	0.076	0.053
	Elastic	1	-26.760	-28.292	-0.519	0.054	0.047
		8	26.763	28.294	-0.622	0.054	0.047
	Residual	1	2.327	1.034	-0.824	0.006	0.012
		8	-2.291	-0.993	-0.835	0.022	0.006
150	Elasto-Plastic	1	-24.654	-28.278	-1.841	0.061	0.057
		8	24.699	28.332	-1.961	0.080	0.051
	Elastic	1	-28.104	-29.714	-0.545	0.056	0.050
		8	28.108	29.716	-0.653	0.056	0.050
	Residual	1	3.450	1.436	-1.295	0.004	0.007
		8	-3.410	-1.384	-1.308	0.023	0.002
200	Elasto-Plastic	1	-24.885	-29.338	-2.358	0.061	0.054
		8	24.928	29.401	-2.483	0.080	0.050
	Elastic	1	-29.451	-31.134	-0.574	0.059	0.052
		8	29.452	31.140	-0.687	0.059	0.052
	Residual	1	4.566	1.796	-1.784	0.002	0.002
		8	-4.523	-1.740	-1.796	0.021	-0.002

As seen from these Figures the plastic zone is different and expands in different directions at the upper and lower surfaces of the plate. When we increase the iteration numbers the residual stress becomes greater.

5.2. Transversly Loaded Plate With Circular Hole

5.2.1 Symmetric or Antisymmetric Laminated Plates of Four Layers

Symmetric or antisymmetric laminated plates of four layers are bonded in the symmetric and antisymmetric form as cross-ply laminated plate $[(0^0/90^0)_2]$ and angle-ply laminated plates $[(30^0/-30^0)_2]$, $[(45^0/-45^0)_2]$ and $[(60^0/-60^0)_2]$. Plate dimensions are 300*300 mm. There is a circular hole at mid of plate. Hole diameter is 20 mm. The transverse uniform load at the yield points of the symmetric and antisymmetric laminated plates is given in Table 5.20.

Table 5.20. The uniform transverse force at the yield points of the four laminated plates. (S: Symmetric laminate, A: Antisymmetric laminate.)

	$[(0^0/90^0)_2]$	$[(30^0/-30^0)_2]$	$[(45^0/-45^0)_2]$	$[(60^0/-60^0)_2]$
S (MPa)	0.1194	0.1152	0.1130	0.1152
A (MPa)	0.1187	0.1174	0.1154	0.1174

As seen from this Table the yield point for antisymmetric angle ply laminated plates is higher than in symmetric ones, except cross-ply laminated plates. The expansion of the plastic zone for symmetric cross-ply $[(0^0/90^0)_2]$ laminated plate is shown in Figure 5.17. Elasto-plastic, elastic and residual stresses at upper surface of the cross-ply laminated plate (point A) for 200, 400, 600 iterations is shown in Table 5.21.

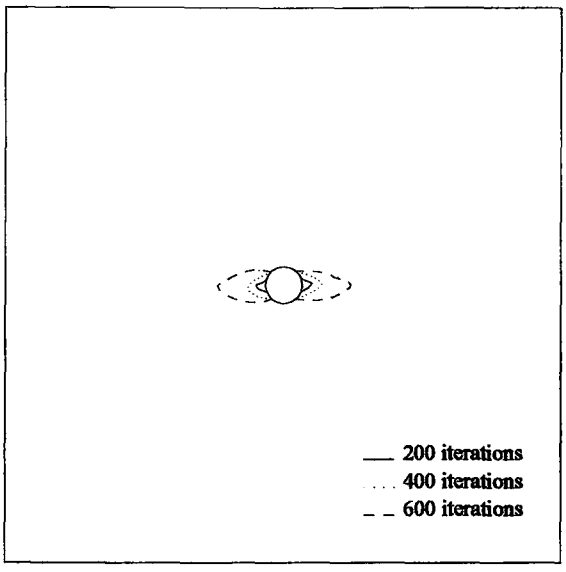

Fig. 5.17. Expansion of plastic zone in the symmetric $[(0^0/90^0)_2]$ laminated plate

Table 5.21. Elastic, elasto-plastic and residual stresses for symmetric cross-ply laminated plate with a circular hole $[(0^0/90^0)_2]$ at point A for 200-400-600 iterations.

Iterations	Stress	σ_x (MPa)	σ_y(MPa)	τ_{xy}(MPa)	τ_{yz}(MPa)	τ_{xz}(MPa)
200	Elasto-Plastic	-31.359	-14.563	1.308	-0.671	-0.079
	Elastic	-31.369	-14.666	1.311	-0.673	-0.087
	Residual	0.010	0.103	-0.003	0.002	0.009
400	Elasto-Plastic	-35.875	-16.492	1.436	-0.758	-0.094
	Elastic	-35.869	-16.770	1.499	-0.770	-0.100
	Residual	-0.006	0.278	-0.063	0.012	0.006
600	Elasto-Plastic	-40.420	-18.271	1.481	-0.839	0.121
	Elastic	-40.370	-18.874	1.687	-0.867	-0.112
	Residual	-0.051	0.603	-0.206	0.027	-0.008

The expansion of residual stress σ_x along AB in symmetric cross-ply $[(0^0/90^0)_2]$ laminated plate is shown Figure 5.18.

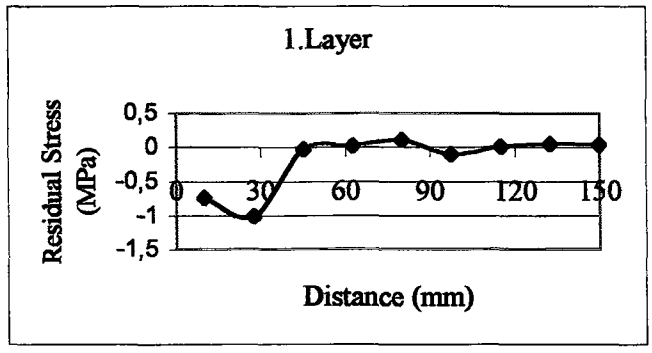

Fig. 5.18. The expansion of residual stress σ_x along AB in the symmetric $[(0^0/90^0)_2]$ laminated plate

The expansion of the plastic zone for symmetric angle-ply $[(30^0/-30^0)_2]$ laminated plate is shown in Figure 5.19. Elasto-plastic, elastic and residual stresses at upper surface of the angle-ply laminated plate (point A) for 200, 400, 600 iterations are given in Table 5.22. The expansion of residual stress σ_x for symmetric angle-ply $[(30/-30)_2]$ laminated plate is shown Figure 5.20.

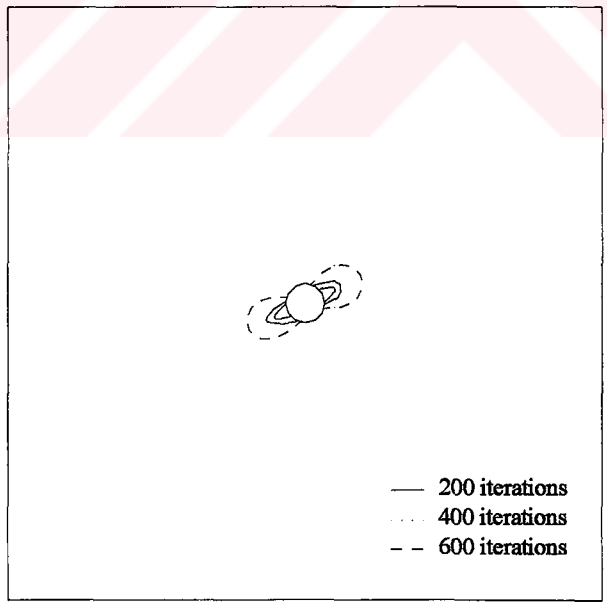

Fig. 5.19. Expansion of plastic zone in the symmetric $[(30^0/-30^0)_2]$ laminated plate

Table 5.22.. Elastic, elasto-plastic and residual stresses for symmetric angle-ply laminated plate with a circular hole $[(30^0/-30^0)_2]$ at point A 200-400-600 iterations.

Iterations	Stress	σ_x (MPa)	σ_y(MPa)	τ_{xy}(MPa)	τ_{yz}(MPa)	τ_{xz}(MPa)
200	Elasto-Plastic	-29.237	-14.375	-0.063	-0.704	-0.170
	Elastic	-29.367	-14.577	0.260	-0.665	-0.115
	Residual	0.131	0.202	-0.323	-0.039	-0.055
400	Elasto-Plastic	-33.575	-16.285	0.381	-0.871	-0.251
	Elastic	-33.711	-16.733	0.298	-0.764	-0.132
	Residual	0.136	0.448	-0.679	-0.107	-0.119
600	Elasto-Plastic	-33.979	-17.983	-0.968	-1.063	-0.415
	Elastic	-38.056	-18.890	0.337	-0.862	-0.149
	Residual	0.096	0.906	-1.305	-0.201	-0.267

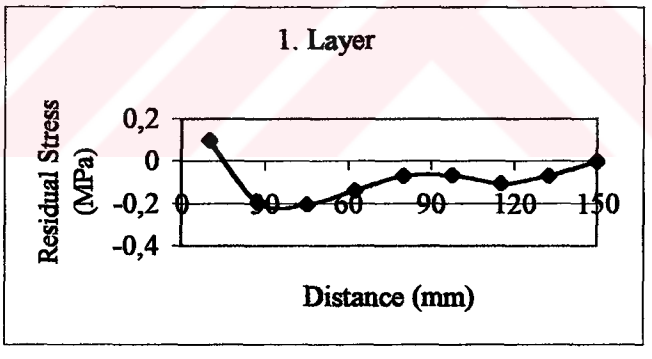

Fig. 5.20. The expansion of residual stress σ_x along AB in the symmetric $[(30^0/-30^0)_2]$ laminated plate

The expansion of the plastic zone for symmetric angle-ply $[(45^0/-45^0)_2]$ laminated plate is shown in Figure 5.21. Elasto-plastic, elastic and residual stresses at upper surface of the angle-ply laminated plate (point A) for 200, 400, 600 iterations are given in Table 5.23. The expansion of residual stress σ_x along AB for symmetric angle-ply $[(45^0/-45^0)_2]$ laminated plate is shown Figure 5.22.

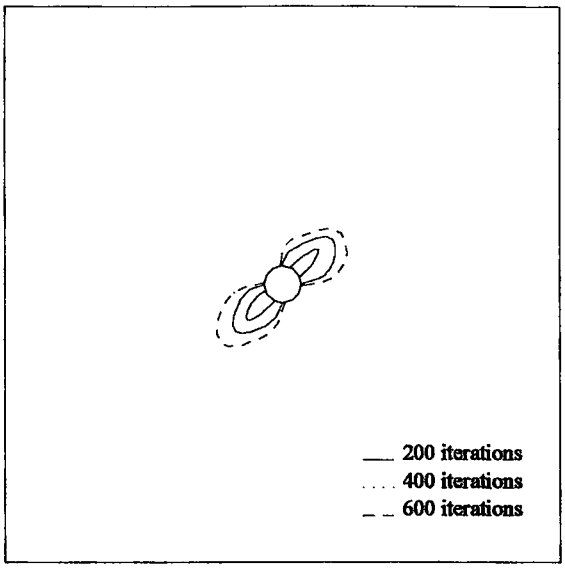

Fig. 5.21. Expansion of plastic zone in the symmetric $[(45^0/-45^0)_2]$ laminated plate

Table 5.23. Elastic, elasto-plastic and residual stresses for symmetric cross-ply laminated plate with a circular hole $[(45^0/-45^0)_2]$ at point A for 200-400-600 iterations.

Iterations	Stress	σ_x (MPa)	σ_y(MPa)	τ_{xy}(MPa)	τ_{yz}(MPa)	τ_{xz}(MPa)
200	Elasto-Plastic	-28.009	-14.438	-0.054	-0.737	-0.171
	Elastic	-28.094	-14.594	0.220	-0.680	-0.113
	Residual	0.085	0.156	-0.274	-0.057	-0.059
400	Elasto-Plastic	-32.162	-16.180	-0.484	-0.926	-0.238
	Elastic	-32.318	-16.789	0.253	-0.782	-0.130
	Residual	0.156	0.609	-0.737	-0.144	-0.108
600	Elasto-Plastic	-34.911	-16.393	-1.953	-1.005	-0.310
	Elastic	-36.543	-18.983	0.286	-0.885	-0.146
	Residual	1.632	2.586	-2.238	-0.121	-0.164

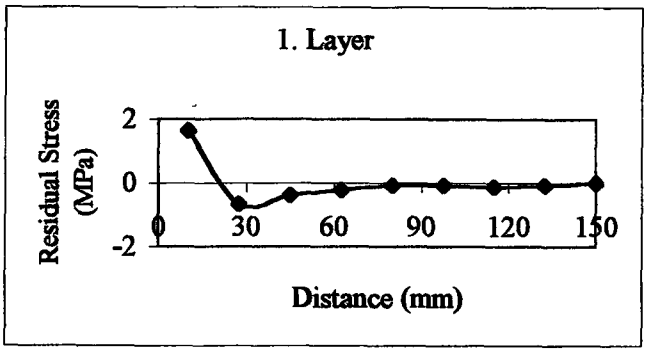

Fig. 5.22. The expansion of residual stress σ_x along AB in the symmetric $[(45^0/-45^0)_2]$ laminated plate

The expansion of the plastic zone for symmetric angle-ply $[(60^0/-60^0)_2]$ laminated plate is shown in Figure 5.23. Elasto-plastic, elastic and residual stresses at upper surface of the angle-ply laminated plate (point A) for 200, 400, 600 iterations are given in Table 5.24. The expansion of residual stress σ_x for symmetric angle-ply $[(60^0/-60^0)_2]$ laminated plate is shown Figure 5.24.

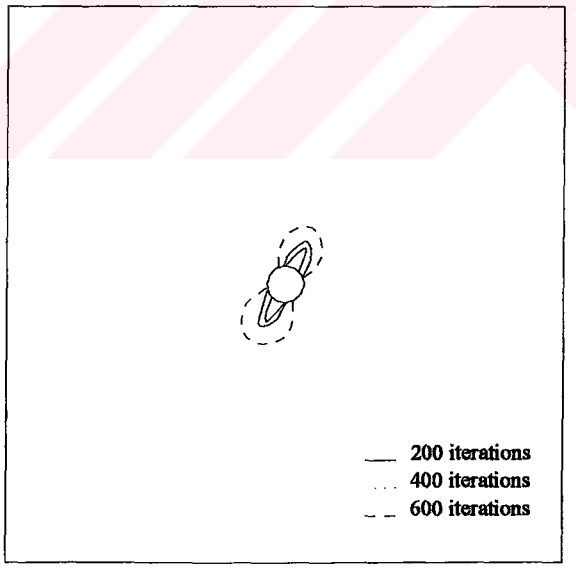

Fig. 5.23. Expansion of plastic zone in the symmetric $[(60^0/-60^0)_2]$ laminated plate

Table 5.24. Elastic, elasto-plastic and residual stresses for symmetric angle-ply laminated plate with a circular hole $[(60^0/-60^0)_2]$ at point A for 200-400-600 iterations.

Iterations		σ_x (MPa)	σ_y(MPa)	τ_{xy}(MPa)	τ_{yz}(MPa)	τ_{xz}(MPa)
200	Elasto-Plastic	-27.160	-14.383	-0.086	-0.738	-0.122
	Elastic	-27.872	-15.005	0.469	-0.720	-0.103
	Residual	0.711	0.622	-0.555	-0.018	-0.019
400	Elasto-Plastic	-28.662	-14.735	-1.462	-0.760	-0.107
	Elastic	-31.995	-17.224	0.538	-0.827	-0.118
	Residual	3.332	2.489	-2.000	0.067	0.011
600	Elasto-Plastic	-30.353	-15.036	-2.973	-0.803	-0.145
	Elastic	-36.118	-19.444	0.608	-0.993	-0.133
	Residual	5.765	4.408	-3.580	0.130	-0.012

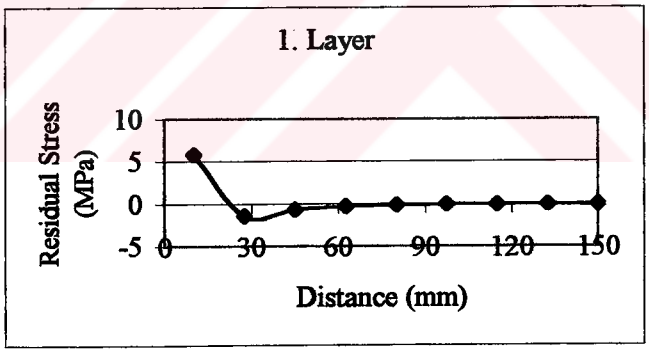

Fig. 5.24. The expansion of residual stress σ_x along AB in the symmetric $[(60^0/-60^0)_2]$ laminated plate

The expansion of the plastic zone at the upper and lower surfaces for antisymmetric cross-ply $[(0^0/90^0)_2]$ laminated plate are shown in Figure 5.25. (a) and (b). In antisymmetric plate, the plastic zone at the upper and lower surface is different. Elasto-plastic, elastic and residual stresses at (point A) upper and lower

surfaces of the cross-ply laminated plate for 200, 400, 600 iterations are given in Table 5.25. The expansion of residual stress σ_x for antisymmetric cross-ply $[(0^0/90^0)_2]$ laminated plate is shown Figure 5.26.

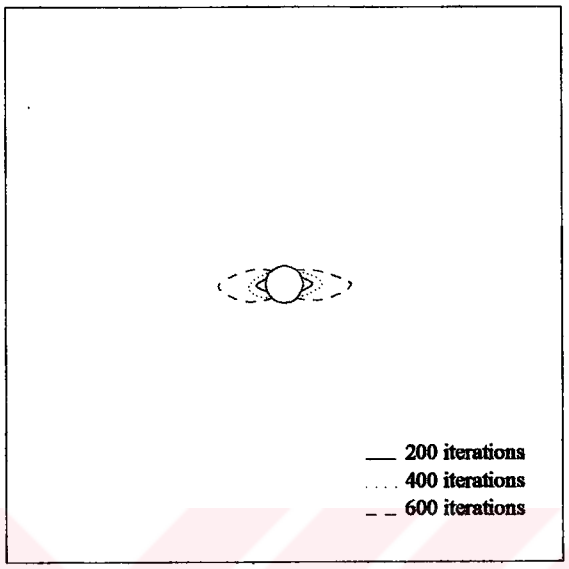

(a)

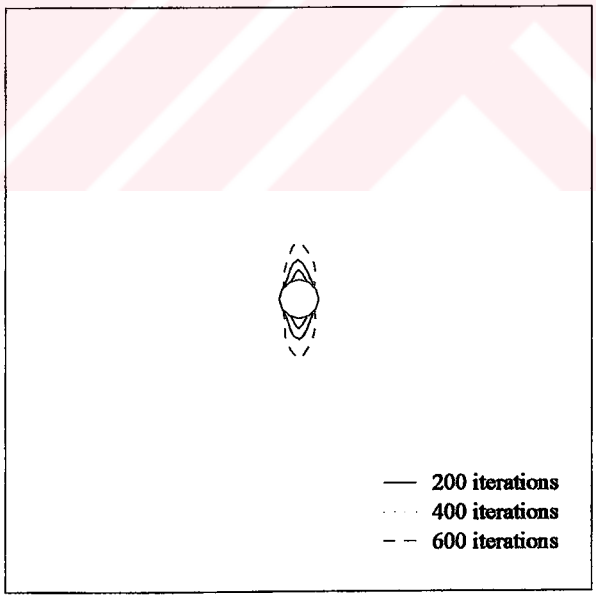

(b)

Fig. 5.25. Expansion of the plastic zone in the antisymmetric $[(0^0/90^0)_2]$ laminated plate **(a)** At the upper surface **(b)** At the lower surface

As seen from these Figures the expansion of plastic zone is different and expands in different directions at the upper and lower surfaces of the antisymmetric laminated plate. Also stress components are different at the upper and lower surfaces of the plate.

Table 5.25.. Elastic, elasto-plastic and residual stresses for antisymmetric cross-ply laminated plate with a circular hole $[(0^0/90^0)_2]$ at point A for 200-400-600 iterations.

Iterations	Stress	Layer	σ_x(MPa)	σ_y(MPa)	τ_{xy}(MPa)	τ_{yz}(MPa)	τ_{xz}(MPa)
200	Elasto-Plastic	1	-31.327	-14.693	1.399	-0.644	-0.034
		8	24.024	14.285	-1.400	-0.609	-0.034
	Elastic	1	-31.006	-14.687	-1.320	-0.711	-0.072
		8	28.090	15.462	-1.333	-0.711	-0.072
	Residual	1	-0.322	-0.007	0.079	0.067	0.039
		8	-4.066	-1.177	-0.068	0.103	0.039
400	Elasto-Plastic	1	-36.046	-16.718	1.591	-0.677	-0.023
		8	24.024	15.339	-1.637	-0.609	-0.023
	Elastic	1	-35.476	-16.804	1.511	-0.814	-0.083
		8	32.140	17.691	-1.525	-0.814	-0.083
	Residual	1	-0.570	0.086	0.080	0.137	0.060
		8	-8.116	-2.353	-0.112	0.205	0.060
600	Elasto-Plastic	1	-40.977	-18.755	1.748	-0.660	0.009
		8	24.025	16.450	-1.847	-0.609	0.008
	Elastic	1	-39.947	-18.922	1.701	-0.916	-0.093
		8	36.191	19.921	-1.717	-0.916	-0.093
	Residual	1	-1.029	0.167	0.048	0.257	0.102
		8	-12.166	-3.471	-0.131	0.308	0.101

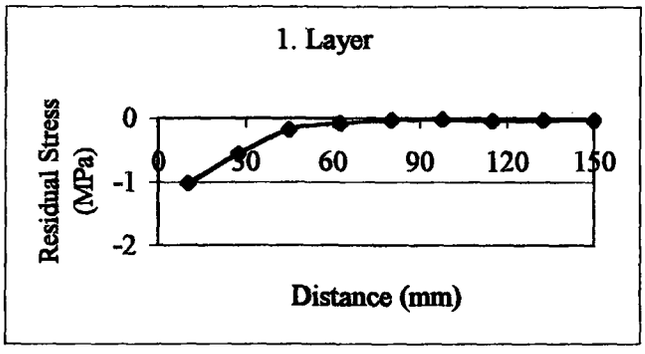

Fig. 5.26. The expansion of residual stress σ_x along AB in the antisymmetric $[(0^0/90^0)_2]$ laminated plate

The expansion of the plastic zone at the upper and lower surfaces for antisymmetric angle-ply $[(30^0/-30^0)_2]$ laminated plate are shown in Figure 5.27 (a) and (b). Elasto-plastic, elastic and residual stresses at (point A) upper and lower surfaces of the angle-ply laminated plate for 200, 400, 600 iterations are given in Table 5.26. The expansion of residual stress σ_x for antisymmetric angle-ply $[(30^0/-30^0)_2]$ laminated plate is shown Figure 5.28.

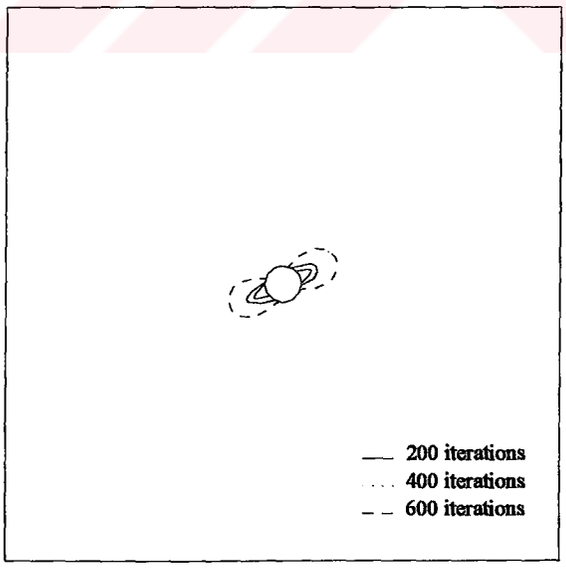

(a)

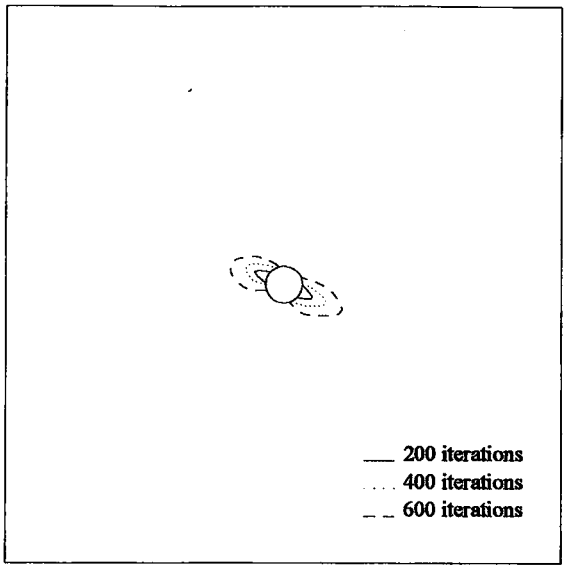

(b)

Fig. 5.27. Expansion of the plastic zone in the antisymmetric $[(30^0/-30^0)_2]$ laminated plate **(a)** At the upper surface **(b)** At the lower surface

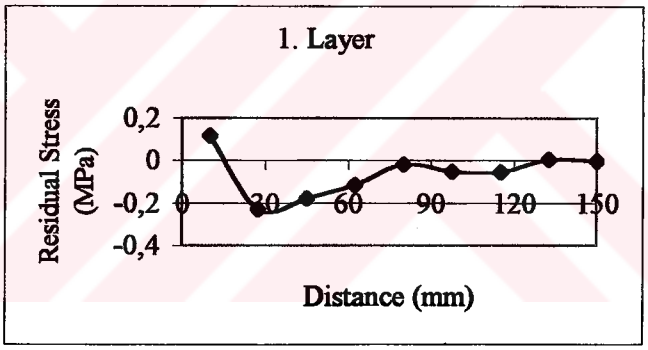

Fig. 5.28. The expansion of residual stress σ_x along AB in the antisymmetric $[(30^0/-30^0)_2]$ laminated plate

The expansion of the plastic zone at the upper and lower surfaces for antisymmetric angle-ply $[(45^0/-45^0)_2]$ laminated plate are shown in Figure 5.29 (a) and (b). Elasto-plastic, elastic and residual stresses at (point A) upper and lower surfaces of the angle-ply laminated plate for 200, 400, 600 iterations are given in Table 5.27. The expansion of residual stress σ_x for antisymmetric angle-ply $[(45^0/-45^0)_2]$ laminated plate is shown Figure 5.30.

Table 5.26. Elastic, elasto-plastic and residual stresses for antisymmetric angle-ply laminated plate with a circular hole $[(30^0/-30^0)_2]$ at point A for 200-400-600 iterations.

Iterations	Stress	Layer	σ_x(MPa)	σ_y(MPa)	τ_{xy}(MPa)	τ_{yz}(MPa)	τ_{xz}(MPa)
200	Elasto-Plastic	1	-29.675	-14.612	0.224	-0.680	-0.109
		8	29.962	14.843	-2.116	-0.680	-0.109
	Elastic	1	-29.797	-14.810	0.464	-0.669	-0.081
		8	29.981	14.932	-2.174	-0.669	-0.081
	Residual	1	0.122	0.198	-0.240	-0.010	-0.029
		8	-0.018	-0.089	0.059	-0.010	-0.029
400	Elasto-Plastic	1	-34.041	-16.561	0.152	-0.826	-0.152
		8	34.373	16.858	-2.436	-0.826	-0.152
	Elastic	1	-34.134	-16.966	0.532	-0.767	-0.092
		8	34.345	17.106	-2.491	-0.767	-0.092
	Residual	1	0.093	0.406	-0.379	-0.059	-0.060
		8	0.029	-0.248	0.055	-0.059	-0.060
600	Elasto-Plastic	1	-38.356	-18.315	-0.039	-0.964	-0.227
		8	38.815	18.721	-2.768	-0.964	-0.227
	Elastic	1	-38.471	-19.122	0.599	-0.864	-0.104
		8	38.709	19.279	-2.807	-0.864	-0.104
	Residual	1	0.115	0.808	-0.639	-0.099	-0.123
		8	0.106	-0.559	0.039	-0.099	-0.123

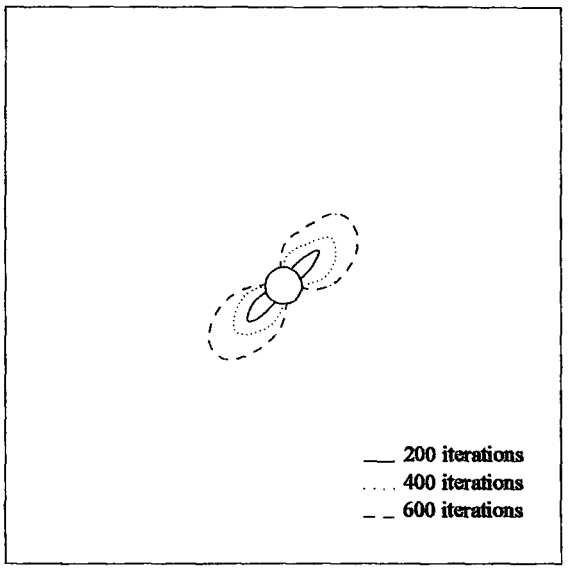

(a)

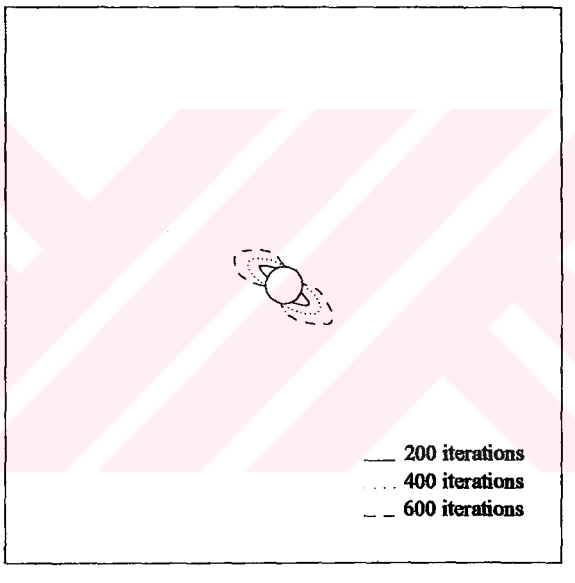

(b)

Fig. 5.29. Expansion of the plastic zone in the antisymmetric $[(45^0/-45^0)_2]$ laminated plate **(a)** At the upper surface **(b)** At the lower surface

As seen from these Figures plastic zone expands in different directions at the upper and lower surfaces of the plate and it spreads at the upper surface more than at the lower surface.

Table 5.27. Elastic, elasto-plastic and residual stresses for antisymmetric angle-ply laminated plate with a circular hole $[(45^0/-45^0)_2]$ at point A for 200-400-600 iterations.

Iteration	Stress	Layer	σ_x(MPa)	σ_y(MPa)	τ_{xy}(MPa)	τ_{yz}(MPa)	τ_{xz}(MPa)
200	Elasto-Plastic	1	-28.477	-14.707	0.334	-0.730	-0.106
		8	28.697	14.933	-2.173	-0.730	-0.106
	Elastic	1	-28.547	-14.852	0.446	-0.684	-0.070
		8	28.731	15.039	-2.198	-0.684	-0.070
	Residual	1	0.070	0.145	-0.112	-0.046	-0.036
		8	-0.034	-0.106	0.025	-0.046	-0.036
400	Elasto-Plastic	1	-31.969	-15.823	-0.171	-0.855	-0.137
		8	32.247	16.126	-2.997	-0.854	-0.136
	Elastic	1	-32.763	-17.046	0.512	-0.785	-0.080
		8	32.975	17.261	-2.523	-0.785	-0.080
	Residual	1	0.795	1.222	-0.682	-0.070	-0.057
		8	-0.727	-1.135	-0.474	-0.069	-0.056
600	Elasto-Plastic	1	-34.460	-15.728	-1.339	-0.911	-0.165
		8	34.971	16.197	-4.381	-0.909	-0.165
	Elastic	1	-36.980	-19.240	0.577	-0.886	-0.090
		8	37.218	19.482	-2.848	-0.886	-0.090
	Residual	1	2.520	3.511	-1.917	-0.025	-0.075
		8	-2.248	-3.285	-1.533	-0.023	-0.074

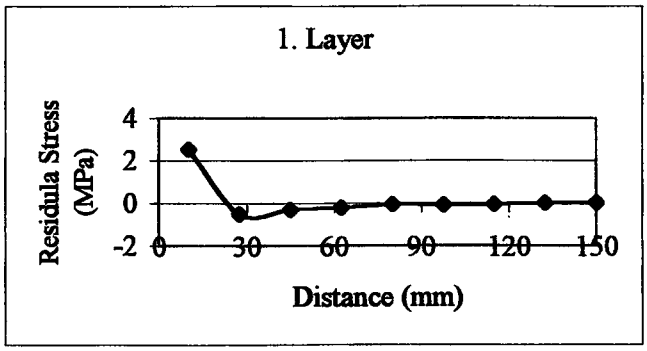

Fig. 5.30. The expansion of residual stress σ_x along AB in the antisymmetric $[(45^0/-45^0)_2]$ laminated plate

The expansion of the plastic zone at the upper and lower surfaces for antisymmetric angle-ply $[(60^0/-60^0)_2]$ laminated plate are illustrated in Figure 5.31. (a) and (b). Elasto-plastic, elastic and residual stresses at (point A) upper and lower surfaces of the angle-ply laminated plate for 200, 400, 600 iterations are given in Table 5.28. The expansion of residual stress σ_x for antisymmetric angle-ply $[(60^0/-60^0)_2]$ laminated plate is shown Figure 5.32.

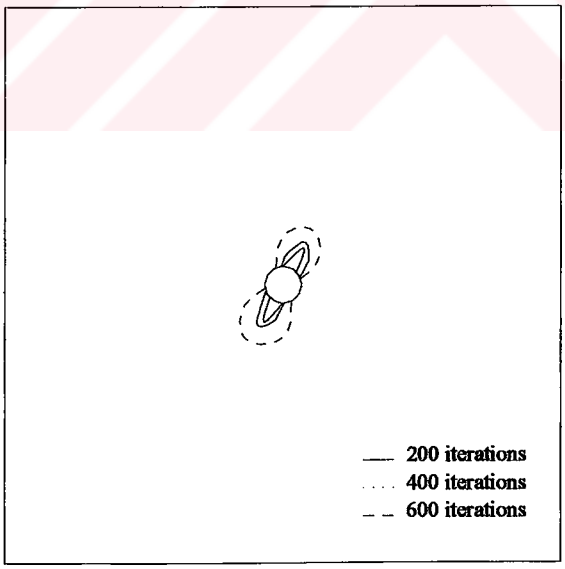

(a)

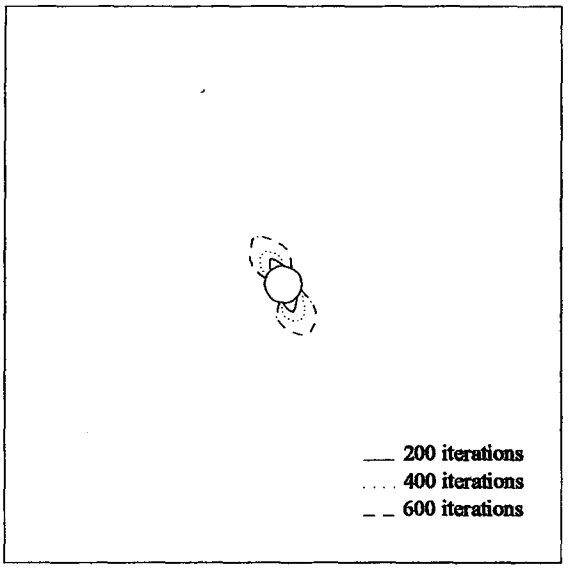

(b)

Fig. 5.31.. Expansion of the plastic zone in the antisymmetric $[(60^0/-60^0)_2]$ laminated plate **(a)** At the upper surface **(b)** At the lower surface

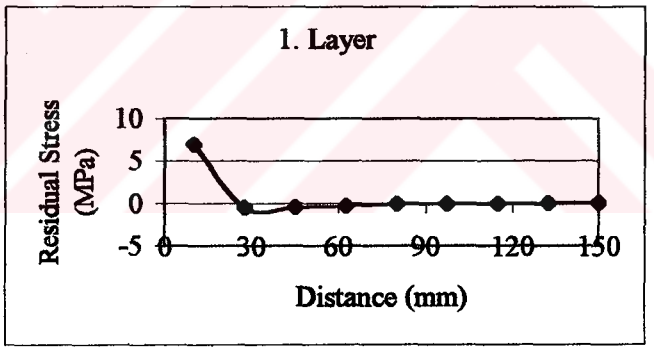

Fig. 5.32. The expansion of residual stress σ_x along AB in the antisymmetric $[(60^0/-60^0)_2]$ laminated plate

Table 5.28. Elastic, elasto-plastic and residual stresses for antisymmetric angle-ply laminated plate with a circular hole $[(60^0/-60^0)_2]$ at point A for 200-400-600 iterations.

Iterations	Stress	Layer	σ_x(MPa)	σ_y(MPa)	τ_{xy}(MPa)	τ_{yz}(MPa)	τ_{xz}(MPa)
200	Elasto-Plastic	1	-26.997	-14.139	0.093	-0.724	-0.076
		8	27.223	14.557	-2.612	-0.727	-0.076
	Elastic	1	-28.284	-15.248	0.667	-0.724	-0.061
		8	28.423	15.458	-2.035	-0.724	-0.061
	Residual	1	1.287	0.929	-0.574	-0.001	-0.014
		8	-1.200	-0.901	-0.578	-0.003	-0.015
400	Elasto-Plastic	1	-28.276	-14.593	-1.067	-0.756	-0.073
		8	28.867	15.004	-4.127	-0.766	-0.073
	Elastic	1	-32.401	-17.467	0.764	-0.829	-0.070
		8	32.561	17.708	-2.331	-0.829	-0.070
	Residual	1	4.125	2.875	-1.831	0.074	-0.003
		8	-3.694	-2.704	-1.796	0.064	-0.003
600	Elasto-Plastic	1	-29.627	-14.818	-2.257	-0.769	-0.073
		8	30.609	15.393	-5.735	-0.780	-0.072
	Elastic	1	-36.518	-19.958	0.861	-0.935	-0.079
		8	36.698	19.958	-2.627	-0.935	-0.079
	Residual	1	6.890	4.869	-3.118	0.165	0.006
		8	-6.089	-4.565	-3.108	0.155	0.007

5.2.2. Antisymmetric Laminated Plates of Four Layers

In this case, the layers are bonded antisymmetrically, as $[(0^0)_2/(90^0)_2]$, $[(30^0)_2/(-30^0)_2]$, $[(45^0)_2/(-45^0)_2]$ and $[(60^0)_2/(-60^0)_2]$. The transverse uniform load at the yield point of the plates is given in Table 5.29.

Table 5.29. The uniform transverse force at the yield points of the antisymmetric four laminated plates.

	$[(0^0)_2/(90^0)_2]$	$[(30^0)_2/(-30^0)_2]$	$[(45^0)_2/(-45^0)_2]$	$[(60^0)_2/(-60^0)_2]$
Transverse load (MPa)	0.1168	0.1154	0.1130	0.1154

The expansion of the plastic zone at the upper and lower surfaces for antisymmetric cross-ply $[(0^0)_2/(90^0)_2]$ laminated plate are shown in Figure 5.33. (a) and (b). In antisymmetric plate, the plastic zone at the upper and lower surface is different. Elasto-plastic, elastic and residual stresses at (point A) upper and lower surfaces of the cross-ply laminated plate for 200, 400, 600 iterations are given in Table 5.30. The expansion of residual stress σ_x for antisymmetric cross-ply $[(0^0)_2/(90^0)_2]$ laminated plate is illustrated Figure 5.34.

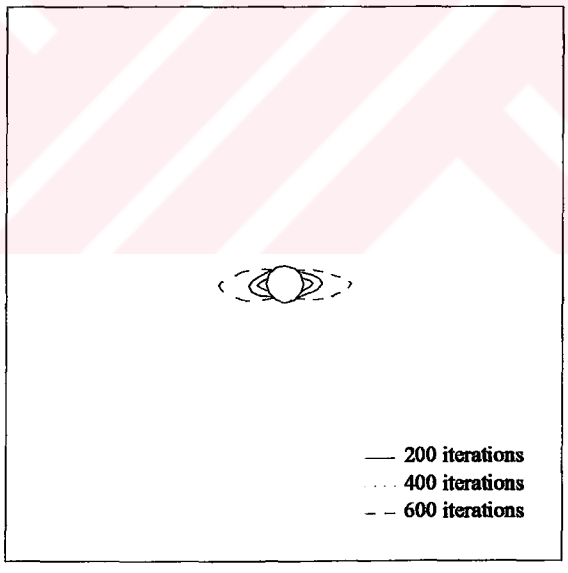

(a)

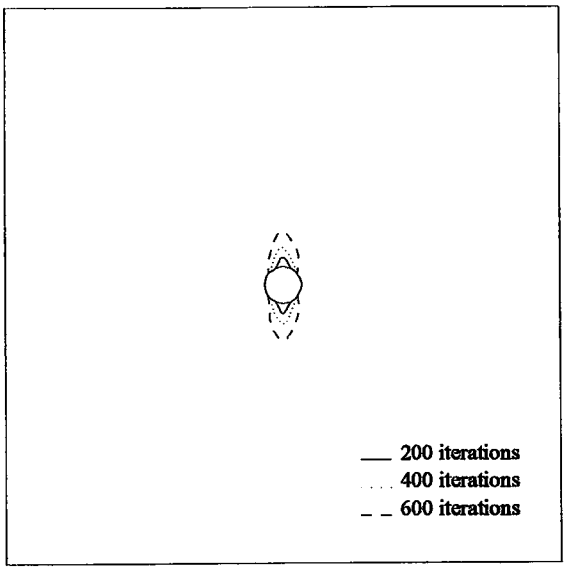

(b)

Fig. 5.33. Expansion of the plastic zone in the antisymmetric $[(0^0)_2/(90^0)_2]$ laminated plate **(a)** At the upper surface **(b)** At the lower surface

As seen from these Figures the plastic zone is different at the upper and lower surfaces of the plate.

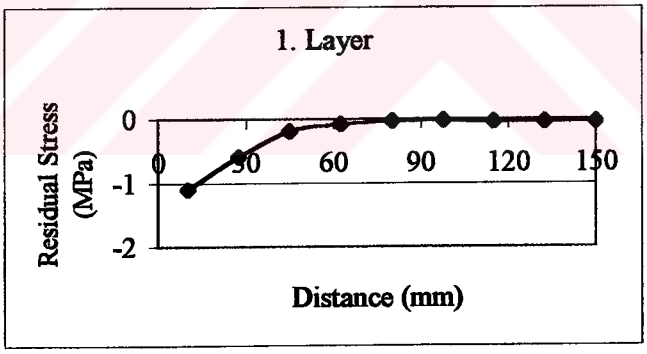

Fig. 5.34. The expansion of residual stress σ_x along AB in the antisymmetric $[(0^0)_2/(90^0)_2]$ laminated plate

Table 5.30. Elastic, elasto-plastic and residual stresses for antisymmetric cross-ply laminated plate with a circular hole $[(0^0)_2/(90^0)_2]$ at point A for 200-400-600 iterations.

Iterations	Stress	Layer	σ_x(MPa)	σ_y(MPa)	τ_{xy}(MPa)	τ_{yz}(MPa)	τ_{xz}(MPa)
200	Elasto-Plastic	1	-30.479	-14.627	1.377	-0.631	-0.031
		8	24.025	13.945	-1.390	-0.598	-0.031
	Elastic	1	-30.418	-14.620	1.296	-0.701	-0.071
		8	28.149	15.140	-1.320	-0.701	-0.071
	Residual	1	-0.330	-0.007	0.081	0.069	0.040
		8	-4.124	-1.195	-0.070	0.102	0.040
400	Elasto-Plastic	1	-35.164	-16.672	1.577	-0.655	-0.015
		8	24.025	14.964	-1.631	-0.598	-0.015
	Elastic	1	-34.556	-16.758	1.485	-0.803	-0.081
		8	32.264	17.353	-1.513	-0.803	-0.081
	Residual	1	-0.608	0.086	0.092	0.148	0.067
		8	-8.239	-2.389	-0.117	0.205	0.067
600	Elasto-Plastic	1	-40.069	-18.729	1.735	-0.628	0.021
		8	24.026	16.043	-1.851	-0.598	0.021
	Elastic	1	-38.964	-18.895	1.675	-0.905	-0.092
		8	36.380	19.566	-1.706	-0.905	-0.092
	Residual	1	-1.105	0.166	0.060	0.278	0.113
		8	-12.353	-3.523	-0.144	0.307	0.113

As seen from this Table stress components are different at the upper and lower surfaces of the plate.

The expansion of the plastic zone at the upper and lower surfaces for antisymmetric angle-ply $[(30^0)_2/(-30^0)_2]$ laminated plate are shown in Figure 5.35. (a) and (b). Elasto-plastic, elastic and residual stresses at (point A) upper and lower

surfaces of the angle-ply laminated plate for 200, 400, 600 iterations is shown in Table 5.31. The expansion of residual stress σ_x for antisymmetric angle-ply $[(30^0)_2/(-30^0)_2]$ laminated plate is shown Figure 5.36.

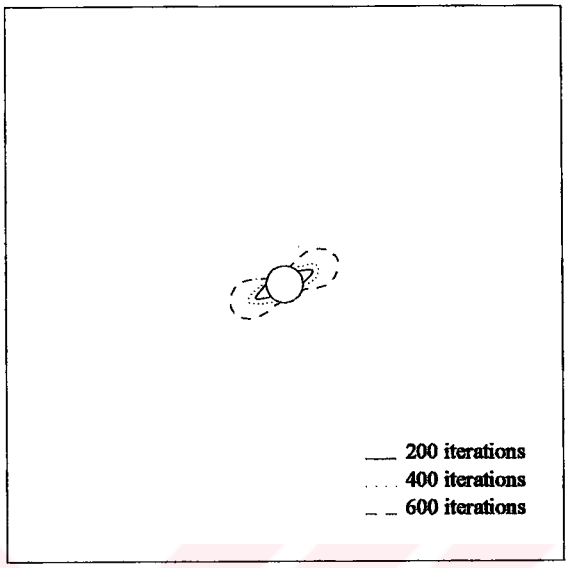

(a)

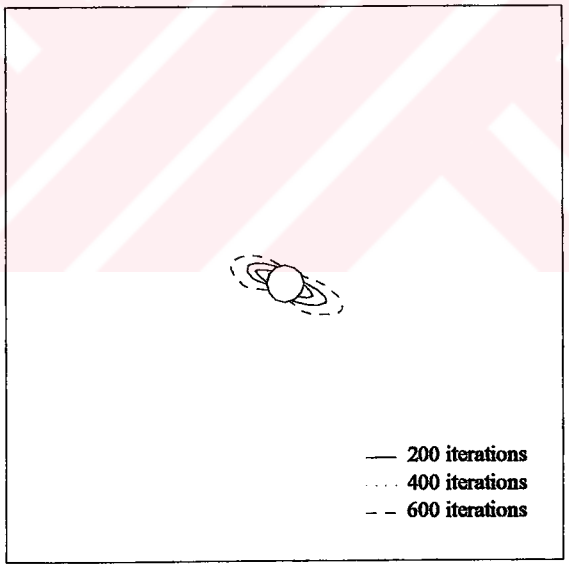

(b)

Fig. 5.35. Expansion of the plastic zone in the antisymmetric $[(30^0)_2/(-30^0)_2]$ laminated plate **(a)** At the upper surface **(b)** At the lower surface

Table 5.31.. Elastic, elasto-plastic and residual stresses for antisymmetric angle-ply laminated plate with a circular hole $[(30^0)_2/(-30^0)_2]$ at point A for 200-400-600 iterations.

Iterations	Stress	Layer	σ_x(MPa)	σ_y(MPa)	τ_{xy}(MPa)	τ_{yz}(MPa)	τ_{xz}(MPa)
200	Elasto-Plastic	1	-29.277	-14.629	0.496	-0.671	-0.109
		8	29.495	14.603	-1.802	-0.671	-0.109
	Elastic	1	-29.405	-14.628	0.738	-0.660	-0.079
		8	29.511	14.690	-1.862	-0.660	-0.079
	Residual	1	0.128	0.199	-0.242	-0.010	-0.029
		8	-0.016	-0.087	0.060	-0.010	-0.029
400	Elasto-Plastic	1	-33.643	-16.364	0.449	-0.820	-0.154
		8	33.905	16.606	-2.079	-0.820	-0.154
	Elastic	1	-33.749	-16.789	0.847	-0.758	-0.091
		8	33.870	16.860	-2.137	-0.758	-0.091
	Residual	1	0.106	0.425	-0.398	-0.063	-0.063
		8	0.036	-0.254	0.058	-0.063	-0.063
600	Elasto-Plastic	1	-37.946	-18.098	0.280	-0.960	-0.234
		8	38.338	18.447	-2.366	-0.960	-0.234
	Elastic	1	-38.092	-18.950	0.956	-0.855	-0.103
		8	38.229	19.030	-2.412	-0.855	-0.103
	Residual	1	0.147	-0.852	-0.676	-0.105	-0.131
		8	0.109	-0.582	0.045	-0.105	-0.131

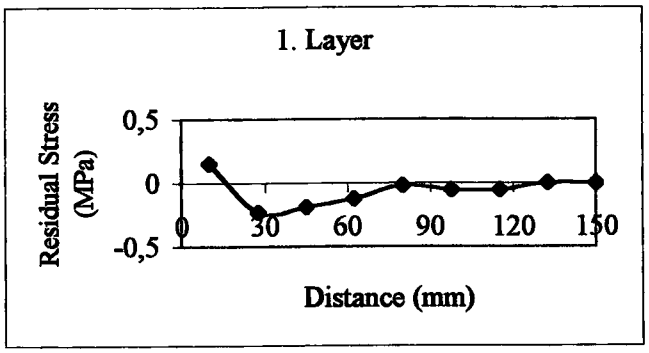

Fig. 5.36. The expansion of residual stress σ_x along AB in the antisymmetric $[(30^0)_2/(-30^0)_2]$ laminated plate

The expansion of the plastic zone at the upper and lower surfaces for antisymmetric angle-ply $[(45^0)_2/(-45^0)_2]$ laminated plate are shown in Figure 5.37. (a) and (b). Elasto-plastic, elastic and residual stresses at (point A) upper and lower surfaces of the angle-ply laminated plate for 200, 400, 600 iterations are given in Table 5.32. The expansion of residual stress σ_x for antisymmetric angle-ply $[(45^0)_2/(-45^0)_2]$ laminated plate is shown Figure 5.38.

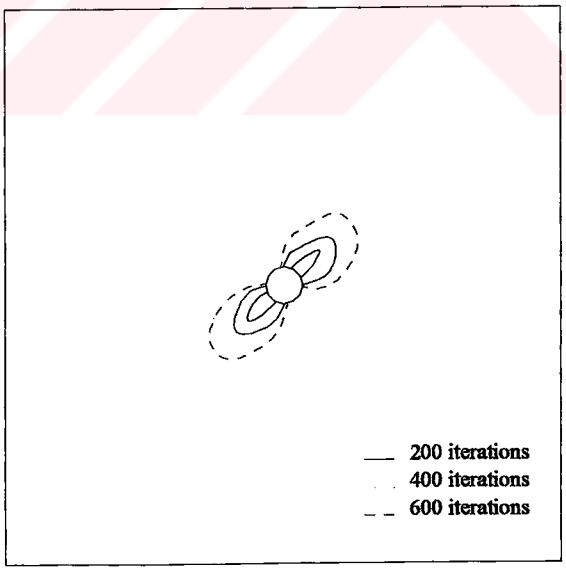

(a)

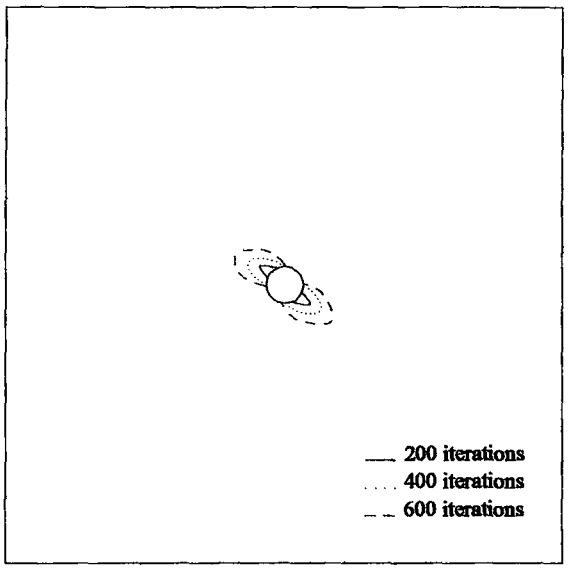

(b)

Fig. 5.37. Expansion of the plastic zone in the antisymmetric $[(45^0)_2/(-45^0)_2]$ laminated plate **(a)** At the upper surface **(b)** At the lower surface

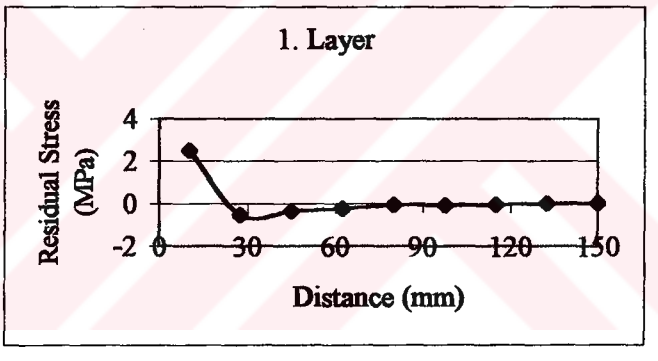

Fig. 5.38. The expansion of residual stress σ_x along AB in the antisymmetric $[(45^0)_2/(-45^0)_2]$ laminated plate

The expansion of the plastic zone at the upper and lower surfaces for antisymmetric angle-ply $[(60^0)_2/(-60^0)_2]$ laminated plate are shown in Figure 5.39. (a) and (b). Elasto-plastic, elastic and residual stresses at (point A) upper and lower surfaces of the angle-ply laminated plate for 200, 400, 600 iterations are given in Table 5.33. The expansion of residual stress σ_x for antisymmetric angle-ply $[(60^0)_2/(-60^0)_2]$ laminated plate is illustrated Figure 5.40.

Table 5.32. Elastic, elasto-plastic and residual stresses for antisymmetric angle-ply laminated plate with a circular hole $[(45^0)_2/(-45^0)_2]$ at point A for 200-400-600 iterations.

Iterations	Stress	Layer	σ_x(MPa)	σ_y(MPa)	τ_{xy}(MPa)	τ_{yz}(MPa)	τ_{xz}(MPa)
200	Elasto-Plastic	1	-28.011	-14.475	0.618	-0.718	-0.105
		8	28.165	-1.834	-0.718	-0.718	-0.105
	Elastic	1	-28.084	-14.625	0.735	-0.671	-0.069
		8	28.196	14.743	-1.861	-0.671	-0.069
	Residual	1	0.073	0.149	-0.117	-0.047	-0.037
		8	-0.030	-0.106	0.027	-0.047	-0.037
400	Elasto-Plastic	1	-31.530	-15.619	0.160	-0.848	-0.141
		8	31.726	15.830	-2.596	-0.848	-0.141
	Elastic	1	-32.307	-16.824	0.845	-0.772	-0.079
		8	32.436	16.960	-2.141	-0.772	-0.079
	Residual	1	0.777	1.204	-0.685	-0.076	-0.062
		8	-0.709	-1.130	-0.454	-0.075	-0.062
600	Elasto-Plastic	1	-34.036	-15.467	-0.985	-0.907	-0.172
		8	34.439	15.839	-3.958	-0.905	-0.172
	Elastic	1	-36.530	-19.023	0.956	-0.873	-0.089
		8	36.676	19.177	-2.421	-0.873	-0.089
	Residual	1	2.494	3.556	-1.941	-0.034	-0.083
		8	-2.236	-3.337	-1.537	-0.032	-0.083

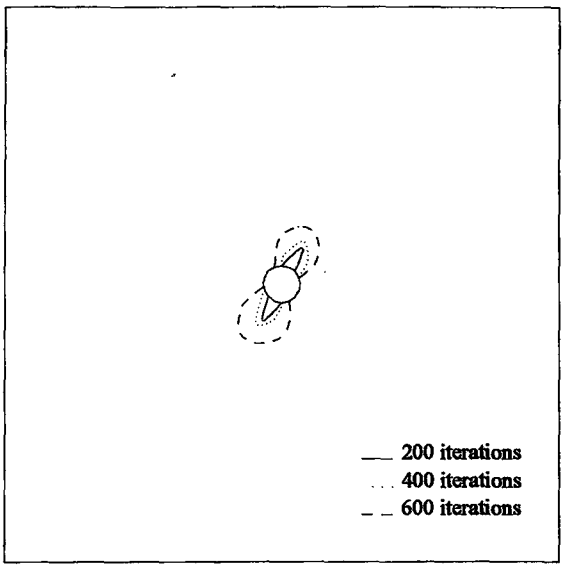

(a)

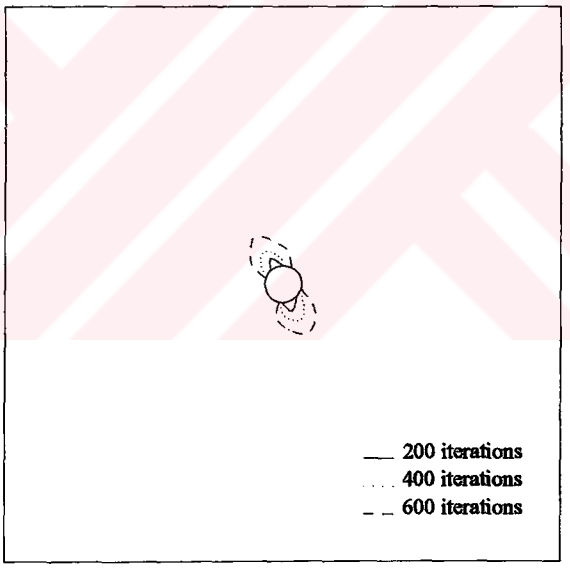

(b)

Fig. 5.39. Expansion of the plastic zone in the antisymmetric $[(60^0)_2/(-60^0)_2]$ laminated plate **(a)** At the upper surface **(b)** At the lower surface

Table 5.33. Elastic, elasto-plastic and residual stresses for antisymmetric angle-ply laminated plate with a circular hole $[(60^0)_2/(-60^0)_2]$ at point A for 200-400-600 iterations.

Iterations	Stress	Layer	σ_x(MPa)	σ_y(MPa)	τ_{xy}(MPa)	τ_{yz}(MPa)	τ_{xz}(MPa)
200	Elasto-Plastic	1	-26.724	-14.192	0.374	-0.720	-0.078
		8	26.899	14.370	-2.289	-0.722	-0.078
	Elastic	1	-27.905	-15.056	0.899	-0.712	-0.061
		8	27.998	15.206	-1.762	-0.712	-0.061
	Residual	1	1.181	0.864	-0.525	-0.007	-0.017
		8	-1.099	-0.836	-0.527	-0.010	-0.017
400	Elasto-Plastic	1	-27.982	-14.443	-0.762	-0.753	-0.077
		8	28.518	14.785	-3.775	-0.764	-0.077
	Elastic	1	-32.027	-17.280	1.032	-0.818	-0.069
		8	32.133	17.452	-2.022	-0.818	-0.069
	Residual	1	4.046	2.837	-1.794	0.065	-0.008
		8	-3.615	-2.667	-1.753	0.054	-0.008
600	Elasto-Plastic	1	-29.298	-14.630	-1.913	-0.767	-0.079
		8	30.283	15.161	-5.346	-0.781	-0.079
	Elastic	1	-36.149	-19.504	1.165	-0.923	-0.078
		8	36.269	19.698	-2.283	-0.923	-0.078
	Residual	1	6.851	4.873	-3.078	0.156	-0.001
		8	-5.986	-4.537	-3.064	0.142	0.000

As seen from these Figures and Tables the expansion of plastic zone and stress components are different at the upper and lower surfaces of the antisymmetric laminated plates.

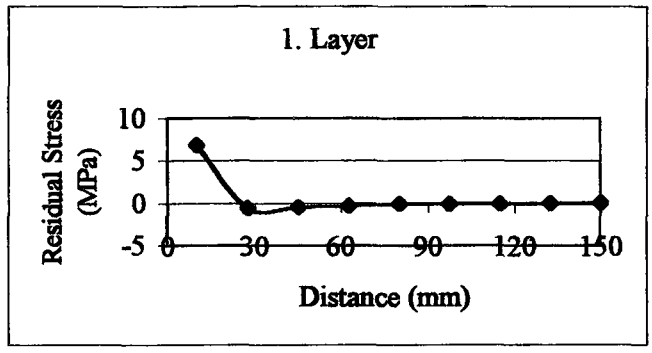

Fig. 5.40. The expansion of residual stress σ_x along AB in the antisymmetric $[(60^0)_2/(-60^0)_2]$ laminated plate

CONCLUSIONS

Elasto-plastic stress analysis has been carried out by using the first order shear deformation theory in aluminum-steel fiber laminated plates under transverse loading. The expansion of the plastic zone and elastic, elasto-plastic, residual stresses are obtained in symmetric and antisymmetric cross-ply and angle-ply laminated plates without a hole and with a hole. The following results of elasto-plastic stress analysis are obtained.

Metal fiber reinforced metal-matrix composite layer gives the higher improved mechanical properties such as, higher yield points and stiffnesses.

The orientation angle affects the yield points of laminated plates.

The yield points of symmetric laminated plates are higher than those of antisymmetric laminated plates without a hole.

The expansion of plastic zone and stress components are the same at the upper and lower surfaces of the symmetric laminated plates in absolutely.

The expansion of plastic zone is different at the upper and lower surface of the antisymmetric laminated plates.

The yield points in antisymmetric laminated plate without a hole as $[(0^0)_2/(90^0)_2]$, $[(30^0)_2/(-30^0)_2]$, $[(45^0)_2/(-45^0)_2]$ and $[(60^0)_2/(-60^0)_2]$ are less than those in the symmetric and antisymmetric $[(0^0/90^0)_2]$, $[(30^0/-30^0)_2]$, $[(45^0/-45^0)_2]$ and $[(60^0/-60^0)_2]$. The yield

points in antisymmetric laminated plate as $(0^0/90^0)$, $(30^0/-30^0)$, $(45^0/-45^0)$ and $(60^0/-60^0)$ are the smallest.

The yield points for plate with a circular hole are higher than the yield points of the plate without a hole.

The yield points in antisymmetric laminated plate with a circular hole as $[(0^0)_2/(90^0)_2]$, $[(30^0)_2/(-30^0)_2]$, $[(45^0)_2/(-45^0)_2]$ and $[(60^0)_2/(-60^0)_2]$ are less than those in the symmetric and antisymmetric $[(0^0/90^0)_2]$, $[(30^0/-30^0)_2]$, $[(45^0/-45^0)_2]$ and $[(60^0/-60^0)_2]$.

In each case for plate with a circular hole yielding occurs around the hole.

If iteration numbers are increased the residual stress components become greater .

The strength of the laminated plates can be increased by using residual stresses.

REFERENCES

Bahei-El-Din, Y.A., & Dvorak, G.J. (1982). Plasticity analysis of laminated composite plates. Transactions of the Asme, 49, 740-746.

Yeh, N.M., & Krempl, E. (1993). The influence of cool-down temperature histories on the residual stresses in fibrous metal-matrix composites. Journal of Composite Materials, 27, 973-995.

Doghri,I., Jansson, D.S., Leckie, F.A., & Lemaitre, J. (1994). Optimization of coating layers in the design of ceramic fiber reinforced metal matrix composites. Journal of Composite Materials, 28,167-187.

Canumalla, S., Dynan, S.A., & Green, D.J. (1995). Mechanical behavior of mullite fiber reinforced aluminum alloy composites. Journal of Composite Materials, 29, 653-669.

Nicolaou, P.D. Piehler, H.R. & Saigal S. (1994). Experimental and finite element analytical guidelines for fabricating continuous fiber (SCS-6) metal matrix (Ti-6AI-4V) composites via the foil/fiber/foil technique. Journal of Composite Materials, 28, 1694-1722.

Karakuzu , R., & Özcan , R. (1997). Exact solution of elasto-plastic stresses in a metal-matrix composite beam of arbitrary orientation subjected to transverse loads. Composite Science and Technology, 56, 1383-1389.

Chou, T.W., Kelly, A. & Okura, A. (1985). Fibre-reinforced metal-matrix composites. Journal of Composite Materials, 16, 187-206.

Kang, C.G., & Kang, S.S. (1994). Effect of extrusion on fibre orientation and breakage of aluminar short fibre composites. Journal of Composite Materials, 28, 155-165.

Cöcen, Ü., Önel, K., & Özdemir, İ. (1997). Microstructures and age hardenability of Al-5% Si-0.2% Mg based composites reinforced with particulate SiC. Composite Science and Technology, 57, 801-808.

Kang, C.G., & Ku, G.S. (1995). An experimental investigation on infiltration limit and the mechanical properties of Al_2O_3 short fiber reinforced metal-matrix composites fabricated by squeeze casting. Journal of Composite Materials, 29, 444-462.

Pitchumani, R., Liaw , P.K., Yao, S.C., Nsu, D.K., & Jeong, H. (1994). An eddy current technique for the measurement of constituent volume fractions in a three-phase metal-matrix composite. Journal of Composite Materials, 28, 1743-1769.

Ananth, C.R., & Chandra, N. (1995). Numerical modeling of fibre push-out test in metalic and intermetalic matrix composites-mechanics of the failure process. Journal of Composite Materials, 29, 1488-1514.

Karakuzu, R., & Sayman, O. (1993). Elasto-plastic finite element analysis of orthotropic rotating discs with holes. Computers and Structures, 51, 695-703.

Karakuzu, R., Özel, A., & Sayman, O. (1997). Elasto-plastic finite element analysis of metal-matrix plates with edge notches. Computers and Structures, 63, 551-558.

Jeronimidis, G., & Parkyn, A.T. (1988). Residual stresses in carbon fibre-thermoplastic matrix laminates. Journal of Composite Materials, 22, 401-415.

Unger, W.J., & Hansen, S. (1993). The effect of thermal processing on residual strain development in unidirectional graphite fiber-reinforced PEEK. Journal of Composite Materials, 27, 59-81.

Pomies, F., & Carlsson, L.A. (1994). Analysis of modulus and strength of dry and wet thermoset and thermoplastic composites loaded in transverse tension. Journal of Composite Materials, 28, 22-35.

Zocher, M.A., Allen, D.H., Groves, S.E., & Feng, W.W. (1995). Evaluation of first ply failure in a three- dimensional load space. Journal of Composite Materials, 29, 1649-1678.

Karakaya, M., & Şehitoğlu, H. (1996). Failure behavior of unidirectional AS4/3501-G carbon-epoxy laminates, Journal of Composite Materials, 30, 1150-1176.

Yang, H.T.Y., & He, C.C. (1994). Three dimensional finite element analysis of free edge stresses and delamination of composite laminates. Journal of Composite Materials, 28, 1394-1412.

Hu, H.T., & Schnobrich, W.C. (1991). Nonlinear finite element analysis of reinforced concrete plates and shells under monotonic loading. Computers and Structures, 38, 637-651.

Choi, C.K., & Kwak, H.G. (1990). The effect of finite element mesh size in nonlinear analysis of reinforced concrete structures. Computers and Structures, 36, 807-815.

Owen, D.R.J. (1983). Anisotropic elasto-plastic finite element analysis of thick and thin plates and shells, Int. Journal for Numerical Methods in Eng., 19, 541-566.

Theo, J, (1981). Stress around rectangular holes in orthotropic plates., Journal of Composite Materials., 15, 311-328.

Lin, C.C., & Kuo, C.S. (1989). Buckling of laminated plates with holes. Journal of Composite Materials, 23, 536-553.

Bathe, K.J. (1982). Finite element procedures in engineering analysis. Prentice-Hall, Inc., Englewood Cliff, New Jersey.

Jones, R.M. (1975). Mechanics of composite materials. McGraw-Hill Kogakusha, Ltd.

Crisfield, M.A. (1991). Non- linear finite element analysis of solids and structures, John Wiley & Sons.

Chkrabarty, J. (1988). Theory of plasticity. McGraw-Hill Book Company.

Zienkiewicz, O.C., Valliappand, S., & King, I.P. (1963). Elasto-plastic solutions of engineering problems 'initial stress', finite element approach. Int. J. Numer. Meth. Eng. 1, 75-100.

Tsai, S.W., & Hahn, H.T. (1980). Introduction to composite materials. Technomic Publishing Company.

Lekhnitskii, S.G., Tsai, S.W., & Cheron, T. (1968). Anisotropic plates. Gordon and Breach Science Publishers.

Mendelson, A. (1968). Plasticity: theory and application. The Macmillan Company, Newyork.

Vinson, J.R., & Chou, T.W. (1975). Composite materials and their use in structures. Applied Science Publishers, London.

Chandrupatla, T.R., & Belegundu, A.D. (1991). Introduction to finite elements in engineering. New Jersey: Prentice-Hall, Inc., Englewood Cliffs.

Nath, B. (1974). Fundamentals of finite elements for engineers. Humanities Press.

Sayman, O., & Aksoy, S. (1987). Kompozit malzemeler, DEÜ Müh. Fak.

Timeshenko, S., & Goodier, J.N. (1951). Theory of elasticity, McGraw Hill Book Company.

Huebner, K.H. (1982). Finite element method for engineers, John Wiley Sons, Newyork.